2016 / Volume 54 / Number 1
ISSN 1641-4640

Folia NEUROPATHOLOGICA

www.folianeuro.termedia.pl

Official Journal of Mossakowski Medical Research Centre Polish Academy of Sciences
and
Polish Association of Neuropathologists

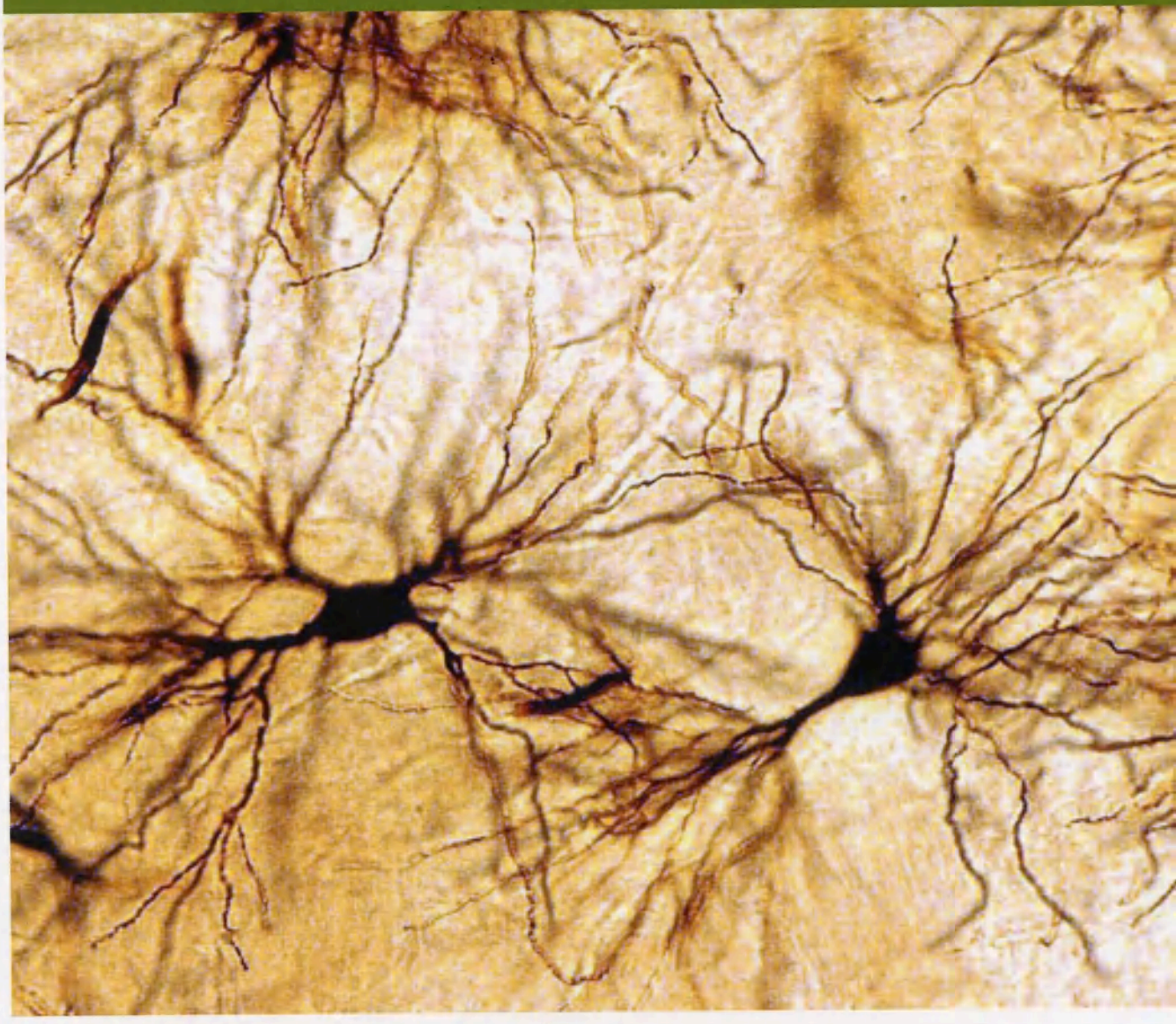

ISSN 1641-4640

Folia Neuropathologica

TERMEDIA Publishing House

Folia
Neuropathologica
former *Neuropatologia Polska*

Official Journal of Mossakowski Medical Research Centre Polish Academy of Sciences and Polish Association of Neuropathologists

The journal is partly financially supported
by the Ministry of Science and Higher Education

termedia

Termedia Publishing House
Kleeberga 2, 61-615 Poznan, Poland
phone/fax: +48 61 822 77 81
e-mail: termedia@termedia.pl
www.termedia.pl
www.folianeuro.termedia.pl

Warsaw office
phone/fax: +48 22 827 75 14
e-mail: biuro.warszawa@termedia.pl

President of the Management Board
of the Termedia Publishing House
Janusz Michalak

Scientific Director
of the Termedia Publishing House
Maciej Banach

Production Editor
Marzena Demska
e-mail: m.demska@termedia.pl

Marketing and Advertising Department
Renata Dolata
phone: +48 61 822 77 81 ext. 508
e-mail: r.dolata@termedia.pl

Distribution Subscription Department
Jolanta Jankowiak
phone: +48 61 656 22 00
e-mail: prenumerata@termedia.pl

Impact Factor for Folia Neuropathologica equals 1.568
MNiSW score for Folia Neuropathologica equals 20
Index Copernicus Value 2014 for Folia Neuropathologica equals 22.61 (154.82)
Position in Index Copernicus ranking systems available at http://www.indexcopernicus.pl

Abstracted and indexed in Index Medicus/MEDLINE, Neuroscience Citation Index, SciSearch, Research Alert, Chemical Abstracts, EMBASE/Excerpta Medica, Polish Medical Bibiography, Index Copernicus

The journal is financially supported by the Ministry of Sciences and Higher Education.

Print run: 450 copies

Folia
Neuropathologica
2016; 54/1: 1-88

Contents

Review paper

Folia Neuropathologica

Emery-Dreifuss muscular dystrophy: the most recognizable laminopathy

Agnieszka Madej-Pilarczyk, Andrzej Kochański

Neuromuscular Unit, Mossakowski Medical Research Centre, Polish Academy of Sciences, Warsaw, Poland

The authors dedicate this review to Prof. Irena Hausmanowa-Petrusewicz.

Folia Neuropathol 2016; 54 (1): 1-8 DOI: 10.5114/fn.2016.58910

Abstract

Emery-Dreifuss muscular dystrophy (EDMD), a rare inherited disease, is characterized clinically by humero-peroneal muscle atrophy and weakness, multijoint contractures, spine rigidity and cardiac insufficiency with conduction defects. There are at least six types of EDMD known so far, of which five have been associated with mutations in genes encoding nuclear proteins. The majority of the EDMD cases described so far are of the emerinopathy (EDMD1) kind, with a recessive X-linked mode of inheritance, or else laminopathy (EDMD2), with an autosomal dominant mode of inheritance. In the work described here, the authors have sought to describe the history by which EDMD came to be distinguished as a separate entity, as well as the clinical and genetic characteristics of the disease, the pathophysiology of lamin-related muscular diseases and, finally, therapeutic issues, prevention and ethical aspects.

Key words: *Emery-Dreifuss muscular dystrophy, emerin, lamin A/C, laminopathy, LMNA gene.*

Introduction

Laminopathies fall within a group of rare diseases connected with structural/functional defects of the proteins making up the nuclear envelope (which is composed of inner and outer nuclear membranes). This explains them also being called envelopathies. Below the inner membrane there lies the so called nuclear lamina formed by intermediate filament proteins called lamins. There are two types of lamins in human beings, with lamin B encountered at all developmental stages, while lamin A/C is a protein characteristic of differentiated cells in adults, which is not therefore present in the early stages of embryonic development [14,35]. Lamin A/C plays the role of a structural integrator in a cell nucleus, ensuring the maintenance of the latter's shape, as well as its mechanical endurance (mechanotransduction). It takes part in regulation of the cell-division cycle, through interaction with chromatin, transcription factors and associated proteins. Lamin A/C is encoded by the *LMNA* gene, which is composed of 12 exons and on the matrix of which two proteins are formed – lamin A and lamin C. Mature lamin A is made of prelamin A, which is subject to posttranslational modifications catalysed by the specific metalloproteinase FACE-1, as encoded by the *ZMPSTE-24* gene [37]. Lamin A not only forms the nuclear lamin, but

Communicating author

Dr Agnieszka Madej-Pilarczyk, Neuromuscular Unit, Mossakowski Medical Research Centre, Polish Academy of Sciences, 5 Pawińskiego St., 02-106 Warsaw, Poland, phone: +48 22 608 66 01, fax: +48 22 608 65 31, e-mail: agamadpil@gmail.com

is also present in smaller amounts in another compartment of the cell nucleus – the nucleoplasm [10].

There are four phenotypic subgroups of laminopathies related to the pathology of A/C lamin, i.e. muscular and peripheral neurogenic, as well as lipodystrophies and premature ageing syndromes [44]. However, the first described envelopathy was not a laminopathy, but an emerinopathy connected with muscular pathology – Emery-Dreifuss muscular dystrophy marked later on as type 1 (EDMD 1).

EDMD1 (emerinopathy): historical remarks, clinical presentation, genetic investigations

Historically the first clinical description of the familiar muscular dystrophy with early contractures was made in 1902 by Cestan and Lejonne [13]. In 1955, Peter Emil Becker recognized a benign form of X-linked muscular dystrophy characterized by later onset than in the Duchenne type, a slow course of disease and slightly decreased average life expectancy [3]. In 1961, Dreifuss and Hogan reported on a large four-generational family in which muscle dystrophy only occurred in 8 males. In contrast to Duchenne-type muscular dystrophy, this disease was reported on by the authors by reference to its extraordinarily slow progression. Even 52-year-old and 44-year-old affected males remained ambulant, and had been able to remain active, working as a school teacher and the owner of a grocery store, respectively [15]. In 1966, Emery and Dreifuss offered a detailed characterization of the clinical features and course of the disease [16], which encompasses atrophy or weakening of muscles, mainly of the brachial and fibular groups; multiarticular contractures and rigidity of the spine; and – in further course – development of cardiomyopathy with conduction disturbances. The first symptoms of the diseases are usually seen in the first decade of life, manifesting as ankle and elbow contractures and spine rigidity. They precede muscle atrophy and weakness, which are typically visible in the 2nd to 3rd decades of life. It is during adolescence, as a young man grows rapidly, that contractures become more evident. Nevertheless, the progression of muscle atrophy is usually slow in the first decades of life, though tending to accelerate subsequently. In EDMD1, symptoms involving the skeletal muscles usually arise before cardiac disease, with the latter initially including sinus bradycardia, supraventricular tachyarrhythmias and paroxysmal atrial fibrillation, with atrial standstill and heart insufficiency then coming to characterize the 4th or 5th decades of life. Sudden death is due mainly to a complete heart block, though this is capable of being averted if a pacemaker is implanted. The full clinical picture with skeletal-muscle and cardiac involvement is to be seen in men. Female carriers never present muscle symptoms or signs, though in the 4th–5th decades of life, around 20% of them may develop overt cardiac disease, with pacemaker implantation and pharmacotherapy necessitated. It was in 1979 that the disease began being referred to as Emery-Dreifuss muscular dystrophy (EDMD, MIM 31030), while 1986 saw Thomas and co-workers succeed in mapping the gene responsible for the disease, i.e. *EMD*, which encodes the nuclear protein emerin, on the X chromosome, in its q27-28 region. The maximum *LOD score* value of 4.29 was obtained in the case of the marker for Factor VIII. Simultaneously, genetic linkage to the Duchenne and Becker muscular dystrophy *locus* Xp21 was excluded, in this way offering a firm confirmation that the genetic identity of Emery-Dreifuss muscular dystrophy is separate [42]. The Warsaw Department of Neurology headed by Professor Irena Hausmanowa-Petrusewicz (1917-2015) contributed to narrowing of the Emery-Dreifuss *locus* to the Xq27.3-qter region and one of the 2 families analysed originated from Poland. Thanks to the highly informative contacts it proved possible to maintain with the Polish family (in which 8 males were affected), the identity of Emery-Dreifuss dystrophy could be narrowed down further [45]. The *EMD* gene was found to contain 6 exons. The mutations in the *EMD* gene first identified as responsible for EDMD1 were: c.3G>A affecting codon start in exon 1, the nonsense c.130C>T in exon 2 and c.653insTGGGC in exon 6, which influences the open reading frame and introduces a premature stop codon at 238 [5]. In the majority of EDMD1 cases, small deletions or splice-site mutations leading to a change of reading frame are observed, while remaining patients have either a nonsense/missense mutation or large deletions [http://www.umd.be/EMD] (Fig. 1). In these circumstances, a lack of emerin can be observed in patients. Mutations are most often located in exons 1 and 2, whereas 26% of mutations are of codons 1 or 34 [6,11,23].

EDMD2 (laminopathy)

In the 1990s, it was determined that EDMD may also be conditioned by laminopathy (EDMD 2 with an autosomal dominant trait of inheritance and

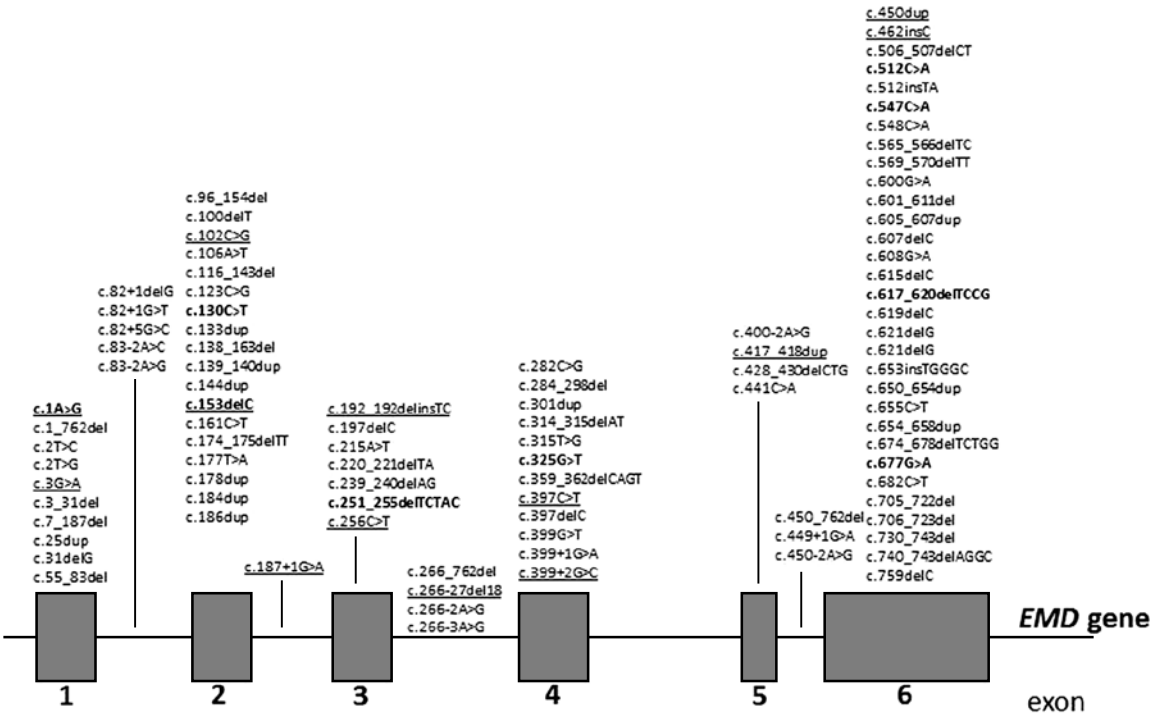

Fig. 1. Mutation spectrum in EDMD1. The most frequent mutations in the *EMD* gene associated with EDMD1 phenotype are marked in bold. Mutations in Polish EDMD1 patients are underlined.
Source: http://www.umd.be/EMD/

EDMD3 with a recessive one) [7,8,33,43]. The symptoms in skeletal muscles in EDMD2 are less stereotypical than those regarding EDMD1. Severe generalized muscle atrophy and joint contractures can occur early, leading to a loss of independent ambulance in some cases. In contrast, in others the phenotype might prove mild, with late onset and slow progression of muscle weakness and joint contractures [8]. Paraspinal ligaments are frequently affected. Weakness of respiratory muscles and chest deformity may cause respiratory failure. The cardiological component is found to be less predictable in EDMD2 than in EDMD1. Apart from conduction disturbances, systolic dysfunction of the left ventricle predominates, while the pathological process affects the ventricles more frequently, leading to dilated cardiomyopathy. Life-threatening ventricular arrhythmia is the main cause of death. As a pacemaker is not found to suffice, implantation of a cardioverter-defibrillator in primary prevention of sudden cardiac death is recommended. In 1999, Bonne *et al.* [7] mapped the locus for EDMD2 on chromosome 1q11-q23, which contains the *LMNA* gene encoding two proteins of the nuclear lamina, i.e. lamin A and lamin C. The first reported mutations in the *LMNA* gene, as associated with EDMD 2, were: the nonsense c.16C>T in exon 1, and the three missense mutations of c.1357C>T in exon 7, as well as c.1580G>C and 1589T>C in exon 9. In 80% of cases of EDMD2, mutations in the *LMNA* gene involve heterozygous missense mutations, which result in synthesis of a mutated lamin A/C with a dominant-negative toxic effect; less often they include deletions/duplications, some of which may lead to loss of function of the final protein [4]. The *LMNA* gene mutations in EDMD2 are disseminated randomly in exons 1-11 of the lamin A/C gene (Fig. 2). A genetic defect is most often localized in exons 1 and 6, while recurrent mutations are seen in codons 377 and 453 [23,25]. In the majority of EDMD2 patients, it is possible to find *de novo* mutation in the *LMNA* gene [9].

Other types of EDMD

Laminopathy or emerinopathy is diagnosed in 40% of patients with the clinical picture of EDMD. A search for mutations in other genes, including those encoding proteins of the nuclear envelope that are functionally related to lamin A/C, allowed

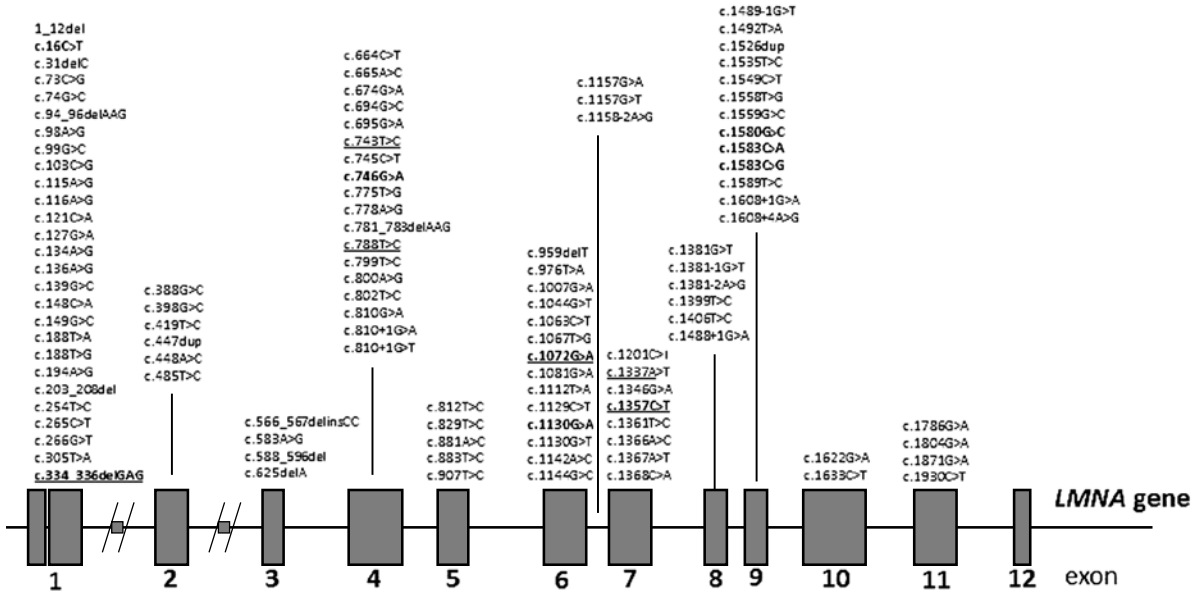

Fig. 2. Mutation spectrum in EDMD2. The most frequent mutations in the *LMNA* gene associated with EDMD2 phenotype are marked in bold. Mutation in Polish EDMD2 patients are underlined. Source: http://www.umd.be/LMNA/

for the identification of *SYNE1* and *SYNE 2* (the *synaptic nuclear envelope protein 1(or 2) genes*), encoding nesprin-1 and nesprin-2, as two genes connected with EDMD, i.e. EDMD4 and EDMD5, respectively [46]. A further candidate gene is the *LAP* gene encoding polypeptides connected with lamins *(lamin-associated protein 2 alpha, LAP2alpha*). Mutations in this gene were also reported in patients with dilated cardiomyopathy, which is clinically similar to laminopathy. In 2009, a few patients with a clinical picture resembling Emery-Dreifuss muscular dystrophy were reported with a mutation in the *FHL-1 (four and a half LIM domains protein 1)* gene located on the X chromosome [21]. The gene is responsible for encoding one of the proteins of the cytoskeleton. A characteristic feature of EDMD6 caused by a mutation of *FHL-1* is hypertrophic cardiomyopathy (as opposed to the dilated cardiomyopathy observed in the case of laminopathy), as well as deltoid hypertrophy and – often – vocal cord paresis.

Pathophysiology

A number of pathological changes can be observed in both laminopathies and emerinopathies, at both the molecular and the cellular levels. In the majority of emerinopathies, a lack or considerable reduction of emerin expression is to be observed [26]. Some *EMD* mutations lead to shortening of emerin, due to premature termination of the amino-acid chain or improper exon splicing. Shortened emerin is deprived of its proper biological function and in the case of a loss of signal of nuclear localization, it may be absent from the nucleus. Ultrastructural examination of cells of skeletal, cardiac-muscle and skin fibroblasts from patients suffering from both types of EDMD has been found to show irregularly-shaped nuclei, losses of nuclear membrane and a change in the density of heterochromatin. In addition, laminopathy causes an escape of nucleoplasm beyond the boundaries of the nucleus due to losses incurred by the nuclear membrane, as well as chromatin decondensation and its detachment from nuclear lamin. In some cases pseudo-inclusions in its area are also created, while the most advanced changes may also entail fragmentation of the nucleus [17,18,34,39].

Lamin A/C is expressed not only in mature myocytes, but also in stem cells of the skeletal muscles and in the satellite cells responsible for muscle regeneration [19]. Satellite cells exit the cell cycle and fuse with muscle fibre when hyperphosphorylated retinoblastoma protein (pRb) inhibits the p21 protein responsible for continued proliferation [22,41]. In skeletal muscle, pRb binds to skeletal muscle-spe-

cific transcriptional regulator, MyoD, induces expression of myogenesis-regulating genes and arrests the cell cycle, promoting differentiation [30]. Lamin A/C regulates the cell cycle through interaction with the pRb-MyoD complex, and via other nucleoplasmic proteins that are partners of lamin A/C, i.e. emerin, LAP2alpha and nesprin. Mutations in the *LMNA* gene responsible for muscular dystrophies cause damage and degeneration of myocytes. Simultaneous expression of mutated lamin A/C in the satellite cells responsible for repair processes hampers the regeneration process and variation of myocytes, thus contributing to the progressive development of muscular dystrophy. In muscle specimens from EDMD1/2 patients, mutations in genes encoding nuclear envelope proteins have been shown to disrupt their interactions with the pRb-MyoD complex, with the result that the process of differentiation of myoblasts into muscle fibres is impaired [2]. A lack of lamin A or emerin decreases levels of the proteins important in muscle differentiation; e.g. pRb, MyoD, desmin and M-cadherin [19]. Since LAP2alpha regulates the proliferation of stem cells in mature tissue [29], it is suggested that LAP2alpha activity in satellite muscle cells can be compromised. The LAP2alpha-lamin A/C complex may be a regulator of MyoD and pRb in the initial step of muscle differentiation. As the inhibition of myoblast proliferation and promotion of differentiation progress, lamin A/C moves from the nucleoplasm to nuclear lamina, and the expression of LAP2alpha is seen to decrease. Introduction of mutated lamin A to nuclei in turn impairs myoblast differentiation. Mutated lamin A accumulates in the nucleoplasm and disrupts the transfer of normal lamin A to nuclear lamina (dominant-negative activity). In addition it increases interaction of LAP2alpa with wild and mutated lamin, leading to sequestration of their complexes in the nucleoplasm [27,32].

Laminopathies are characterized by great intrafamilial and interfamilial variability, as regards both the phenotype generated by a given mutation (possible overlapping syndromes with other laminopathies) and the severity of the disease, from life-threatening to symptom-free carrier state [12]. Interfamilial and intrafamilial variability in patients with the same mutation may depend on phenotype modifiers: concomitant mutation in various genes – oligogenic inheritance [20,28], single nucleotide polymorphisms in the mutated or another gene, various expression of the protein, impaired promoter methylation, interactions with other nuclear proteins, modifying emerin/lamin A/C function and the existence of an allele with a high or low expression at the LMNA locus [36].

Treatment, prevention and management of Emery-Dreifuss muscular dystrophy carriers

There is no specific treatment for EDMD. Patients should have mild dynamic physical therapy with stretching exercises to prevent contractures. Severe contractures may be treated surgically. The best effects are obtained for ankle contractures, and the results of operation persist for longer if this is done after the adolescent growth spurt. Cardiological treatment includes implantation of a pacemaker or cardioverter-defibrillator, as well as pharmacotherapy aiming to delay heart remodeling (using ACE inhibitors), to treat arrhythmia and cardiac failure (using ACE inhibitors, diuretics and beta-blockers) and to prevent thromboembolism (using anticoagulants and antiplatelets). In patients with a preserved respiratory function and without severe muscle involvement, but who have treatment-resistant severe cardiomyopathy, heart transplantation might be considered. Patients with respiratory failure sometimes require respiratory support, especially at night.

Males diagnosed with EDMD1 and all patients with EDMD2 should be involved in regular annual cardiological screening, with this including clinical examination, ECG, echocardiography and 24-hour ECG monitoring. Obligatory female carriers of EDMD1 (i.e. daughters of men affected by it) and those with a carrier state confirmed genetically (i.e. the sisters of men affected by EDMD1, the daughters and sisters of known female carriers) should be informed about the risk of cardiomyopathy, and familiarized with the potential symptoms of cardiac insufficiency. In the case of any cardiac symptoms, the first cardiological consultation – including clinical examination, ECG and echocardiography – should be held in early adulthood, then annually; otherwise every 5 years from the age of 25 years onwards. The above guidelines are based on the recommendations of the Working Group of the National Consultant in Cardiology on cardiological supervision in Duchenne and Becker muscular dystrophy and the prevention of cardiomyopathy in female carriers of DMD/BMD [40], given that these could be taken to apply to EDMD patients as well.

Since the penetrance of *LMNA* mutations, especially in relation to cardiac symptoms which might be life-threatening and even initially manifest as sudden cardiac death, is high and greater with age (being almost complete by the age of 60), patients with a subclinical course of the disease, including asymptomatic carriers of *LMNA* mutations, require careful assessment of the cardiological risk [31]. Although the muscle symptoms in EDMD usually precede heart involvement, and although the latter is seen typically in early adulthood, this sequence is generally true of EDMD1, while the clinical picture is seen to be more unpredictable in EDMD2. Some EDMD patients may have conduction disturbances or atrial arrhythmia as early as in the middle of the second decade of life [23]. Children from families affected with EDMD should therefore be observed for early signs of the disease, especially joint contractures and spine rigidity. Molecular testing should be done in the case of any abnormalities on neurological examination.

Ethical issues as regards genetic testing in Emery-Dreifuss muscular atrophy

In terms of genetic counselling, Emery-Dreifuss muscular dystrophy should be considered separately from other neuromuscular disorders limited to damage of the skeletal muscle, given the high risk of heart-rhythm disturbances and even sudden death in EDMD families. In particular, in the case of the novel *EMD* or *LMNA* mutations reported in single families, the question of penetrance remains unanswered. The marked clinical variability of EDMD, even as regards recurrent *EMD/LMNA* mutations, ensures that an individual risk of severe heart complications is notably hard to predict. Furthermore, in young EDMD patients, a positive result of genetic testing may result in fatalism and a deterministic attitude to further life. Indeed, a positive test result in a young patient may give rise to anxiety and distress. Moreover, molecular diagnosis of EDMD may be associated with a person feeling threatened by sudden death and thus regarding his/her own life as being of limited value. The "right not to know" confirmed by both the Council of Europe Convention on Human Rights and Biomedicine (Article 10.2) and the UNESCO Declaration on the Human Genome (Article 5c) should be considered carefully during the EDMD genetic counselling process [24]. According to some authors, in the case of a direct threat to life (also present in EDMD), the right "not to know" is of limited value [1]. Nevertheless, in young patients especially, a possible EDMD diagnosis should always entail consideration being given to the question of genetic testing and the disclosure of genetic results. In turn, clinically-healthy members of families affected by EDMD, who do not want to undergo and do not undergo genetic screening for the disease should be aware of potential cardiological symptoms, which may occur later in life and serve as the first indicator of laminopathy. In that case, prompt cardiological assessment is necessary, with genetic screening performed where the results prove to be abnormal. Similarly, the question of genetic testing for EDMD assumes special value in regard to preimplantation genetic diagnosis (PGD) and prenatal testing. In fact, in the cases of both PGD and prenatal testing for EDMD, genetic counselling deals only with the prediction of the possible phenotype, provoking ethical questions where decisions regarding embryo transfer or abortion are concerned. Additionally, due to the unknown long-term consequences of blastomere removal in PGD, the ethical dilemmas associated with EDMD-directed PGD are not to be omitted [38].

Disclosure

Authors report no conflict of interest.

References

1. Andorno R. The right not to know: an autonomy based approach. J Med Ethics 2004; 30: 435-440.
2. Bakay M, Wang Z, Melcon G, Schiltz L, Xuan J, Zhao P, Sartorelli V, Seo J, Pegoraro E, Angelini C, Shneiderman B, Escolar D, Chen YW, Winokur ST, Pachman LM, Fan C, Mandler R, Nevo Y, Gordon E, Zhu Y, Dong Y, Wang Y, Hoffman EP. Nuclear envelope dystrophies show a transcriptional fingerprint suggesting disruption of Rb-MyoD pathways in muscle regeneration. Brain 2006; 129: 996-1013.
3. Becker PE, Kiener F. Eine neue X-chromosomale Muskeldystrophie. Arch Psychiat Nervenkrank 1955; 193: 427-448.
4. Benedetti S, Menditto I, Degano M, Rodolico C, Merlini L, D'Amico A, Palmucci L, Berardinelli A, Pegoraro E, Trevisan CP, Morandi L, Moroni I, Galluzzi G, Bertini E, Toscano A, Olivè M, Bonne G, Mari F, Caldara R, Fazio R, Mammì I, Carrera P, Toniolo D, Comi G, Quattrini A, Ferrari M, Previtali SC. Phenotypic clustering of lamin A/C mutations in neuromuscular patients. Neurology 2007; 69: 1285-1292.
5. Bione S, Maestrini E, Rivella S, Mancini M, Regis S, Romeo G, Toniolo D. Identification of a novel X-linked gene responsible for Emery-Dreifuss muscular dystrophy. Nat Genet 1994; 8: 323-327.

6. Bonne G, Quijano-Roy S. Emery-Dreifuss muscular dystrophy, laminopathies, and other nuclear envelopathies. Handb Clin Neurol 2013; 113: 1367-1376.
7. Bonne G, Di Barletta MR, Varnous S, Bécane HM, Hammouda EH, Merlini L, Muntoni F, Greenberg CR, Gary F, Urtizberea JA, Duboc D, Fardeau M, Toniolo D, Schwartz K. Mutations in the gene encoding lamin A/C cause autosomal dominant Emery-Dreifuss muscular dystrophy. Nat Genet 1999; 21: 285-288.
8. Bonne G, Mercuri E, Muchir A, Urtizberea A, Bécane HM, Recan D, Merlini L, Wehnert M, Boor R, Reuner U, Vorgerd M, Wicklein EM, Eymard B, Duboc D, Penisson-Besnier I, Cuisset JM, Ferrer X, Desguerre I, Lacombe D, Bushby K, Pollitt C, Toniolo D, Fardeau M, Schwartz K, Muntoni F. Clinical and molecular genetic spectrum of autosomal dominant Emery-Dreifuss muscular dystrophy due to mutations of the lamin A/C gene. Ann Neurol 2000; 48: 170-180.
9. Bonne G, Leturcq F, Ben Yaou R. Emery-Dreifuss Muscular Dystrophy. In: Pagon RA, Adam MP, Ardinger HH, Wallace SE, Amemiya A, Bean LJH, Bird TD, Fong CT, Mefford HC, Smith RJH, Stephens K. GeneReviews® [Internet]. University of Washington, Seattle 1993-2015; 2004 Sep 29 [Updated 2013 Jan 17].
10. Bridger JM, Kill IR, O'Farrell M, Hutchison CJ. Internal lamin structures within G1 nuclei of human dermal fibroblasts. J Cell Sci 1993; 104: 297-306.
11. Brown CA, Scharner J, Felice K, Meriggioli MN, Tarnopolsky M, Bower M, Zammit PS, Mendell JR, Ellis JA. Novel and recurrent EMD mutations in patients with Emery-Dreifuss muscular dystrophy, identify exon 2 as a mutation hot spot. J Hum Genet 2011; 56: 589-594.
12. Carboni N, Mura M, Mercuri E, Marrosu G, Manzi RC, Cocco E, Nissardi V, Isola F, Mateddu A, Solla E, Maioli MA, Oppo V, Piras R, Marini S, Lai C, Politano L, Marrosu MG. Cardiac and muscle imaging findings in a family with X-linked Emery-Dreifuss muscular dystrophy. Neuromuscul Disord 2012; 22: 152-158.
13. Cestan R, Lajonne NJ. Dystrophie musculaire. Iconogr Salpetriere 1902; 155: 35.
14. Dauer WT, Worman HJ. The nuclear envelope as a signaling node in development and disease. Dev Cell 2009; 17: 626-638.
15. Dreifuss FE, Hogan GR. Survival in X-chromosomal muscular dystrophy. Neurology 1961; 11: 734-737.
16. Emery AE, Dreifuss FE. Unusual type of benign x-linked muscular dystrophy. J Neurol Neurosurg Psychiatry 1966; 29: 338-342.
17. Fidziańska A, Toniolo D, Hausmanowa-Petrusewicz I. Ultrastructural abnormality of sarcolemmal nuclei in Emery-Dreifuss muscular dystrophy (EDMD). J Neurol Sci 1998; 159: 88-93.
18. Fidziańska A, Hausmanowa-Petrusewicz I. Architectural abnormalities in muscle nuclei: ultrastuctural differences between X-linked and autosomal dominant forms of EDMD. J Neurol Sci 2003; 210: 47-51.
19. Frock RL, Kudlow BA, Evans AM, Jameson SA, Hauschka SD, Kennedy BK. Lamin A/C and emerin are critical for skeletal muscle satellite cell differentiation. Genes Dev 2006; 20: 486-500.
20. Granger B, Gueneau L, Drouin-Garraud V, Pedergnana V, Gagnon F, Ben Yaou R, Tezenas du Montcel S, Bonne G. Modifier locus of the skeletal muscle involvement in Emery-Dreifuss muscular dystrophy. Hum Genet 2011; 129: 149-159.
21. Gueneau L, Bertrand AT, Jais JP, Salih MA, Stojkovic T, Wehnert M, Hoeltzenbein M, Spuler S, Saitoh S, Verschueren A, Tranchant C, Beuvin M, Lacene E, Romero NB, Heath S, Zelenika D, Voit T, Eymard B, Ben Yaou R, Bonne G. Mutations of the FHL1 gene cause Emery-Dreifuss muscular dystrophy. Am J Hum Genet 2009; 85: 338-353.
22. Halevy O, Novitch BG, Spicer DB, Skapek SX, Rhee J, Hannon GJ, Beach D, Lassar AB. Correlation of terminal cell cycle arrest of skeletal muscle with induction of p21 by MyoD. Science 1995; 267: 1018-1021.
23. Hausmanowa-Petrusewicz I, Madej-Pilarczyk A, Marchel M, Opolski G. Emery-Dreifuss dystrophy: a 4-year follow-up on a laminopathy of special interest. Neurol Neurochir Pol 2009; 43: 415-420.
24. Kochański A, Demkow U. Next generation sequencing-ethical and social issues. In: Clinical Applications for Next Generation Sequencing. Demkow U, Ploski R (eds.). Elsevier, London 2016; pp: 295-300.
25. Madej-Pilarczyk A, Kotruchow K, Kabzinska D, Cegielska J, Kochanski A, Hausmanowa-Petrusewicz I. Emery-Dreifuss muscular dystrophy type 2 associated (?) with mild peripheral polyneuropathy. Folia Neuropathol 2015; 53: 270-274.
26. Manilal S, Recan D, Sewry CA, Hoeltzenbein M, Llense S, Leturcq F, Deburgrave N, Barbot J, Man N, Muntoni F, Wehnert M, Kaplan J, Morris GE. Mutations in Emery-Dreifuss muscular dystrophy and their effects on emerin protein expression. Hum Mol Genet 1998; 7: 855-864.
27. Markiewicz E, Venables R, Mauricio-Alvarez-Reyes, Quinlan R, Dorobek M, Hausmanowa-Petrusewicz I, Hutchison C. Increased solubility of lamins and redistribution of lamin C in X-linked Emery-Dreifuss muscular dystrophy fibroblasts. J Struct Biol 2002; 140: 241-253.
28. Muntoni F, Bonne G, Goldfarb LG, Mercuri E, Piercy RJ, Burke M, Yaou RB, Richard P, Récan D, Shatunov A, Sewry CA, Brown SC. Disease severity in dominant Emery Dreifuss is increased by mutations in both emerin and desmin proteins. Brain 2006; 129: 1260-1268.
29. Naetar N, Korbei B, Kozlov S, Kerenyi MA, Dorner D, Kral R, Gotic I, Fuchs P, Cohen TV, Bittner R, Stewart CL, Foisner R. Loss of nucleoplasmic LAP2alpha-laminA complexes causes erythroid and epidermal progenitor hyperproliferation. Nat Cell Biol 2008; 10: 1341-1348.
30. Novitch BG, Mulligan GJ, Jacks T, Lassar AB. Skeletal muscle cells lacking the retinoblastoma protein display defects in muscle gene expression and accumulate in S and G2 phases of the cell cycle. J Cell Biol 1996; 135: 441-456.
31. Pasotti M, Klersy C, Pilotto A, Marziliano N, Rapezzi C, Serio A, Mannarino S, Gambarin F, Favalli V, Grasso M, Agozzino M, Campana C, Gavazzi A, Febo O, Marini M, Landolina M, Mortara A, Piccolo G, Viganò M, Tavazzi L, Arbustini E. Long-term outcome and risk stratification in dilated cardiolaminopathies. J Am Coll Cardiol 2008; 52: 1250-1260.
32. Politano L, Carboni N, Madej-Pilarczyk A, Marchel M, Nigro G, Fidziaóska A, Opolski G, Hausmanowa-Petrusewicz I. Advances in basic and clinical research in laminopathies. Acta Myol 2013; 32: 18-22.
33. Raffaele Di Barletta M, Ricci E, Galluzzi G, Tonali P, Mora M, Morandi L, Romorini A, Voit T, Orstavik KH, Merlini L, Trevisan C, Biancalana V, Hausmanowa-Petrusewicz I, Bione S, Ricotti R, Schwartz K, Bonne G, Toniolo D. Different mutations in the LMNA gene cause autosomal dominant and autosomal reces-

sive Emery-Dreifuss muscular dystrophy. Am J Hum Genet 2000; 66: 1407-1412.
34. Reichart B, Klafke R, Dreger C, Krüger E, Motsch I, Ewald A, Schäfer J, Reichmann H, Müller CR, Dabauvalle MC. Expression and localization of nuclear proteins in autosomal-dominant Emery-Dreifuss muscular dystrophy with LMNA R377H mutation. BMC Cell Biol 2004; 5: 12.
35. Rober RA, Weber K, Osborn M. Differential timing of nuclear lamin A/C expression in the various organs of the mouse embryo and the young animal: a developmental study. Development 1989; 105: 365-378.
36. Rodríguez S, Eriksson M. Low and high expressing alleles of the LMNA gene: implications for laminopathy disease development. PLoS One 2011; 6: e25472.
37. Rusinol AE, Sinensky MS. Farnesylated lamins, progeroid syndromes and farnesyl transferase inhibitors. J Cell Sci 2006; 119: 3265-3272.
38. Sampino S, Zacchini F, Swiergiel AH, Modlinski AJ, Loi P, Ptak G. Effects of blastomere biopsy on postnatal growth and behavior in mice. Hum Reprod 2014; 29: 1875-1883.
39. Sewry CA, Brown SC, Mercuri E, Bonne G, Feng L, Camici G, Morris GE, Muntoni F. Skeletal muscle pathology in autosomal dominant Emery-Dreifuss muscular dystrophy with lamin A/C mutations. Neuropathol Appl Neurobiol 2001; 27: 281-290.
40. Sinkiewicz W, Droździ J, Dubiel JS, Filipiak KJ, Rozentryt P, Wierzchowiecki M, Opolski G. Guidelines of National Consultant in the issue of cardiologic care of patients with Duchenne's and Becker's muscular dystrophy and cardiomyopathy prevention in woman with DMD/BMD mutations (mothers and sisters of patients with dystrophies. Kardiol Pol 2007; 65: 223-228.
41. Takahashi C, Bronson RT, Socolovsky M, Contreras B, Lee KY, Jacks T, Noda M, Kucherlapati R, Ewen ME. Rb and N-ras function together to control differentiation in the mouse. Mol Cell Biol 2003; 23: 5256-5268.
42. Thomas NS, Williams H, Elsas LJ, Hopkins LC, Sarfarazi M, Harper PS. Localisation of the gene for Emery-Dreifuss muscular dystrophy to the distal long arm of the X chromosome. J Med Genet 1986; 23: 596-598.
43. Vytopil M, Benedetti S, Ricci E, Galluzzi G, Dello Russo A, Merlini L, Boriani G, Gallina M, Morandi L, Politano L, Moggio M, Chiveri L, Hausmanova-Petrusewicz I, Ricotti R, Vohanka S, Toman J, Toniolo D. Mutation analysis of the lamin A/C gene (LMNA) among patients with different cardiomuscular phenotypes. J Med Genet 2003; 40: e132.
44. Worman HJ, Bonne G. "Laminopathies": a wide spectrum of human diseases. Exp Cell Res 2007; 313: 2121-2133.
45. Yates JR, Affara NA, Jamieson DM, Ferguson-Smith MA, Hausmanowa-Petrusewicz I, Zaremba J, Borkowska J, Johnston AW, Kelly K. Emery-Dreifuss muscular dystrophy: localisation to Xq27.3--- qter confirmed by linkage to the factor VIII gene. J Med Genet 1986; 23: 587-590.
46. Zhang Q, Bethmann C, Worth NF, Davies JD, Wasner C, Feuer A, Ragnauth CD, Yi Q, Mellad JA, Warren DT, Wheeler MA, Ellis JA, Skepper JN, Vorgerd M, Schlotter-Weigel B, Weissberg PL, Roberts RG, Wehnert M, Shanahan CM. Nesprin-1 and -2 are involved in the pathogenesis of Emery-Dreifuss muscular dystrophy and are critical for nuclear envelope integrity. Hum Mol Genet 2007; 16: 2816-2833.

Original article

Folia Neuropathologica

Histopathological comparison of Kearns-Sayre syndrome and PGC-1α-deficient mice suggests a novel concept for vacuole formation in mitochondrial encephalopathy

Levente Szalardy[1], Mate Molnar[1], Rita Torok[1], Denes Zadori[1], Laszlo Vecsei[1,2], Peter Klivenyi[1], Paweł Piotr Liberski[3], Gabor Geza Kovacs[4]

[1]Department of Neurology, Faculty of Medicine, Albert Szent-Györgyi Clinical Center, University of Szeged, Szeged, Hungary, [2]MTA-SZTE Neuroscience Research Group, Szeged, Hungary, [3]Department of Molecular Pathology and Neuropathology, Chair of Oncology, Medical University of Lodz, Lodz, Poland, [4]Institute of Neurology, Medical University of Vienna, Vienna, Austria

Folia Neuropathol 2016; 54 (1): 9-22 DOI: 10.5114/fn.2016.58911

Abstract

Despite the current hypotheses about myelinic and astrocytic ion-dyshomeostasis underlying white (WM) and grey matter (GM) vacuolation in mitochondrial encephalopathies, there is a paucity of data on the exact mechanism of vacuole formation. To revisit the concepts of vacuole formation associated with mitochondrial dysfunction, we performed a comparative neuropathological analysis in Kearns-Sayre syndrome (KSS) and full-length peroxisome proliferator-activated receptor-γ coactivator-1α (FL-PGC-1α)-deficient mice, a recently proposed morphological model of mitochondrial encephalopathies. Brain tissues from an individual with genetically proven KSS (22-year-old man) and aged FL-PGC-1α-deficient and wild-type (male, 70-75-week-old) mice were analysed using ultrastructural and immunohistochemical methods, with a specific focus on myelin-related, oligodendroglial, axonal and astrocytic pathologies. Besides demonstrating remarkable similarities in the lesion profile of KSS and FL-PGC-1α-deficient mice, this study first provides morphological evidence for the identical origin of WM and GM vacuolation as well as for the presence of intracytoplasmic oligodendroglial vacuoles in mitochondriopathies. Based on these observations, the paper proposes a theoretical model for the development of focal myelin vacuolation as opposed to the original concepts of intramyelin oedema. Placing oligodendrocytes in the centre of tissue lesioning in conditions related to defects in mitochondria, our observations support the rationale for cytoprotective targeting of oligodendrocytes in mitochondrial encephalopathies, and may also have implications in brain aging and multiple sclerosis, as discussed.

Key words: *Kearns-Sayre syndrome, PGC-1α, mitochondrial encephalopathy, vacuole, myelin, oligodendrocyte.*

Introduction

Mitochondrial diseases comprise a group of inherited or sporadic neurological disorders in which proper mitochondrial function is compromised. Either the mitochondrial or nuclear genome is involved by the genetic alterations. Based on the symptomatic appearance, such diseases are divided into characteristic syndromes, including MELAS (mitochondrial

Communicating author

Prof. Gabor Geza Kovacs, Institute of Neurology, Medical University of Vienna, Währinger Gürtel 18-20, 1090 Vienna, Austria, e-mail: gabor.kovacs@meduniwien.ac.at

encephalomyopathy, lactic acidosis, and stroke-like episodes), MERRF (myoclonic epilepsy with ragged red fibres), LHON (Leber's hereditary optic neuropathy), MNGIE (mitochondrial neurogastrointestinal encephalopathy), NARP (neuropathy, ataxia, retinitis pigmentosa), Leigh's syndrome and Kearns-Sayre syndrome (KSS) [4,6,9,47], as well as the more recently characterized LBSL (leukoencephalopathy with brainstem and spinal cord involvement and lactate elevation) [39,48] and HBSL (hypomyelination with brainstem and spinal cord involvement and leg spasticity) [44]. The leading symptoms develop due to the progressive pathology in organs with high energy demand, resulting usually in early death. Though the distribution of neuropathological alterations is characteristic of a particular syndrome, all mitochondrial encephalopathies present in various degrees of vacuolation in the white (WM) and grey matter (GM), regional neurodegeneration with reactive astrogliosis and, less generally, capillary proliferation [4,6,9,47].

Recently, mice deficient in the expression of full-length peroxisome proliferator-activated receptor gamma coactivator-1α (PGC-1α) protein (FL-PGC-1α) have been suggested as a morphological model for mitochondrial diseases [43]. PGC-1α is a nuclear-encoded protein that plays important roles in the transcriptional regulation of mitochondrial function at several levels, including mitochondrial biogenesis, glucose and lipid metabolism as well as oxidative stress defence, and its dysfunction has been implicated in the pathogenesis of a number of neurodegenerative diseases both in humans and experimental animals [37,43]. FL-PGC-1α-deficient mice develop liver disease, decreased locomotion and muscle weakness [23], together with a spongiform leukoencephalopathy with wide-spread vacuolation accompanied by reactive astrogliosis in the brainstem and the cerebellar nuclei, resembling the neuropathological alterations seen in KSS [43].

According to the current notion, WM vacuoles in mitochondrial encephalopathies are linked to intramyelin 'oedema' due to preferential mitochondrial dysfunction in oligodendrocytes, presenting as intramyelin 'bubbles' due to splitting of the myelin sheath at the intraperiod line. In contrast, GM neuropil vacuoles are presumed to develop because of the failure of ATP-dependent ion transporters in astrocytic membranes [32,40,46]. While intraperiod line splitting is a common finding in cases with status spongiosus, the mechanism through which focal and circumscribed fluid accumulation develops in an extracellular compartment is only poorly understood. Thus, our knowledge about the origin of intramyelin and neuropil vacuolation remains speculative.

Our first study on FL-PGC-1α-deficient mice indicated that the majority of the observed vacuoles were associated with myelin in the absence of apparent axonal involvement [43]. Based on these observations, we aimed to evaluate the origin and nature of vacuole formation in aged FL-PGC-1α-deficient mice, in comparison with a human case of KSS. Our results emphasize the novel pathogenic role of the oligodendrocytes in the formation of both WM and GM vacuoles. Besides providing a better understanding of tissue lesioning in mitochondrial encephalopathies, our observations may also have implications for WM damage in multiple sclerosis as well as in the aging brain, related pathologies where mitochondrial dysfunction may also play key roles in the pathogenesis.

Material and methods

Patient and animals

Brain tissue of a male KSS patient with a 4.9 kbp common deletion in mtDNA died at 22 years of age was used for neuropathological analysis. The mother gave informed consent prior to the neuropathological work-up. The study was adhered to the tenets of the most recent revision of the Declaration of Helsinki.

For comparison, 70-75-week-old FL-PGC-1α-deficient and age-matched wild-type C57Bl/6J male mice were involved in this study. The animals were housed in cages (maximum 4 per cage) in standard conditions with 12-12 h light-dark cycle and *ad libitum* access to standard pellet food and water. The experiments were performed in accordance with the European Communities Council Directive (86/609/EEC) and were approved by the local Animal Care Committee.

Immunohistochemistry and histology

Formalin-fixed paraffin-embedded blocks of different regions of the KSS brain, including several neocortical areas, basal ganglia, thalamus, hippocampus, amygdala, brainstem and cerebellum, as well as a double hemispheric block at the levels of WM lesions were examined. The murine brains were removed on ice and halved at the midline immediately following decapitation. Half brains were fixed

in 4% paraformaldehyde overnight and kept in 15% glycerol in 4°C until embedding in paraffin. The other halves of the murine brains were used for the frozen sections (i.e. for Oil Red O staining).

3-µm-thick sections were stained with Klüver-Barrera (Luxol and Fast red) and Oil Red O stainings. For immunohistochemistry we applied the following monoclonal antibodies (cross-reacting with mouse): anti-amyloid precursor protein (APP) (1 : 500, Millipore, Billerica, Mass., USA), phosphorylated and non-phosphorylated neurofilaments (clones SMI-31 and SMI-32, markers of axons and neuronal cell bodies; 1 : 5000 and 1 : 200, respectively, Covance, Berkeley, CA, USA), TPPP/p25 (1 : 2000; a marker of mature oligodendrocytes [15]) and microtubule associated protein-2 (MAP-2, marker of neuronal cell bodies and dendrites; Millipore). Furthermore, the following polyclonal antibodies were used: anti-glial fibrillary acidic protein (GFAP; 1 : 3000, Dako, Glostrup, Denmark), MBP (myelin basic protein; 1 : 400, Dako) and Iba1 (1 : 1000, Wako Chemicals, Osaka, Japan). The DAKO EnVision detection kit, peroxidase/DAB, rabbit/mouse (Dako) was used for visualization of antibody reactions. When applying mouse antibodies, we used the M.O.M. kit (Vector Laboratories, Burlingame, Calif., USA) to prevent the aspecific background staining of endogenous mouse immunoglobulins.

Electron microscopy

Human KSS samples from the basal ganglia (internal capsule) and WM lesions were immersion-fixed in 4% glutaraldehyde for 3 days. The animals used for electron microscopy were anaesthetised with isoflurane and were perfused transcardially with modified Hamori fixative (1.5% glutaraldehyde and 1% formaldehyde in phosphate buffer) for 18 min with a 10 ml/min flow, prior to decapitation and subsequent sample preparation.

The obtained central nervous system (CNS) samples were postfixed in 1% osmium tetroxide for 1-2 h, dehydrated through a series of graded ethanols and propylene oxide, and then embedded in Embed 812 resin (Electron Microscopy Sciences, EMS 14120). Semi-thin sections were stained with toluidine blue, blocks trimmed, and ultrathin sections stained with lead citrate and uranyl acetate. Specimens were examined using a JEM-100C transmission electron microscope.

Results

Comparison of lesion profiles

Vacuolation

Klüver-Barrera staining revealed a widespread spongiform change in both the KSS brain and FL-PGC-1α-deficient mice. In both, the vacuolation predominated in the WM; however, vacuoles in the GM neuropil were also observed with apparently lower frequency (Fig. 1A-F). The vacuolation commonly affected the internal capsule, striatal pencil fibres, cerebellar WM, thalamic fascicules, pyramidal tracts and, less intensively, the corpus callosum. Vacuoles were commonly present in the neuropil, most intensively in the brainstem, but also consistently present in the basal ganglia, thalamic nuclei and less intensively in the neocortex, where they showed a predilection toward the deep cortical layers. The severity of vacuolation was more prominent in the KSS brain than in experimental animals; in some regions with coarse cystic-necrotic lesions and myelin pallor, while in some others with demyelinated foci (e.g. postcentral region, cerebellar WM, some of the pencil fibres) (Fig. 1C and F). Demyelination and cystic-necrotic lesions were undetected in FL-PGC-1α-deficient mice. Notably, the examined aged wild-type brains presented vacuoles showing similar appearance and distribution as their FL-PGC-1α-deficient counterparts; however, their frequency was remarkably lower in all examined regions (Fig. 1A-B, D-E).

Astrogliosis

GFAP staining revealed moderate to severe reactive astrogliosis in the brainstem and cerebellum of both the KSS and the FL-PGC-1α-deficient brains (Fig. 1G-I). In the KSS brain, astroglial reaction was observed in the tectal midbrain, the area of the inferior olive in the medulla oblongata, the dentate nucleus of the cerebellum and the Purkinje cell layer (Bergmann gliosis). In the FL-PGC-1α-deficient mice, severe reaction was present in the medulla oblongata and the pons often in a confluent pattern involving large areas without being limited to certain groups of nuclei, whereas mild reaction with patchy astrocytosis was observed in the midbrain and in the deep cerebellar nuclei. Notably, the caudate-putamen of PGC-1α-deficient mice were free of astroglial reaction even at this age (Fig. 2), supporting our prior observations [43].

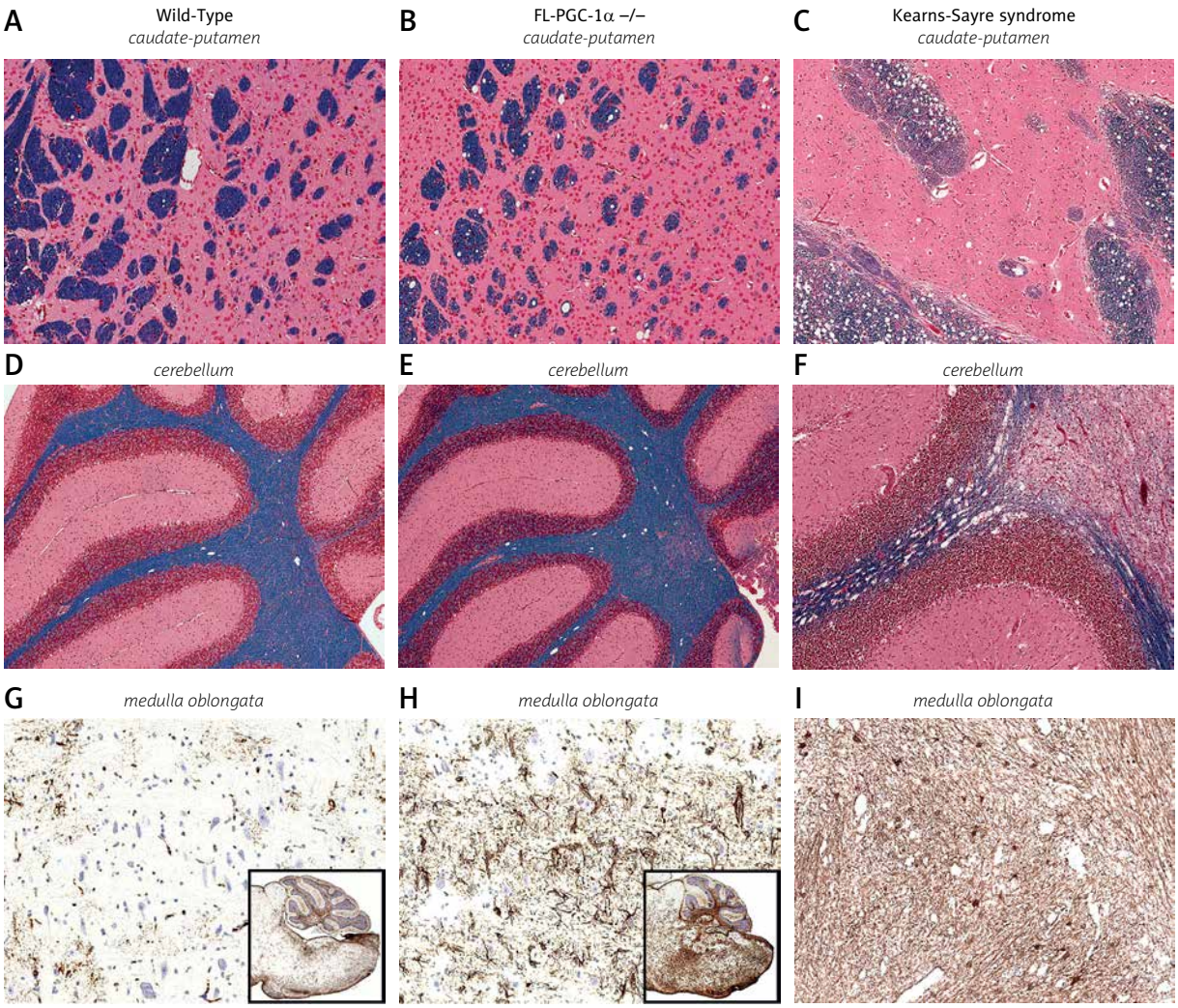

Fig. 1. Vacuolation and astroglial reaction. Aged FL-PGC-1α-deficient mice develop moderate to severe vacuolation (**B** and **E**) in areas corresponding to severe to devastating vacuolation in KSS (**C** and **F**) and mild vacuolation in aged wild-type mice (**A** and **D**; Klüver-Barrera). Vacuoles are in association with WM structures. Note the patchy areas of myelin pallor in the pencil fibres of the caudate-putamen (**C**) and the demyelinated cystic-necrotic lesion in the cerebellar WM in KSS (**F**). Reactive astrogliosis indicative of neuronal degeneration is present in the brainstem of FL-PGC-1α-deficient mice and the KSS case (**H** and **I**; GFAP).

Axonal pathology

The intensity of axonal destruction in the KSS brain was variable and generally followed that of the vacuolar change. Only the severely affected cystic-necrotic lesions showed axonal loss or swelling, whereas most of the moderately vacuolated areas were devoid of axonal pathology (Fig. 3C), except for scattered swellings and APP-positive spheroids indicating acute-subacute impairment of axonal transport (Fig. 3F). Regions with severe axonal involvement were accompanied by reactive microgliosis (Fig. 3I). The axons in the FL-PGC-1α-deficient mice were generally well preserved, and the patterns of APP, neurofilament and microglia stainings were similar to that observed in wild-type (Fig. 3A-B, D-E and G-H).

Characterization of vacuoles

White matter vacuoles

Vacuoles within the WM were surrounded by rings of MBP-positive myelin in both the KSS and FL-PGC-1α-deficient brains (Fig. 4A). The vacuoles

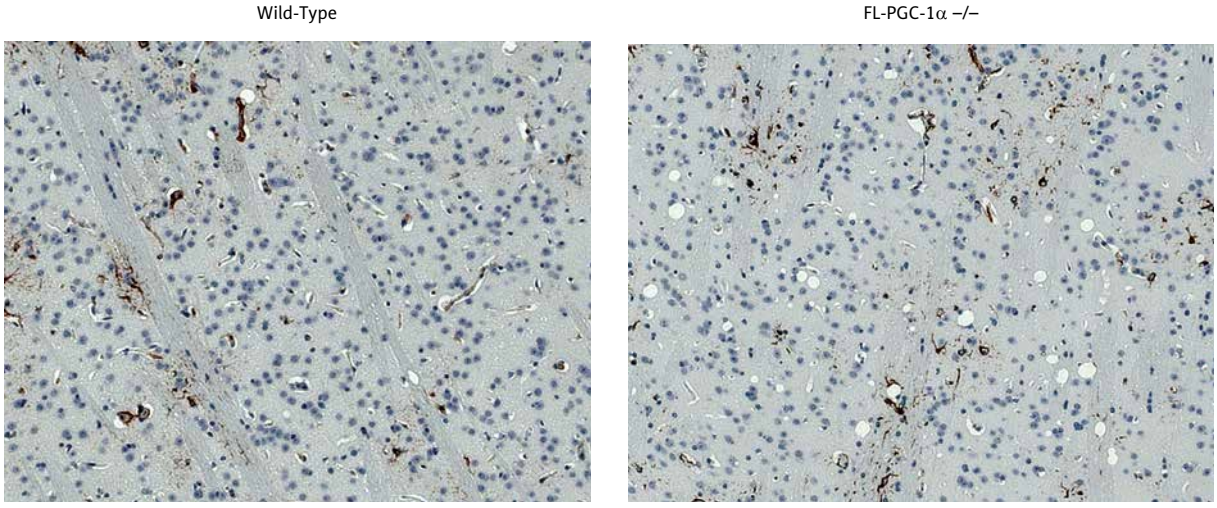

Fig. 2. The caudate-putamen of FL-PGC-1α-deficient mice is free of reactive astrogliosis (GFAP) – an indicator of chronic neuronal degeneration – even in this aged population, suggesting that this murine strain is not a model for Huntington's disease, as it was previously suggested.

were usually ovoid with their longitudinal axis paralleling the direction of axons. They often formed chain-like structures in longitudinal or sieve-like lesions in transverse sections. No apparent macrophage activity was present even in the areas of severe vacuolation, and no signs of active myelin degradation could be detected by Oil Red O (not shown). Electron microscopy revealed that myelin 'bubbles' in the WM were formed by splitting at the intraperiod lines, and occasionally between the axons and the innermost myelin lamellae (adaxonal vacuoles); the vacuoles were 'empty' or contained various amount of debris with myelin-like figures (Fig. 5A-B, Fig. 6).

Neuropil vacuoles

Staining for neuronal (MAP-2 and SMI-32) or astrocytic (GFAP) antigens sparsely revealed associations of neuropil vacuoles with these cell-types in either the KSS or the FL-PGC-1α-deficient brains (Fig. 7). Staining for MBP, however, unveiled that the vast majority of neuropil vacuoles were clearly encompassed by a myelin-positive rim, suggesting the same intramyelinic localization as for vacuoles within the WM (Fig. 4B). Neuropil vacuoles were also frequently associated with oligodendrocytes in sections immunostained for TPPP/p25 (Fig. 4C). Such close contacts of oligodendrocytes and vacuoles were also observed by electron microscopy. Furthermore, vacuoles (sometimes multiloculated) could frequently be identified within the cytoplasm of glial cells, which, due to the lack of glial fibres observed in the cytoplasm, also appeared to be oligodendrocytic (Fig. 5C). Likewise myelin 'bubbles', these membrane-bound vacuoles often contained myelin-like figures, and they occasionally coalesced occupying most of the oligodendroglial cytoplasm and lead to the swelling of the cells (Fig. 5C). These observations were seen in both the KSS and the FL-PGC-1α-deficient brains.

Discussion

In addition to its central role in mitochondrial encephalopathies, mitochondrial dysfunction has been associated with various neurodegenerative CNS disorders [17], and is supposed to play important roles in the pathogenesis of WM lesioning in multiple sclerosis (MS) [7] as well in the aging brain [38]. Though the exact mechanism of vacuole formation in mitochondrial encephalopathies is not yet revealed, intramyelin WM vacuoles are presumed to develop due to intramyelin oedema secondary to mitochondrial dysfunction of oligodendrocytes, manifesting in splitting of the myelin sheath at the intraperiod line [32,40,46]. On the other hand, GM neuropil vacuoles are presumed to develop due to ion transport disorder of astrocytic membranes [32,40,46].

Revisiting the above concepts of vacuole formation in conditions associated with mitochondrial

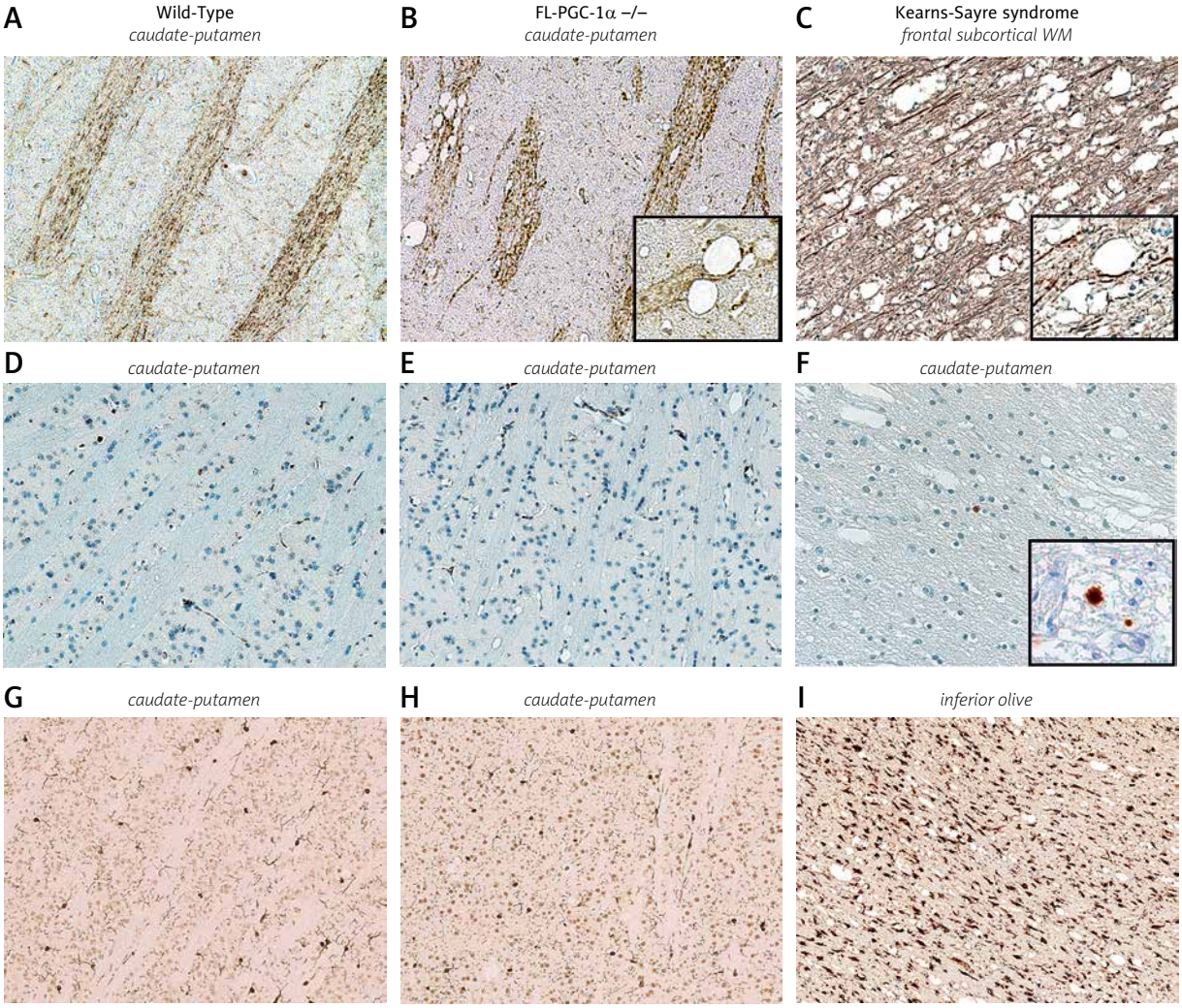

Fig. 3. Axonal pathology. Axons in areas with moderate vacuolation in KSS were relatively intact with sparse presence of axonal swellings (**C**; SMI-31). Such areas also showed scattered appearence of APP+ axonal spheroids indicative of subacute axonal transport impairment in KSS (**F**; APP). Regions with cystic-necrotic lesions showed robust microglia accumulation in KSS (**I**; Iba). These pathologies were virtually absent in the FL-PGC-1α-deficient mice and the immunohistochemical patterns were rather similar to that in aged wild-types (**A-B**, **D-E** and **G-H**). Note the well-preserved axons dodging between multiple vacuoles (**B**), similarly to that seen in KSS (**C**).

dysfunction, our study provided two main novelties. A major finding of our study is that it demonstrates commonalities of vacuolation in the WM and GM, placing oligodendrocytes in the centre of disease pathogenesis. Indeed, our observation that the vast majority of GM neuropil vacuoles are clearly myelin-bound in both the KSS and FL-PGC-1α-deficient brains indicates that the cellular localization and thus the mechanism of vacuole-formation is most likely similar, irrespective of whether they are in WM or GM. This observation can explain the phenomenon widely observed in mitochondrial encephalopathies – including PGC-1α-deficient mice – that cortical vacuoles show a predilection toward the deeper layers of the neocortex, as the density of myelinated fibres apparently gradually decreases by approaching the superficial layers. Importantly, this could also explain the predilection of GM neuropil vacuoles toward the reticular area of the brainstem, thalamus, deep cerebellar nuclei, and basal ganglia adjacent to the internal capsule, as these GM regions are intermingled with the WM. Interestingly, these regions are

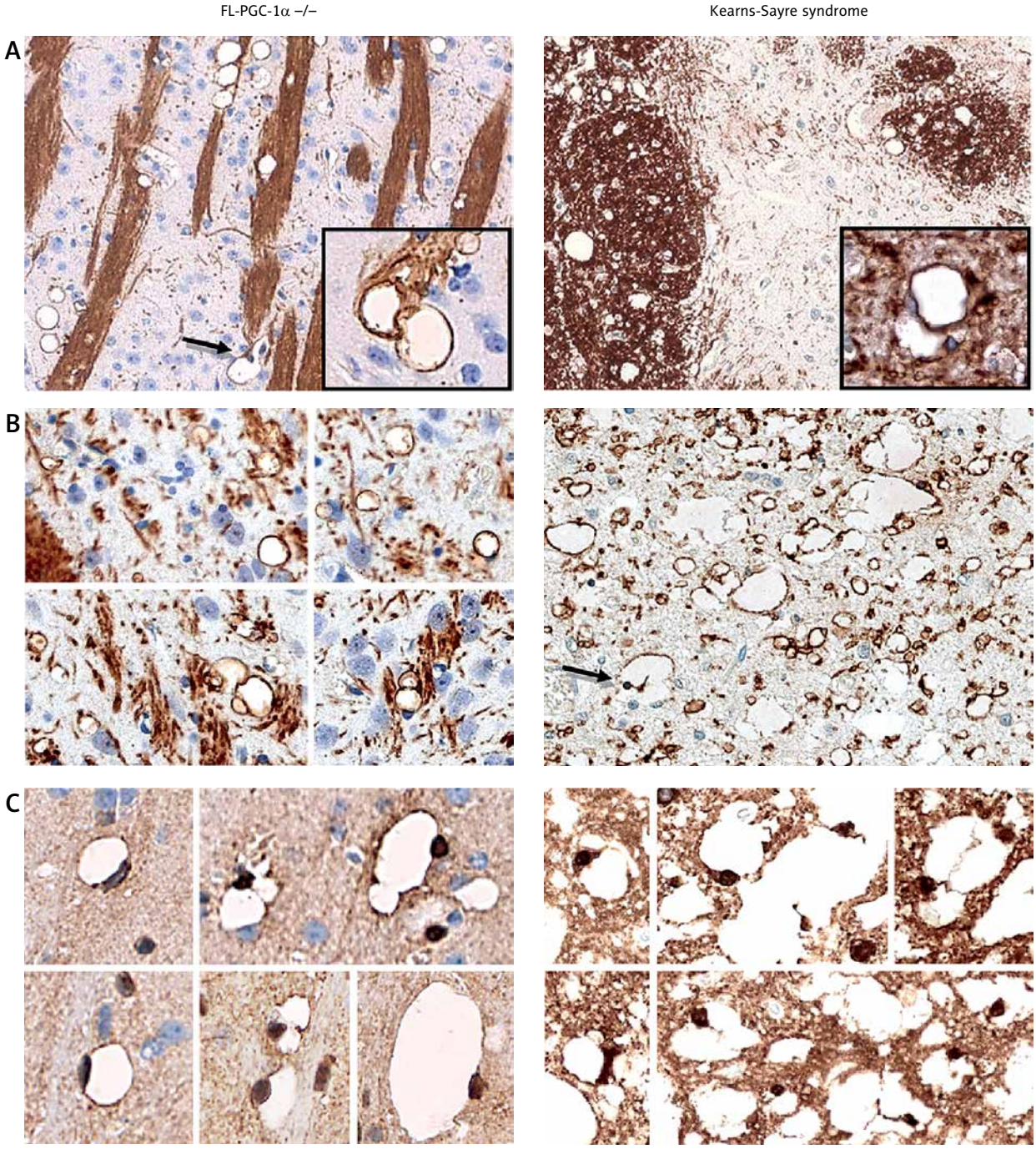

Fig. 4. Immunohistochemical characterization of vacuoles. Vacuoles within the WM are surrounded by rings of myelin (**A**; MBP). Likewise WM myelin 'bubbles', vacuoles within the GM neuropil are also encompassed by a myelin-positive rim, suggesting an identical origin (**B**; MBP). Oligodendroglial cells in close contact with and/or localized within the inner edge of either single or multiloculated vacuoles can frequently be detected by immunohistochemistry (**C**; TPPP/p25), suggesting an important role of oligodendrocytes in vacuole formation. Note some of the larger vacuoles being separated to multiple chambers by oligodendroglial processes (**C**). Note also the glial cell encompassing a vacuole with its MBP+ process (indicated by arrows, **A** – left, **B** – right).

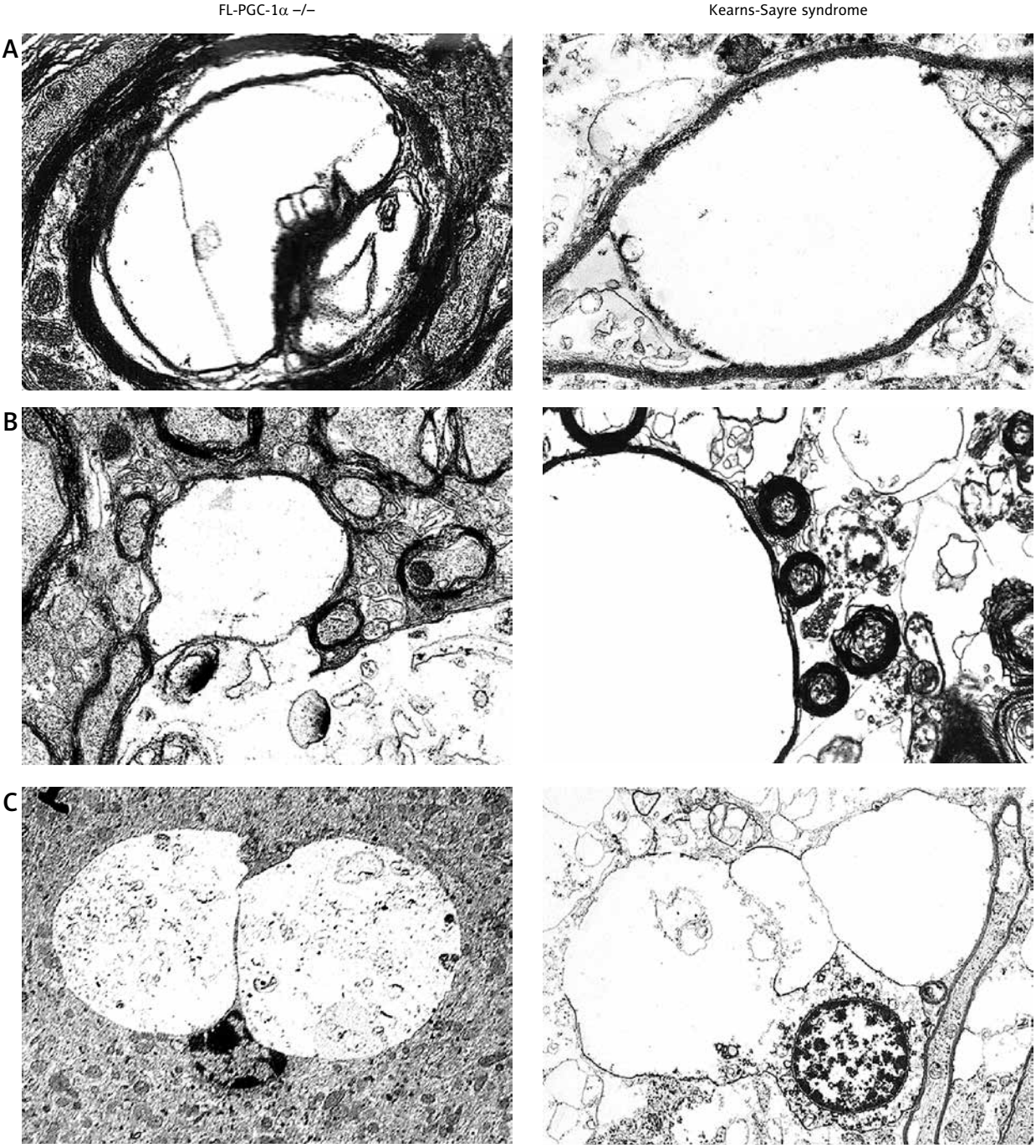

Fig. 5. Ultrastructural characterization of vacuoles. Intramyelin vacuolation can be identified also by electron microscopy (longitudinal section, **A**; transverse section, **B**). In accordance with immunohistochemical findings, vacuoles, often multiloculated, can frequently be identified within the cytoplasm of oligodendroglial cells by electron microscopy (**C**).

the predilection areas for the development of GM vacuolation in hepatic encephalopathy as well [52]. Considering this overlapping predilection of spongy change between hepatic and mitochondrial encephalopathies, and that mitochondrial disorders, including PGC-1α deficiency [23], also present with hepatic involvement, the contribution of liver insufficiency to the development of mitochondrial status spongio-

sus cannot be excluded either. Notably, intramyelin vacuolation has been frequently described in other experimental, veterinary and human metabolic conditions (Table I), suggesting that this change might be a general response to various insults that compromise the metabolism of the myelin sheath and/or oligodendrocytes.

As a second novelty, the ultrastructural analysis revealed the common appearance of intracellular, often multiloculated formation of vacuoles within oligodendroglial cells both in the KSS case and the FL-PGC-1α-deficient mice. This finding was supported by the immunohistochemical observation of TPPP/p25-positive oligodendrocytes directly attaching to and sometimes bulging into vacuoles within the neuropil. The finding, however, that some vacuoles were observed closely attached to and partly encompassed by neuronal structures in MAP-2 and SMI-32 stainings suggests that at least a small proportion of vacuoles within the neuropil can be of neuronal origin, and that the mechanisms which lead to excessive intracellular membrane-bound fluid accumulation may affect different cell-types within the CNS, though to different extents. This hypothesis is supported by the report on CNS vacuoles observed also in neuron-specific PGC-1α knockout mice [25].

Interestingly, though intracellular oligodendroglial vacuoles have not been previously described in mitochondrial diseases, their presence is not unprecedented in pathologies associated with mitochondrial dysfunction and/or severe cellular stress. Indeed, chronic feeding of mice with cuprizone, a copper-chelating mitochondrial toxin associated with megamitochondria [41] and alterations in complex IV and superoxide dismutase (SOD) activity [1], evokes a CNS pathology comprising vacuole formation in the pons, midbrain, thalamus, cerebral and cerebellar WM, as well as in deep cortical layers [42]. It was described that cuprizone-induced intramyelin vacuolation was due to splitting at the intraperiod line and were not stained by Sudan IV (equivalent with Oil Red O in our study) [42]. Additionally, the authors reported the presence of oligodendrocytes with enlarged cytoplasm containing multiloculated vesicles, and that some of these cells were juxtaposed to myelin sheaths, where a thin myelin layer appeared to form the glial membrane [42]. These findings are strikingly similar to those observed in our study. A further similarity between cuprizone-induced and mitochondrial status spongiosus is that cuprizone toxicity in doses evoking demyelination associates with oligodendroglial apoptosis [1], a phenomenon recently described in KSS [22]. Our observation of intra-oligodendroglial vacuolation in mitochondrial encephalopathy expands the spectrum of disorders where this has been described (Table II).

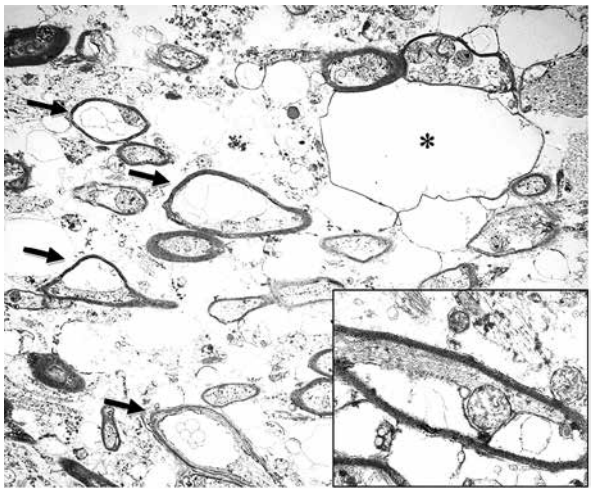

Fig. 6. Distinct types of intramyelin vacuoles in Kearns-Sayre syndrome (KSS). Asterisk denotes a huge 'classical' intramyelin vacuole originating from splitting at the intraperiod line. Arrows indicate the multiple presence of adaxonal vacuoles, some of which appear to originate from splitting between the two innermost myelin lamellae at higher power. The frequent appearance of adaxonal vacuoles may underpin the role of intra-oligodendroglial vacuolar change in the development of intramyelin vacuoles in mitochondrial encephalopathies such as KSS.

Though the neuropathological alterations in MS are results of a complex aetiology including autoimmunity, demyelination, neuronal and axonal degeneration, the central role of oligodendrocytes has also been suggested [15], which gives our observations a wider implication. The interrelation between mitochondrial leukoencephalopathies and MS is well exemplified by the fact that the above mentioned cuprizone intoxication, presenting with a highly similar neuropathology to that observed in KSS and FL-PGC-1α-deficient mice in our study, is in fact a widely applied toxin model of MS [1,27]. It has also been suggested that though a moderate mitochondrial dysfunction alone may not cause selective demyelination directly, its effect to evoke a disintegrated myelin structure may expose the sheath to

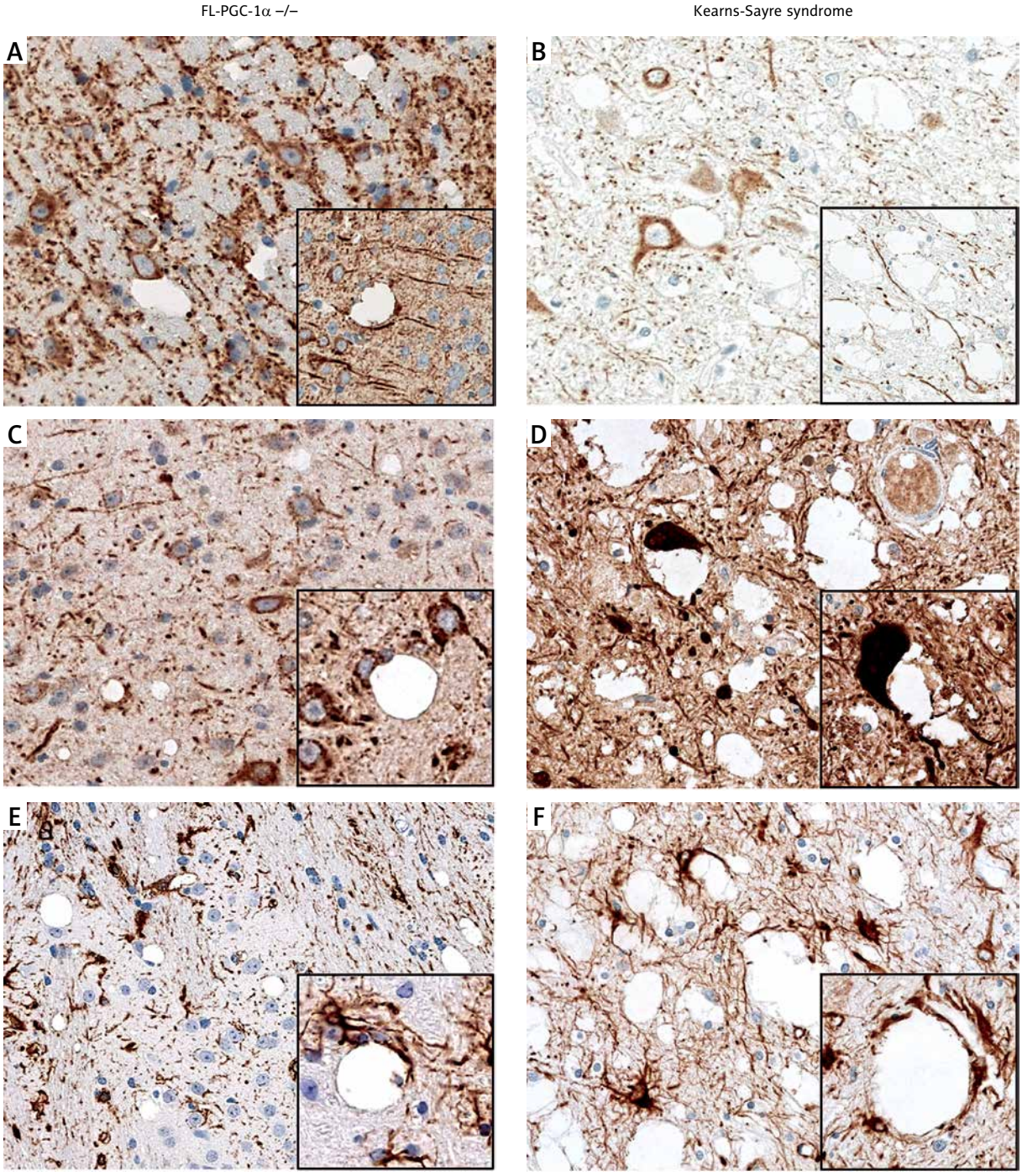

Fig. 7. Rare findings of vacuoles being in close contact with structures positive for staining against neuronal (**A-B**, MAP-2; **C-D**, SMI-32) or astroglial (**E-F**, GFAP) antigens. Notably, the vast majority of GM neuropil vacuoles have no immunohistochemically detectable associations with such structures, which are often merely pushed by vacuoles of most probably distinct origin.

further damage, e.g. by complex immune-mediated mechanisms [20]. Indeed, mtDNA mutations have been proposed to affect the CNS on a common metabolic basis, which may occasionally aggravate or initiate autoimmune pathology leading to MS-like lesions [20].

Besides demyelinating WM disease, our study also has implications for understanding WM lesions

Table I. Animal and human pathologies with intramyelin vacuolation

Experimental pathologies	Reference
Intoxication by	
actinomycin D	[36]
copper	[16]
cuprizone	[33], [42]
ethidium bromide	[50]
hexachlorophene	[18]
isonicotinic acid hydrazide	[21]
lysolecithin	[5]
triethyltin	[2]
Genetic models of	
mitochondrial dysfunction	reviewed in [43]
altered proteolipid expression	[3]
Models of scrapie	[24], [33]
Veterinary pathologies of various aetiology	
Helichrysum poisoning in sheep and a goat	[49]
Tetrapterys poisoning in sheep	[35]
Maple syrup urine disease in calves	[31]
Hereditary spongy degeneration of dogs	[29], [53]
Hereditary spongy degeneration of silver foxes	[13]
Human pathologies	
Aging	reviewed in [34]
Aspartoacylase deficiency (Canavan's disease)	reviewed in [12]
Hepatic encephalopathy	reviewed in [12]
Heroin-induced spongiform leukoencephalopathy	[51]
Maple syrup urine disease	reviewed in [12]
Mitochondrial disorders	reviewed in [12]
Urea cycle disorders	reviewed in [12]

Table II. Experimental and veterinary pathologies with oligodendroglial vacuolation

Experimental pathologies	Reference
Cuprizone intoxication	[42]
Ionizing radiation	[26]
Methionine sulfoximine intoxication	[14]
Triethyltin intoxication in quaking mice	[28]
Twitcher mouse	[45]
Zitter rat	[19]
Veterinary pathologies	
Hereditary ataxia of the rabbit	[30]
Hereditary spongy degeneration of silver foxes	[13]

in the aging brain, a frequent pathology which includes the formation of intramyelin 'balloons' due to intraperiod line splitting [34], similar to that seen in mitochondrial disorders. Our observation that aged wild-type mice also develop vacuoles to an apparently slighter extent but at the same predilection areas as their FL-PGC-1α-deficient counterparts recapitulates previous observations [10]. Based on these, we propose that vacuole formation in mitochondrial encephalopathies and their representative animal models (e.g. PGC-1α-deficient mice) might also be regarded as an accelerated form of 'normal' WM degeneration, which underpins the role of (oligodendroglial) mitochondrial dysfunction in aging.

Although the potential role of oligodendrocytes in WM vacuolation in mitochondrial encephalopathies has already been suggested, the fundamental concepts included (1) a disrupted ion-homeostasis of the sheath, (2) a dysfunction of the blood-brain barrier, in both cases with consequent development of 'intramyelin oedema' [32,40,46]. These hypotheses, however, do not explain why vacuoles develop focally and how multiple vacuoles can be found within the same internode, instead of a complete splitting and diffuse loosening of the sheath between all lamellae. We propose that chronic mitochondrial dysfunction in a yet unknown pathway leads to the formation of multiple intra-oligodendroglial fluid-filled vacuoles. Increased intracellular content might provoke splitting between the intracellular surfaces of the myelin sheath (major dense line). Due to their firm connections at the macromolecular level, this would cause tears and focal myelin disruptions, allowing the vacuolar content to access into the virtual space between the loosely attached extracellular surfaces (intraperiod lines). Consequently, this could evoke the formation of focal splits and eventually myelin bubbles. Accordingly, disruption of the lateral loops would result in intraperiod line splitting at the corresponding levels, whereas leakage from the inner tongue would cause adaxonal swelling between the axolemma and the innermost myelin lamellae or between the two innermost layers. Supporting

this theoretical consideration, such distinct types of intramyelin vacuoles have indeed been described in experimental status spongiosus [36,50], and could also be observed in our study (Fig. 6).

Conclusions

In addition to a detailed comparative neuropathological characterization of a recently proposed murine model of mitochondrial encephalopathy and human KSS, this study first provides morphological evidence for the identical intramyelinic nature of WM and GM vacuolation as well as for the presence of intra-oligodendroglial vacuoles in mitochondrial disease, which may have a pathogenetic role in the development of intramyelin vacuoles, providing a possible source of focal myelin splitting. Our observations place oligodendrocytes in the centre of the pathogenesis of CNS lesioning in association with chronic mitochondrial dysfunction both in WM and GM, which is in line with the recognition that oligodendrocytes, contrasting astrocytes [11], are most sensitive to mitochondrial stress, exceeding the vulnerability of neurons [8]. This may serve as rationale for cytoprotective targeting of the oligodendrocytes in mitochondrial encephalopathies as well as in other disorders with vacuole formation and myelin degeneration.

Acknowledgements

The study was supported by the Hungarian Brain Research Program – Grant No. KTIA_13_NAP-A-II/18., the European Union and the State of Hungary, co-financed by the European Social Fund in the framework of TÁMOP 4.2.4. A/2-11-1-2012-0001 'National Excellence Program', TÁMOP-4.2.2/B-10/1-2010-0012, and TÁMOP-4.2.2.A-11/1/KONV-2012-0052. P.P.L. is supported by OEAD and Healthy Ageing Research Centre project (REGPOT-2012-2013-1, 7FP). P.P.L. and G.G.K. are supported by ÖAD Austria-Poland (PL 04/2014). We are grateful to Agnes Herczegfalvi, Albert C. Ludolph and Patrick Weydt for their valuable contribution.

Disclosure

Authors report no conflict of interest.

References

1. Acs P, Selak MA, Komoly S, Kalman B. Distribution of oligodendrocyte loss and mitochondrial toxicity in the cuprizone-induced experimental demyelination model. J Neuroimmunol 2013; 262: 128-131.
2. Aleu FP, Katzman R, Terry RD. Fine structure and electrolyte analyses of cerebral edema induced by alkyl tin intoxication. J Neuropathol Exp Neurol 1963; 22: 403-413.
3. Anderson TJ, Schneider A, Barrie JA, Klugmann M, McCulloch MC, Kirkham D, Kyriakides E, Nave KA, Griffiths IR. Late-onset neurodegeneration in mice with increased dosage of the proteolipid protein gene. J Comp Neurol 1998; 394: 506-519.
4. Betts J, Lightowlers RN, Turnbull DM. Neuropathological aspects of mitochondrial DNA disease. Neurochem Res 2004; 29: 505-511.
5. Blakemore WF. Observations on remyelination in the rabbit spinal cord following demyelination induced by lysolecithin. Neuropathol Appl Neurobiol 1978; 4: 47-59.
6. Brown GK, Squier MV. Neuropathology and pathogenesis of mitochondrial diseases. J Inherit Metab Dis 1996; 19: 553-572.
7. Campbell GR, Worrall JT, Mahad DJ. The central role of mitochondria in axonal degeneration in multiple sclerosis. Mult Scler 2014; 20: 1806-1813.
8. Dewar D, Underhill SM, Goldberg MP. Oligodendrocytes and ischemic brain injury. J Cereb Blood Flow Metab 2003; 23: 263-274.
9. Filosto M, Tomelleri G, Tonin P, Scarpelli M, Vattemi G, Rizzuto N, Padovani A, Simonati A. Neuropathology of mitochondrial diseases. Biosci Rep 2007; 27: 23-30.
10. Fraser H. Neuropathology of scrapie: the precision of the lesions and their significance. In: Prusiner SB, Hadlow WJ (eds.). Slow Transmittible Diseases of the Nervous System. Academic Press, New York 1979; pp. 397-406.
11. Goldberg MP, Choi DW. Combined oxygen and glucose deprivation in cortical cell culture: calcium-dependent and calcium-independent mechanisms of neuronal injury. J Neurosci 1993; 13: 3510-3524.
12. Greenfield JG, Love S, Louis DN, Ellison D. Greenfield's neuropathology. 8th ed. Hodder Arnold, London 2008.
13. Hagen G, Blakemore WF, Bjerkås I. Ultrastructural findings in spongy degeneration of white matter in silver foxes (Vulpes vulpes). A naturally occurring demyelinating disease with oligodendrocyte vacuolation. Acta Neuropathol 1990; 80: 590-596.
14. Harris B. Cortical alterations due to methionine sulfoximine. Ultrastructure during seizure activity. Arch Neurol 1964; 11: 388-407.
15. Höftberger R, Fink S, Aboul-Enein F, Botond G, Olah J, Berki T, Ovadi J, Lassmann H, Budka H, Kovacs GG. Tubulin polymerization promoting protein (TPPP/p25) as a marker for oligodendroglial changes in multiple sclerosis. Glia 2010; 58: 1847-1857.
16. Howell JM, Blakemore WF, Gopinath C, Hall GA, Parker JH. Chronic copper poisoning and changes in the central nervous system of sheep. Acta Neuropathol 1974; 29: 9-24.
17. Johri A, Beal MF. Mitochondrial dysfunction in neurodegenerative diseases. J Pharmacol Exp Ther 2012; 342: 619-630.
18. Kanno T, Sasaki S, Yamada N, Kawasako K, Tsuchitani M. Hexachlorophene and cuprizone induce the spongy change of the developing rat brain by different mechanisms: the role of 2', 3'-cyclic

nucleotide 3'-phosphodiesterase (CNPase). J Vet Med Sci 2012; 74: 837-843.
19. Kondo A, Sendoh S, Miyata K, Takamatsu J. Spongy degeneration in the zitter rat: ultrastructural and immunohistochemical studies. J Neurocytol 1995; 24: 533-544.
20. Kovács GG, Höftberger R, Majtényi K, Horváth R, Barsi P, Komoly S, Lassmann H, Budka H, Jakab G. Neuropathology of white matter disease in Leber's hereditary optic neuropathy. Brain 2005; 128: 35-41.
21. Lampert PW, Schochet SS. Electron microscopic observations on experimental spongy degeneration of the cerebellar white matter. J Neuropathol Exp Neurol 1968; 27: 210-220.
22. Lax NZ, Campbell GR, Reeve AK, Ohno N, Zambonin J, Blakely EL, Taylor RW, Bonilla E, Tanji K, DiMauro S, Jaros E, Lassmann H, Turnbull DM, Mahad DJ. Loss of myelin-associated glycoprotein in kearns-sayre syndrome. Arch Neurol 2012; 69: 490-499.
23. Leone TC, Lehman JJ, Finck BN, Schaeffer PJ, Wende AR, Boudina S, Courtois M, Wozniak DF, Sambandam N, Bernal-Mizrachi C, Chen Z, Holloszy JO, Medeiros DM, Schmidt RE, Saffitz JE, Abel ED, Semenkovich CF, Kelly DP. PGC-1alpha deficiency causes multi-system energy metabolic derangements: muscle dysfunction, abnormal weight control and hepatic steatosis. PLoS Biol 2005; 3: e101.
24. Liberski PP, Yanagihara R, Wells GA, Gibbs CJ Jr, Gajdusek DC. Ultrastructural pathology of axons and myelin in experimental scrapie in hamsters and bovine spongiform encephalopathy in cattle and a comparison with the panencephalopathic type of Creutzfeldt-Jakob disease. J Comp Pathol 1992; 106: 383-398.
25. Ma D, Li S, Lucas EK, Cowell RM, Lin JD. Neuronal inactivation of peroxisome proliferator-activated receptor gamma coactivator 1alpha (PGC-1alpha) protects mice from diet-induced obesity and leads to degenerative lesions. J Biol Chem 2010; 285: 39087-39095.
26. Maxwell DS, Kruger L. The reactive oligodendrocyte. An electron microscopic study of cerebral cortex following alpha particle irradiation. Am J Anat 1966; 118: 437-459.
27. Miron VE, Kuhlmann T, Antel JP. Cells of the oligodendroglial lineage, myelination, and remyelination. Biochim Biophys Acta 2011; 1812: 184-193.
28. Nagara H, Suzuki K, Tiffany CW, Suzuki K. Triethyl tin does not induce intramyelinic vacuoles in the cns of the quaking mouse. Brain Res 1981; 225: 413-420.
29. Neer TM, Kornegay JN. Leucoencephalomalacia and cerebral white matter vacuolar degeneration in two related Labrador retriever puppies. J Vet Intern Med 1995; 9: 100-104.
30. O'Leary JL, Harris AB, Fox RR, Smith JM, Tidwell M. Ultrastructural lesions in rabbit hereditary ataxia. Arch Neurol 1965; 13: 238-262.
31. O'Toole D, Montgomery DL, Steadman L, O'Rourke B, Russell W, Dennis J. Status spongiosus of white matter in newborn Gelbvieh-cross calves. J Vet Diagn Invest 2005; 17: 546-553.
32. Oldfors A, Fyhr IM, Holme E, Larsson NG, Tulinius M. Neuropathology in Kearns-Sayre syndrome. Acta Neuropathol 1990; 80: 541-546.
33. Pattison IH, Jebbett JN. Histopathological similarities between scrapie and cuprizone toxicity in mice. Nature 1971; 230: 115-117.
34. Peters A. The effects of normal aging on myelin and nerve fibers: a review. J Neurocytol 2002; 31: 581-593.
35. Riet-Correa G, Riet-Correa F, Schild AL, Barros SS, Soares MP. Abortion and neonatal mortality in sheep poisoned with Tetrapterys multiglandulosa. Vet Pathol 2009; 46: 960-965.
36. Rizzuto N, Gambetti PL. Status spongiosus of rat central nervous system induced by actinomycin D. Acta Neuropathol 1976; 36: 21-30.
37. Róna-Vörös K, Weydt P. The role of PGC-1alpha in the pathogenesis of neurodegenerative disorders. Curr Drug Targets 2010; 11: 1262-1269.
38. Santos RX, Correia SC, Zhu X, Smith MA, Moreira PI, Castellani RJ, Nunomura A, Perry G. Mitochondrial DNA oxidative damage and repair in aging and Alzheimer's disease. Antioxid Redox Signal 2013; 18: 2444-2457.
39. Scheper GC, van der Klok T, van Andel RJ, van Berkel CG, Sissler M, Smet J, Muravina TI, Serkov SV, Uziel G, Bugiani M, Schiffmann R, Krägeloh-Mann I, Smeitink JA, Florentz C, Van Coster R, Pronk JC, van der Knaap MS. Mitochondrial aspartyl-tRNA synthetase deficiency causes leukoencephalopathy with brain stem and spinal cord involvement and lactate elevation. Nat Genet 2007; 39: 534-539.
40. Sparaco M, Bonilla E, DiMauro S, Powers JM. Neuropathology of mitochondrial encephalomyopathies due to mitochondrial DNA defects. J Neuropathol Exp Neurol 1993; 52: 1-10.
41. Suzuki K. Giant hepatic mitochondria: production in mice fed with cuprizone. Science 1969; 163: 81-82.
42. Suzuki K, Kikkawa Y. Status spongiosus of CNS and hepatic changes induced by cuprizone (biscyclohexanone oxalyldihydrazone). Am J Pathol 1969; 54: 307-325.
43. Szalardy L, Zadori D, Plangar I, Vecsei L, Weydt P, Ludolph AC, Klivenyi P, Kovacs GG. Neuropathology of partial PGC-1alpha deficiency recapitulates features of mitochondrial encephalopathies but not of neurodegenerative diseases. Neurodegener Dis 2013; 12: 177-188.
44. Taft RJ, Vanderver A, Leventer RJ, Damiani SA, Simons C, Grimmond SM, Miller D, Schmidt J, Lockhart PJ, Pope K, Ru K, Crawford J, Rosser T, de Coo IF, Juneja M, Verma IC, Prabhakar P, Blaser S, Raiman J, Pouwels PJ, Bevova MR, Abbink TE, van der Knaap MS, Wolf NI. Mutations in DARS cause hypomyelination with brain stem and spinal cord involvement and leg spasticity. Am J Hum Genet 2013; 92: 774-780.
45. Takahashi H, Igisu H, Suzuki K, Suzuki K. The twitcher mouse: an ultrastructural study on the oligodendroglia. Acta Neuropathol 1983; 59: 159-166.
46. Tanji K, DiMauro S, Bonilla E. Disconnection of cerebellar Purkinje cells in Kearns-Sayre syndrome. J Neurol Sci 1999; 166: 64-70.
47. Tanji K, Kunimatsu T, Vu TH, Bonilla E. Neuropathological features of mitochondrial disorders. Semin Cell Dev Biol 2001; 12: 429-439.
48. van der Knaap MS, van der Voorn P, Barkhof F, Van Coster R, Krägeloh-Mann I, Feigenbaum A, Blaser S, Vles JS, Rieckmann P, Pouwels PJ. A new leukoencephalopathy with brainstem and spinal cord involvement and high lactate. Ann Neurol 2003; 53: 252-258.
49. van der Lugt JJ, Olivier J, Jordaan P. Status spongiosis, optic neuropathy, and retinal degeneration in Helichrysum argyro-

sphaerum poisoning in sheep and a goat. Vet Pathol 1996; 33: 495-502.
50. Yajima K, Suzuki K. Ultrastructural changes of oligodendroglia and myelin sheaths induced by ethidium bromide. Neuropathol Appl Neurobiol 1979; 5: 49-62.
51. Yin R, Lu C, Chen Q, Fan J, Lu J. Microvascular damage is involved in the pathogenesis of heroin induced spongiform leukoencephalopathy. Int J Med Sci 2013; 10: 299-306.
52. Zachary JF, McGavin MD. Pathologic Basis of Veterinary Disease. 5th ed. Elsevier Health Sciences Mosby, St Louis 2011.
53. Zachary JF, O'Brien DP. Spongy degeneration of the central nervous system in two canine littermates. Vet Pathol 1985; 22: 561-571.

Original article

Folia Neuropathologica

Identification of a novel inherited *ALK* variant M1199L in the WNT type of medulloblastoma

Joanna Trubicka[1], Małgorzata Szperl[2], Wiesława Grajkowska[3], Agnieszka Karkucińska-Więckowska[4], Magdalena Tarasińska[5], Katarzyna Falana[1], Bożenna Dembowska-Bagińska[5], Maria Łastowska[3,4]

[1]Department of Medical Genetics, The Children's Memorial Health Institute, Warsaw, [2]Molecular Biology Laboratory, The Cardinal Stefan Wyszyński Institute of Cardiology, Warsaw, [3]Department of Experimental and Clinical Neuropathology, Mossakowski Medical Research, Centre Polish Academy of Sciences, Warsaw, [4]Department of Pathology, The Children's Memorial Health Institute, Warsaw, [5]Clinic of Oncology, The Children's Memorial Health Institute, Warsaw, Poland

Folia Neuropathol 2016; 54 (1): 23-30 DOI: 10.5114/fn.2016.58912

Abstract

Rearrangements involving the ALK gene were identified in a variety of cancers, including paediatric tumour neuroblastoma where presence of ALK expression is also associated with adverse prognosis. Microarrays data indicate that ALK is expressed in another paediatric tumour – medulloblastoma. Therefore, we investigated if the ALK gene is mutated in medulloblastoma and performed simultaneously the molecular profiling of tumours.

Tumours from sixty-four medulloblastoma patients were studied for detection of ALK alterations in exons 23 and 25 using Sanger method. The molecular subtypes of tumours were identified by detection of mutations in the CTNNB1 gene, monosomy 6 and by immunohistochemistry using a panel of representative antibodies.

Among three ALK variants detected two resulted in intron variants (rs3738867, rs113866835) and the third one was a novel heterozygous variant c.3595A>T in exon 23 identified in the WNT type of tumour. It resulted in methionine to leucine substitution at codon position 1199 (M1199L) of the kinase domain of ALK protein. Results of analysis using three in silico algorithms confirmed the pathogenicity of this single nucleotide variation. The same gene alteration was detected in both patient and maternal peripheral blood leukocytes indicating an inherited type of the detected variant. Presence of ALK expression in tumour tissue was confirmed by immunohistochemistry. The tumour was diagnosed as classic medulloblastoma, however with visible areas of focal anaplastic features. The patient has been disease free for 6 years since diagnosis.

This is the first evidence of an inherited ALK variant in the WNT type of medulloblastoma, what altogether with presence of ALK expression may point towards involvement of the ALK gene in this type of tumours.

Key words: *medulloblastoma, ALK gene, WNT type.*

Communicating author

Maria Łastowska, Department of Pathology, The Children's Memorial Health Institute, Al. Dzieci Polskich 20, 04-730 Warsaw, Poland, phone: +48 22 815 19 72, e-mail: m.lastowska@czd.pl

Introduction

The *ALK* gene encodes a tyrosine kinase receptor which is expressed in the developing nervous systems [13]. The *ALK* gene is also expressed in neuroblastoma, the most common extracranial childhood tumour originating in the sympathetic nervous system and presence of expression is associated with adverse prognosis [8,26]. Importantly, *ALK* gene defects were reported both in terms of copy number changes and presence of somatic mutations in up to 10% of tumours, with two hotspot mutations in exon 23 (F1174L) and in exon 25 (R1275Q) [1]. Also germline *ALK* mutations were identified in both sporadic and familial cases of neuroblastoma [16,21] which altogether points to *ALK* as a key oncogene associated with this disease. Distribution of *ALK* mutations may be not random but typical for a particular molecular subtype of tumour. For example, F1174L substitution occurs more frequently in tumours with *MYCN* amplification [6].

Medulloblastoma, on the other hand, is the most common malignant intracranial childhood tumour of neuronal origin. Recent molecular studies revealed the existence of at least four molecular subtypes which display distinctive profiles of gene expression: Wingless (WNT), Sonic Hedgehog (SHH), Group 3 and Group 4 tumours [3,18,22]. Microarrays data indicate that *ALK* expression is associated with the WNT group, since the *ALK* gene was identified among top 50 most highly expressed genes in WNT tumours as compared to all other groups [18, in supplementary data]. Recent next generation sequencing studies in medulloblastoma based on analyses of 'discovery sets' of 37-92 tumours did not reveal any *ALK* gene alterations [17,23,24]. However the WNT groups analysed in all of these studies were small (from 5 to 7 tumours), thus preventing from discovery of changes occurring at low frequency. In support of that, the first *ALK* germline variant (3605delG) was discovered recently in a medulloblastoma patient pointing to a possible role of this gene in medulloblastoma [5].

Therefore, we further analysed exons 23 and 25 of the *ALK* gene together with molecular characteristics of tumours and found the second novel inherited *ALK* likely pathogenic variant in the WNT subtype of medulloblastoma.

Material and methods

Patients and tumour material

Sixty-four medulloblastoma patients treated from 1999 to 2014 in the Children's Memorial Health Institute (CMHI) in Warsaw, Poland were included in the analysis.

Analysis was performed on frozen and formalin-fixed paraffin embedded (FFPE) tumours obtained at diagnosis. Hematoxylin-eosin-stained slides were analysed according to the current WHO 2007 criteria [20]. Large cell/anaplastic tumours (LCA) were diagnosed where anaplastic features were identified in the majority of analysed areas.

Additionally, genomic DNA extracted from the patient with *ALK* M1199L alteration and his parents' peripheral blood leukocytes was used to confirm the germline character and parental origin of identified alteration.

Informed consent was obtained to use tumour and blood material according to the procedures outlined by the CMHI's Ethical Committee.

Detection of molecular subtypes of tumours

The molecular subtypes of tumours were identified as follows:

1. WNT tumours by presence of at least two features as recommended by the International Medulloblastoma Working Group [12]: *CTNNB1* mutation, immunohistochemical positive nuclear reaction against β-catenin (BD #610154, San Jose, USA, dilution 1 : 800) and presence of chromosome 6 monosomy detected either by interface fluorescence in situ hybridisation (FISH) or by multiplex ligation-dependent probe amplification (MLPA).
2. SHH tumours by presence of immunohistochemical positive reaction with anti-GAB1 (Abcam, Cambridge, USA, #ab27439 and/or ab #59362, dilution 1 : 100) and anti-YAP1 (Santa Cruz Biotechnology, Dallas, USA, #sc-101199, dilution 1 : 50) antibodies, as described by Ellison *et al*. [9].
3. Non-WNT/SHH tumours were the remaining tumours, tested negative for the above features.

Mutations in exon 3 of the *CTNNB1*

Mutations in exon 3 of the *CTNNB1* gene were detected in genomic DNA obtained from frozen tumour tissues using the Sanger direct method. The

PCR reactions were carried out with the following primers: CTNNB1_3F:CCCTGGCTATCATTCTGCTT and CTNNB1_3R:TCTCTTTTCTTCACCACAACATTT using Amplitaq Gold DNA Polymerase (Roche, Basel, Switzerland) under the following conditions: 95°C for 8 min; 35 cycles of 95°C for 1 min; 57°C for 5 min; 72°C for 1 min, then a final extension step at 72°C for 7 min. Sequencing reactions were performed using a BigDye Terminator v.3.1 Cycle Sequencing Kit (Life Technologies) according to the manufacturer's protocol. Sequencing products were analyzed in ABI Prism 3130 Genetic Analyzer (Applied Biosystems, Foster City, CA, USA). Sequences of the analyzed fragments were compared with the *CTNNB1* cDNA (GenBank RefSeq: NM_001904.3) using Mutation Surveyor software version 3.30 (Soft Genetics, LLC, State Collage, PA, USA). The positions of the identified nucleotide changes were determined based on comparison with the reference sequence, with the A of the ATG translation initiation codon designated as nucleotide +1.

Multiplex ligation-dependent probe amplification

Multiplex ligation-dependent probe amplification was carried out on genomic DNA extracted from frozen tumour tissues for detection of copy number changes of chromosome 6. The analysis was performed using the SALSA MLPA kit P301-A2 (MRC-Holland, Amsterdam, the Netherlands) according to the manufacturer's protocol. Probe amplification products were run an ABI Prism 3130 Genetic Analyzer (Applied Biosystems, Foster City, CA, USA). Peak plots were visualized and normalized, and the dosage ratios were calculated using GeneMarker software v 2.2.0 (Soft Genetics, LLC, State Collage, PA, USA).

Fluorescence *in situ* hybridisation

Fluorescence in situ hybridisationwas performed on FFPE tissue preparations for detection of monosomy 6 using chromosome 6 Satellite Enumeration Probe (Kreatech, Amsterdam, the Netherlands) according to the protocols for the manufacturer of probes.

Detection of *ALK* variants and gene expression

A total of 20 ng of genomic DNA isolated from tumour tissue and/or peripheral blood lymphocytes by automated method (MagnaPure, Roche) was used to amplify coding and intronic flanking regions of exons 23 and 25 of the *ALK* gene.

The PCR reactions were carried out with the following primers: ALK_23F:GGAGCCTGCTGTGGTTCTTC and ALK_23R:AGTTGACACCCTGGGTTCC as well as ALK_25F:GGAAATATAGGGAAGGGAAGGAACTA and ALK_25R:TGATGTAAGGGACAAGCAGCC, using Amplitaq Gold DNA Polymerase (Roche, Basel, Switzerland) under the following conditions: 95°C for 8 min; 35 cycles at 95°C for 1 min; 62°C (exon 23)/60°C (exon 25) for 1 min; 72°C for 1 min, then a final extension step at 72°C for 7 min. Bidirectional sequencing was performed using a 3130 genetic analyser (Applied Biosystems, Foster City, CA, USA). The sequences were determined on both DNA strands from at least two independent PCR products. The analysed sequence fragments were compared with the ALK cDNA (GenBank RefSeq: NM_004304.4) and protein (GenBank RefSeq: NP_004295.2) sequences using Mutation Surveyor software version 3.30 (Soft Genetics, LLC, State Collage, PA, USA). Variant positions were numbered according to HGVS recommendations (with +1 corresponding to the A of the ATG translation initiation codon in the appropriate reference sequence).

Prediction of possible functional effects of novel alternations was performed using three different algorithms, which are web-based tools for the annotation of pathological variants in proteins: FATHMM (http://fathmm.biocompute.org.uk/index.html), PolyPhen-2 (http://genetics.bwh.harvard.edu/pph2/), and Mutation Taster (http://www.mutationtaster.org/). The identified novel variants were also screened against mutation and SNP databases: NCBI (www.ncbi.nlm.nih.gov/SNP) and the Human Gene Mutation Database Professional (HGMD; www.hgmd.cf.ac.uk/ac/validate.php). Additionally, the amino acid position of all selected changes in functional domains and posttranslational modifications was verified using NCBI Protein (http://www.ncbi.nlm.nih.gov/protein) and Alamut-2.4-6 Software.

Expression of ALK was detected by immunohistochemistry using antibody clone ALK1 (DAKO #M 7195, Agilent Technologies, Santa Clara, USA, dilution 1 : 20).

Results

Patients and tumours characteristics

Tumours from sixty four paediatric patients with medulloblastoma were analysed. The average age of patients at diagnosis was nine years, range 0.5-17 years. Forty patients were males, 24 patients were females.

Molecular groups included: ten WNT tumours, eight SHH tumours, 41 non-WNT/SHH tumours and 5 tumours without determined molecular features due to lack of tumour material for extensive analyses. A summary of patients and tumour characteristics is presented in Table I.

Detection of *ALK* variants

Among sixty four tumours, five variants were detected in exons 23 and 25 presented in Table II. In four cases they resulted in an intron variant without impact on the function of the encoded protein and were not considered further.

In one tumour, a novel heterozygous likely pathogenic variant c.3595A>T was detected in exon 23 that resulted in a methionine to leucine substitution at codon position 1199 (M1199L) in the kinase domain of ALK protein (Fig. 1A). Analysis of genomic DNA obtained from proband's peripheral blood leukocytes confirmed the germline nature of the

Table I. Characteristics of 64 patients with medulloblastoma analysed for *ALK* variants

	ALL	WNT	SHH	Non-WNT/SHH	Not determined
No. of patients	64	10	8	41	5
Age (years)					
Average; range	8.8; 0.5-17	9.3; 5-14	5.6; 0.5-11	9.2; 3-17	7.7; 2-15
0-3	5	0	4	0	1
4-17	59	10	4	41	4
Gender					
Male	40	5	3	30	2
Female	24	5	5	11	3
Histopathology					
Classic	44	10	1	32	1
LCA[1]	12	0	1	9	2
DN[2]	5	0	5	0	0
MBEN[3]	1	0	1	0	0
Not available	2	–	–	–	2
ALK status					
Variant	5	2	0	2	1
Normal	59	8	8	39	4

[1]LCA – large cell/anaplastic, [2]DN – desmoplastic/nodular, [3]MBEN – medulloblastoma tumour with extensive nodularity

Table II. Alterations in the *ALK* gene in five medulloblastoma tumours

Group	ALK alterations[1]		Function
	Exon 23	Exon 25	
WNT	c.3595A>T p. Met1199Leu	No change	Missense
WNT	No change	c.3744-32A>G (rs3738867)	Intron variant
Non-WNT/SHH	No change	c.3744-32A>G (rs3738867)	Intron variant
Non-WNT/SHH	No change	c.3744-32A>G (rs3738867)	Intron variant
Not determined	c.3516-62A>G (rs113866835)	No change	Intron variant

[1]Alterations include intronic flanking regions of exons 23 and 25

detected variant. Also maternal DNA sample showed c.3595A>T alteration indicating an inherited type of the alteration.

Variant M1199L is located in the inhibitor binding region of the kinase domain with no recorded SNP site. To predict whether the identified variant is tolerated or deleterious, we used the combined results of three different algorithms (see methods), which confirmed the pathogenicity of the novel p.Met1199Leu variant in the *ALK* gene (FATHMM, PolyPhen-2, Mutation Taster Scores: –2.51, 0.7; 0.99; respectively). A novel variant position relative to two hot spots mutations found in neuroblastoma and the only mutation previously detected in medulloblastoma is presented in Figure 1B.

Characteristics of the patient and tumour with c.3595A>T *ALK* likely pathogenic variant

A ten-year-old boy was diagnosed in 2008 with brain tumour in the posterior fossa midline location. The tumour was surgically totally removed and no metastases were detected on magnetic resonance imaging examination. The patient is still alive and has been disease free for 6 years since diagnosis.

Histopathologically the tumour was diagnosed as classic medulloblastoma, however with clearly visible areas of focal anaplastic features (Fig. 2A-C).

Analysis of DNA extracted from frozen tumour revealed presence of *CTNNB1* mutation in exon 3 (c.98C>A; p.S33Y) and loss of whole chromosome 6 detected by MLPA analysis. In addition, positive nuclear reaction against β-catenin was identified by immunohistochemistry (Fig. 2D) what altogether classifies this tumour to the WNT group. Presence of *ALK* expression at the protein level was confirmed by immunohistochemistry using ALK1 antibody (Fig. 2E).

Discussion

Up to now around 30 recurrent chromosomal translocations involving the *ALK* gene have been identified in different cancers, mainly anaplastic large cell lymphoma (ALCL), non-small cell lung cancer (NSCLC), inflammatory myofibroblastic tumour (IMT) and other tumours (review in [25]).

However, no fusion genes involving *ALK* have been found in neuroblastoma and recently described *ALK* translocations in neuroblastoma are not expected to result in a fusion transcript [10]. Therefore, mutations both somatic and germinal, leading to *ALK* activation are characteristic for this disease. It

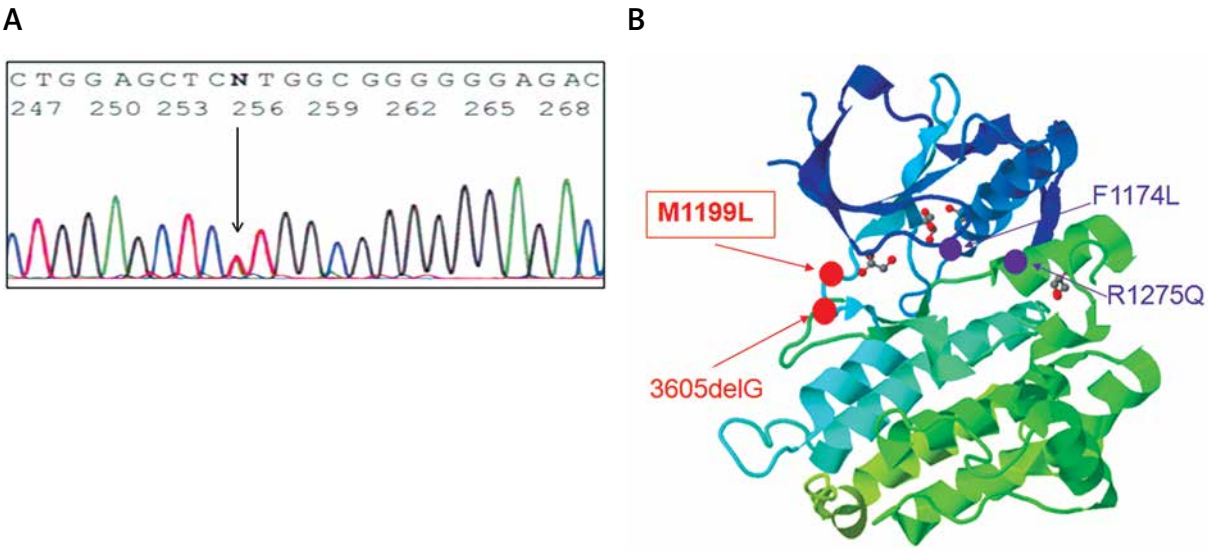

Fig. 1. *ALK* molecular variants in medulloblastoma and neuroblastoma. **A**) A novel *ALK* likely pathogenic variant c.3595A>T (M1199L) in exon 23 in medulloblastoma. **B**) A "ribbon" rainbow diagram of human ALK protein. Red dots indicate location of mutations in medulloblastoma. The M1199L variant detected in this study is located in a hinge region of the kinase domain of the ALK protein. Purple dots indicate two hot spots mutations in neuroblastoma. F1174 is located in C-helix region and R1275Q in the activation segment of the kinase domain of the ALK protein. The view is prepared from protein data bank file RCSB PDB ID: 3L9P.

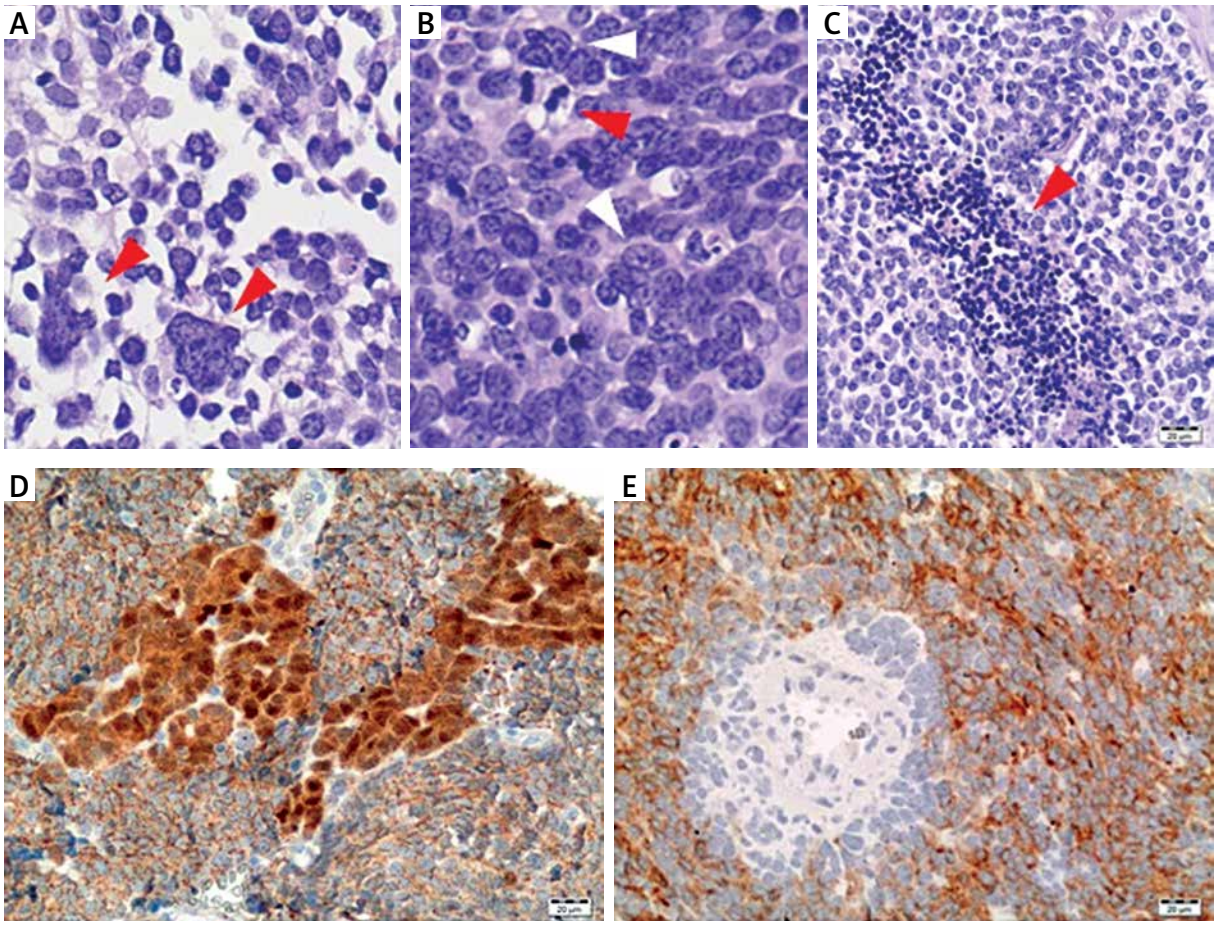

Fig. 2. Images of medulloblastoma tumour with presence of the M1199L variant. Hematoxylin-eosin-stained slides indicating presence of anaplastic features within the tumour (**A-C**). **A**) Red arrowheads indicate pleomorphic cells. **B**) Red arrowhead indicates mitotic cell and white arrowheads indicate cell-cell wrapping. **C**) Red arrowhead shows the area of apoptotic cells. **D**) Positive nuclear reaction against β-catenin. **E**) Positive reaction with anti-ALK1 antibody. Original magnification of images 200×.

is likely that additional genetic changes (e.g. *MYCN* amplification) are required for neuroblastoma tumorigenesis. Mouse model experiments revealed that knock-in mice carrying Alk F1178L mutation (equivalent to human F1174L) were characterized by an increased number of sympathetic neuroblasts and a prolonged proliferation of sympathetic neurons but they did not develop neuroblastoma tumours [2].

We have analysed 64 medulloblastoma tumours, including ten of the WNT type, and found a novel *ALK* M1199L likely pathogenic variant in a binding region of the kinase domain, likely to be deleterious and inherited from maternal origin. This variant may be linked to the ALK inhibitors resistance since the contact maintained by methionine residue M-1199 is most important for the effective binding and stability of the ALK-crizotinib complex [19]. The neighbouring region includes also the sites of secondary acquired *ALK* alterations L1996M and L1998P in EML4-ALK fusion positive lung cancers which confer resistance to crizotinib, and G1202R, which confers resistance to a second-generation ALK inhibitor alectinib and other ALK inhibitors [4,7,14,15]. Therefore, a precise character of the detected variant is critical for further therapeutic considerations.

Although the *ALK* gene was expressed at the protein level, it is possible that M1199L alteration is not sufficient for tumorigenesis alone and mutations in other genes are necessary for tumour development e.g. in *CTNNB1* or as yet unknown genes from chromosome 6. On the other hand, mouse experiments uncovered that activating mutations in *Ctnnb1* alone,

although caused the abnormal accumulation of cells on the embryonic dorsal brainstem, did not lead to the development of tumours [11]. This altogether emphasizes a requirement for a cooperative genetic event, similarly to neuroblastoma, in the development of the WNT type of medulloblastoma.

Germline deletion 3605delG found previously in medulloblastoma [5] is located within a short distance from the variant identified by us (c.3595A>T). However it is a nonsense mutation resulting in a frameshift producing a premature stop codon in exon 25 and putative truncated protein consisting of 1256 amino acids, as compared to 1620 of the wild-type. Its role in signal transduction remains to be determined. Also the molecular type of the tumour with *ALK* mutation was not established. Remarkably, both identified alterations occurred in tumours with presence of anaplastic features, which is in line with observation that *ALK* mutations are characteristic for de-differentiated tumours.

Very recent investigation of 37 medulloblastoma tumours did not reveal any mutations in exon 23 and exon 25 of the *ALK* gene [27]. It is likely that other alterations may be detected in medulloblastoma by application of e.g. next generation sequencing, similarly to intragenic *ALK* rearrangements detected recently in neuroblastoma [10].

In summary, this is the first evidence of inherited *ALK* likely pathogenic variant in the WNT type of medulloblastoma, what altogether with presence of ALK expression may point towards involvement of the *ALK* gene in this type of tumours.

Acknowledgements

The study was funded by the National Science Centre, Poland, Grants no. 2011/01/B/NZ4/01066 (M.Ł.) and 6917/B/P01/2011/40 (J.T.) and by Internal Funding from the Children's Memorial Health Institute, Warsaw, Poland, Grant no. S124/2012 (M.Ł.) and 233/15 (J.T.).

Disclosure

Authors report no conflict of interest.

References

1. Carén H, Abel F, Kogner P, Martinsson T. High incidence of DNA mutations and gene amplifications of the ALK gene in advanced sporadic neuroblastoma tumours. Biochem J 2008; 416: 153-159.
2. Cazes A, Lopez-Delisle L, Tsarovina K, Pierre-Eugène C, De Preter K, Peuchmaur M, Nicolas A, Provost C, Louis-Brennetot C, Daveau R, Kumps C, Cascone I, Schleiermacher G, Prignon A, Speleman F, Rohrer H, Delattre O, Janoueix-Lerosey I. Activated Alk triggers prolonged neurogenesis and Ret upregulation providing a therapeutic target in ALK-mutated neuroblastoma. Oncotarget 2014; 9: 2688-2702.
3. Cho YJ, Tsherniak A, Tamayo P, Santagata S, Ligon A, Greulich H, Berhoukim R, Amani V, Goumnerova L, Eberhart CG, Lau CC, Olson JM, Gilbertson RJ, Gajjar A, Delattre O, Kool M, Ligon K, Meyerson M, Mesirov JP, Pomeroy SL. Integrative genomic analysis of medulloblastoma identifies amolecular subgroup that drives poor clinical outcome. J Clin Oncol 2011; 29: 1424-1430.
4. Choi YL, Soda M, Yamashita Y, Ueno T, Takashima J, Nakajima T, Yatabe Y, Takeuchi K, Hamada T, Haruta H, Ishikawa Y, Kimura H, Mitsudomi T, Tanio Y, Mano H; ALK Lung Cancer Study Group. EML4-ALK mutations in lung cancer that confer resistance to ALK inhibitors. N Engl J Med 2010; 363: 1734-1739.
5. Coco S, De Mariano M, Valdora F, Servidei T, Ridola V, Andolfo I, Oberthuer A, Tonini GP, Longo L. Identification of ALK germline mutation (3606del) in pediatric anaplastic medulloblastoma. J Hum Genet 2012; 57: 682-684.
6. De Brouwer S, De Preter K, Kumps C, Zabrocki P, Porcu M, Westerhout EM, Lakeman A, Vandesompele J, Hoebeeck J, Van Maerken T, De Paepe A, Laureys G, Schulte JH, Schramm A, Van Den Broecke C, Vermeulen J, Van Roy N, Beiske K, Renard M, Noguera R, Delattre O, Janoueix-Lerosey I, Kogner P, Martinsson T, Nakagawara A, Ohira M, Caron H, Eggert A, Cools J, Versteeg R, Speleman F. Metaanalysis of neuroblastomas reveals a skewed ALK mutation spectrum in tumors with MYCN amplification. Clin Cancer Res 2010; 16: 4353-4362.
7. Doebele RC, Pilling AB, Aisner DL, Kutateladze TG, Le AT, Weickhardt AJ, Kondo KL, Linderman DJ, Heasley LE, Franklin WA, Varella-Garcia M, Camidge DR. Mechanisms of resistance to crizotinib in patients with ALK gene rearranged non-small cell lung cancer. Clin Cancer Res 2012; 18: 1472-1482.
8. Duijkers FA, Gaal J, Meijerink JP, Admiraal P, Pieters R, de Krijger RR, van Noesel MM. High anaplastic lymphoma kinase immunohistochemical staining in neuroblastoma and ganglioneuroblastoma is an independent predictor of poor outcome. Am J Pathol 2012; 180: 1223-1231.
9. Ellison DW, Dalton J, Kocak M, Nicholson SL, Fraga C, Neale G, Kenney AM, Brat DJ, Perry A, Yong WH, Taylor RE, Bailey S, Clifford SC, Gilbertson RJ. Medulloblastoma: clinicopathological correlates of SHH, WNT, and non-SHH/WNT molecular subgroups. Acta Neuropathol 2011; 121: 381-396.
10. Fransson S, Hansson M, Ruuth K, Djos A, Berbegall A, Javanmardi N, Abrahamsson J, Palmer RH, Noguera R, Hallberg B, Kogner P, Martinsson T. Intragenic anaplastic lymphoma kinase (ALK) rearrangements: Translocations as a novel mechanism of ALK activation in neuroblastoma tumours. Genes Chromosomes Cancer 2015; 54: 99-109.
11. Gibson P, Tong Y, Robinson G, Thompson MC, Currle DS, Eden C, Kranenburg TA, Hogg T, Poppleton H, Martin J, Finkelstein D, Pounds S, Weiss A, Patay Z, Scoggins M, Ogg R, Pei Y, Yang ZJ, Brun S, Lee Y, Zindy F, Lindsey JC, Taketo MM, Boop FA, Sanford RA, Gajjar A, Clifford SC, Roussel MF, McKinnon PJ, Gutmann DH,

Ellison DW, Wechsler-Reya R, Gilbertson RJ. Subtypes of medulloblastoma have distinct developmental origins. Nature 2010; 468: 1095-1099.
12. Gottardo NG, Hansford JR, McGlade JP, Alvaro F, Ashley DM, Bailey S, Baker DL, Bourdeaut F, Cho YJ, Clay M, Clifford SC, Cohn RJ, Cole CH, Dallas PB, Downie P, Doz F, Ellison DW, Endersby R, Fisher PG, Hassall T, Heath JA, Hii HL, Jones DT, Junckerstorff R, Kellie S, Kool M, Kotecha RS, Lichter P, Laughton SJ, Lee S, McCowage G, Northcott PA, Olson JM, Packer RJ, Pfister SM, Pietsch T, Pizer B, Pomeroy SL, Remke M, Robinson GW, Rutkowski S, Schoep T, Shelat AA, Stewart CF, Sullivan M, Taylor MD, Wainwright B, Walwyn T, Weiss WA, Williamson D, Gajjar A. Medulloblastoma Down Under 2013: a report from the third annual meeting of the International Medulloblastoma Working Group. Acta Neuropathol 2014; 127: 189-201.
13. Hallberg B, Palmer RH. Mechanistic insight into ALK receptor tyrosine kinase in human cancer biology. Nat Rev Cancer 2013; 13: 685-700.
14. Heuckmann JM, Hölzel M, Sos ML, Heynck S, Balke-Want H, Koker M, Peifer M, Weiss J, Lovly CM, Grütter C, Rauh D, Pao W, Thomas RK. ALK mutations conferring differential resistance to structurally diverse ALK inhibitors. Clin Cancer Res 2011; 17: 7394-7401.
15. Ignatius Ou SH, Azada M, Hsiang DJ, Herman JM, Kain TS, Siwak-Tapp C, Casey C, He J, Ali SM, Klempner SJ, Miller VA. Next-generation sequencing reveals a novel NSCLC ALK F1174V mutation and confirms ALK G1202R mutation confers high-level resistance to alectinib (CH5424802/RO5424802) in ALK-rearranged NSCLC patients who progressed on crizotinib. J Thorac Oncol 2014; 9: 549-553.
16. Janoueix-Lerosey I, Lequin D, Brugières L, Ribeiro A, de Pontual L, Combaret V, Raynal V, Puisieux A, Schleiermacher G, Pierron G, Valteau-Couanet D, Frebourg T, Michon J, Lyonnet S, Amiel J, Delattre O. Somatic and germline activating mutations of the ALK kinase receptor in neuroblastoma. Nature 2008; 455: 967-970.
17. Jones DT, Jäger N, Kool M, Zichner T, Hutter B, Sultan M, Cho YJ, Pugh TJ, Hovestadt V, Stütz AM, Rausch T, Warnatz HJ, Ryzhova M, Bender S, Sturm D, Pleier S, Cin H, Pfaff E, Sieber L, Wittmann A, Remke M, Witt H, Hutter S, Tzaridis T, Weischenfeldt J, Raeder B, Avci M, Amstislavskiy V, Zapatka M, Weber UD, Wang Q, Lasitschka B, Bartholomae CC, Schmidt M, von Kalle C, Ast V, Lawerenz C, Eils J, Kabbe R, Benes V, van Sluis P, Koster J, Volckmann R, Shih D, Betts MJ, Russell RB, Coco S, Tonini GP, Schüller U, Hans V, Graf N, Kim YJ, Monoranu C, Roggendorf W, Unterberg A, Herold-Mende C, Milde T, Kulozik AE, von Deimling A, Witt O, Maass E, Rössler J, Ebinger M, Schuhmann MU, Frühwald MC, Hasselblatt M, Jabado N, Rutkowski S, von Bueren AO, Williamson D, Clifford SC, McCabe MG, Collins VP, Wolf S, Wiemann S, Lehrach H, Brors B, Scheurlen W, Felsberg J, Reifenberger G, Northcott PA, Taylor MD, Meyerson M, Pomeroy SL, Yaspo ML, Korbel JO, Korshunov A, Eils R, Pfister SM, Lichter P. Dissecting the genomic complexity underlying medulloblastoma. Nature 2010; 488: 100-105.
18. Kool M, Koster J, Bunt J, Hasselt NE, Lakeman A, van Sluis P, Troost D, Meeteren NS, Caron HN, Cloos J, Mrsić A, Ylstra B, Grajkowska W, Hartmann W, Pietsch T, Ellison D, Clifford SC, Versteeg R. Integrated genomics identifies five medulloblastoma subtypes with distinct genetic profiles, pathway signatures and clinicopathological features. PLoS One 2008; 3: e3088.
19. Kumar A, Ramanathan K. Exploring the structural and functional impact of the ALK F1174L mutation using bioinformatics approach. J Mol Model 2014; 20: 2324.
20. Louis DN, Ohgaki H, Wiestler OD, Cavenee WK, Burger PC, Jouvet A, Scheithauer BW, Kleihues P. The 2007 WHO classification of tumours of the central nervous system. Acta Neuropathol 2007; 114: 97-109.
21. Mossé YP, Laudenslager M, Longo L, Cole KA, Wood A, Attiyeh EF, Laquaglia MJ, Sennett R, Lynch JE, Perri P, Laureys G, Speleman F, Kim C, Hou C, Hakonarson H, Torkamani A, Schork NJ, Brodeur GM, Tonini GP, Rappaport E, Devoto M, Maris JM. Identification of ALK as a major familial neuroblastoma predisposition gene. Nature 2008; 455: 930-935.
22. Northcott PA, Korshunov A, Witt H, Hielscher T, Eberhart CG, Mack S, Bouffet E, Clifford SC, Hawkins CE, French P, Rutka JT, Pfister S, Taylor MD. Medulloblastoma comprises four distinct molecular variants. J Clin Oncol 2011; 29: 1408-1414.
23. Pugh TJ, Weeraratne SD, Archer TC, Pomeranz Krummel DA, Auclair D, Bochicchio J, Carneiro MO, Carter SL, Cibulskis K, Erlich RL, Greulich H, Lawrence MS, Lennon NJ, McKenna A, Meldrim J, Ramos AH, Ross MG, Russ C, Shefler E, Sivachenko A, Sogoloff B, Stojanov P, Tamayo P, Mesirov JP, Amani V, Teider N, Sengupta S, Francois JP, Northcott PA, Taylor MD, Yu F, Crabtree GR, Kautzman AG, Gabriel SB, Getz G, Jäger N, Jones DT, Lichter P, Pfister SM, Roberts TM, Meyerson M, Pomeroy SL, Cho YJ. Medulloblastoma exome sequencing uncovers subtype-specific somatic mutations. Nature 2012; 488: 106-110.
24. Robinson G, Parker M, Kranenburg TA, Lu C, Chen X, Ding L, Phoenix TN, Hedlund E, Wei L, Zhu X, Chalhoub N, Baker SJ, Huether R, Kriwacki R, Curley N, Thiruvenkatam R, Wang J, Wu G, Rusch M, Hong X, Becksfort J, Gupta P, Ma J, Easton J, Vadodaria B, Onar-Thomas A, Lin T, Li S, Pounds S, Paugh S, Zhao D, Kawauchi D, Roussel MF, Finkelstein D, Ellison DW, Lau CC, Bouffet E, Hassall T, Gururangan S, Cohn R, Fulton RS, Fulton LL, Dooling DJ, Ochoa K, Gajjar A, Mardis ER, Wilson RK, Downing JR, Zhang J, Gilbertson RJ. Novel mutations target distinct subgroups of medulloblastoma. Nature 2012; 488: 43-48.
25. Roskoski R Jr. Anaplastic lymphoma kinase (ALK): Structure, oncogenic activation, and pharmacological inhibition. Pharmacol Res 2013; 68: 68-94.
26. Wang M, Zhou C, Sun Q, Cai R, Li Y, Wang D, Gong L. ALK amplification and protein expression predict inferior prognosis in neuroblastomas. Exp Mol Pathol 2013; 95: 124-130.
27. Yan B, Kuick CH, Lim M, Yong MH, Lee CK, Low SY, Low DC, Lim D, Soh SY, Chang KT. Characterization of anaplastic lymphoma kinase-positive medulloblastomas. J Clin Neurosci 2016; 23: 120-122.

Original paper

Folia Neuropathologica

Analysis of Olig2 and YKL-40 expression: a clinicopathological/ immunohistochemical study for the distinction between subventricular zone II and III glioblastomas

Kelvin Manuel Piña Batista[1], Bruno Augusto Lourenco Costa[2], Isabel Cuervo-Arango Herreros[1], Ivan Fernandez Vega[3], Julio Cesar Gutierrez Morales[1], Aitana Vallina Alvarez[4], Pablo Isidro Marron[4], Ángela Meilán[5], Aurora Astudillo[3], Kenia Yoelvi Alvarez[6]

[1]Department of Neurosurgery, Hospital Universitario Central de Asturias, [2]Department of Neurosurgery, Hospitais da Universidade de Coimbra, [3]Department of Neuropathology, Hospital Universitario de Araba, [4]IUOPA biobank, Hospital Universitario Central de Asturias, [5]Department of Neuroradiology, Hospital Universitario Central de Asturias, [6]Hospital Álvarez Buylla, Asturias, Spain

Folia Neuropathol 2016; 54 (1): 31-39 DOI: 10.5114/fn.2016.58913

Abstract

Glioblastomas (GBs) are the most common and lethal primary brain tumors in the adults. Glioblastomas originates either from astrocytes that have accumulated mutations and de-differentiated or from neural stem cells within the subventricular zone (SVZ) in close contact with the vasculature. Recently, several studies have hypothesized that gliomagenesis occurs in perivascular niches with highly invasive peripheral proliferating zones. The purpose of our study was to investigate the pathological and clinical significance of Olig2 and YKL40 immunoexpression in 152 GBs in relationship to the SVZ II and III. Olig2 expressions were successfully detected in 12 (15.58%) of 77 SVZ type II GBs and 16 (21.3%) of 75 SVZ type III GBs, respectively. YKL-40 expression was observed in 45 (58.4%) of 77 SVZ type II GBs and in 17 (22.6%) of 75 SVZ type III GBs, respectively. Stepwise multivariate Cox proportional hazards models were used, and the prognostic factors to significantly impact OS were: PFS < 54 weeks (HR: 5.86; CI: 3.02-11.33; p = 0.00); radiotherapy (HR: 0.34; CI: 0.18-0.60; p = 0.00); radio- and chemotherapy (HR: 0.05; CI: 0.03-0.10; p = 0.0), and YKL-40+ GBs (HR: 1.61; CI: 1.28-2.31; p = 0.01).

Key words: *glioblastoma, subventricular zone, Olig2, YKL-40, clinicopathological, immunohistochemical.*

Introduction

Glioblastoma (GB) is the most common primary brain tumor in the adults. Median survival of GB patients treated with aggressive multimodal therapy, including total resection, combined radiation and chemotherapy, and adjuvant chemotherapy is about 12 months [9,18,24,25]. Glioblastoma is actually considered a heterogeneous and dynamic disease [13,17,21]. Recent studies demonstrate that GB originates either from astrocytes that have accumulated mutations and de-differentiated or from neural stem cells within the subventricular zone (SVZ) in close

Communicating author

Kelvin Manuel Piña Batista, MD, MSc, MBA, PhD, Department of Neurosurgery, Hospital Universitario Central de Asturias, Av. de Las Segadas 22, 4a 33006 Oviedo, Spain, phone: +34 693 86 24 81, e-mail: pineappledr@gmail.com

contact with the vasculature. In animal models, those neural stem cells may play a role in the gliomagenesis, recurrence, and resistance to therapies [17,28]. Probably, survival may be strongly affected by the tumor's relationship to the SVZ. Based on the MRI spatial relationship of the GB, Lim *et al.* [21] distinguish 4 types: type I, tumor contacting the SVZ and infiltrating cortex; type II, tumor contacting the SVZ only; type III, tumor involving the cortex but not involving the SVZ, and type IV, tumors spare both the cortex and the SVZ.

The precise origin of glioma stem cells (GSCs) is still unclear. Recent research efforts hypothesize that gliomagenesis occurs in perivascular niches with highly invasive peripheral proliferating zones [6,12,29]. Several studies report that Olig2 expression is limited in GSCs [7,12,22] and is probably being related to the SVZ type II as a proliferation regulator and glioma progenitor cell marker. Olig2 (a basic helix-loop-helix transcription factor) is expressed in the postnatal SVZ and plays a critical role in the lineage specification of progenitor cells into neurons and oligodendrocytes [20]. However, the literature on Olig2 and its association with glioblastoma prognosis is ambivalent [1,11,12,22]. Recent reports have found associations between glioblastoma and neural stem cells expressing Olig2 [8,12,20,35]. Therefore, a significant amount of the ongoing GB research is focused on better understanding how cells expressing Olig2 contribute to the gliomagenesis and therapeutic targets.

YKL-40 (also known as CHI3LI), a member of mammalian chitinase-like protein, is a growth factor for connective tissue cells that (although its function is not well defined) may play a role in the migration of endothelial cells, inflammation and tissue remodeling. It is also overexpressed in glioblastoma compared to anaplastic gliomas and low-grade gliomas [26,30,36].

The localization of YKL-40 expression related to the SVZ remains unclear. Given that YKL-40 immunoexpression is associated with poor prognosis and Olig2 is linked to the neural stem/progenitor cells, we investigated the clinical/prognostic significance of YKL-40 and Olig2 expression related to SVZ type II/III GBs.

Material and methods

Patients and samples

A retrospective study was performed on 152 patients harboring GBs in the SVZ type II/III treated by subtotal resection between 2006 and 2010. Paraffin-embedded samples were obtained from the Biobank of Asturias, in Central of Asturias University Hospital, Spain. For each case, the hematoxylin-eosin sections were reviewed and all cases were classified according to the World Health Organization (WHO) classification system as glioblastoma multiforme by a senior neuropathologist. Detailed data regarding clinical presentation, pathological analysis, progression-free survival, and overall survival outcome were recorded. Tumors were classified as limited to the cortex or type II (77 GBs) or limited to the SVZ or type III (75 GBs). Both, YKL-40 and Olig2 expressions were investigated by immunohistochemistry in all of the aforementioned cases. All samples used in this study were obtained with the approval of the Committee for Ethical Review Board of Central of Asturias University Hospital.

The extent of resection was determined on the basis of MRI results (within 48 hours after surgery). Subtotal and total resection were defined as those tumors with residual and no residual enhancement, respectively, achieved by comparing pre- and postoperative MRI. The extent of resection was classified as total (> 95%), subtotal (< 95%) or biopsy by a neuroradiologist blinded to patient outcomes. Patients with a Karnofsky Performance Scale (KPS) score ≥ 70 and age < 60 were included to receive conventional radiotherapy and chemotherapy after surgical resection: 1.8-2.0 Gy per day, over a period of 6 weeks, for a total dose of 60 Gy and temozolomide therapy at a dose of 75 mg/m^2 per day, seven days a week for 42 consecutive days during radiotherapy (as used in the EORTC study by Stupp *et al.*) [19,31,33].

Immunohistochemistry

Monoclonal antibodies for YKL-40 (ab86428; Abcam, Cambridge, UK; dilution 1 : 500), and polyclonal anti-Olig2 antibody (ab9610; EDM Millipore, Massachusetts, USA; dilution 1 : 500) were used. Five-micrometer consecutive sections were cut from the paraffin-embedded samples. Each tissue section was deparaffinized and rehydrated with graded ethanol. Antigen retrieval was accomplished by boiling the sections for 15 minutes in 10 mmol/l EDTA, pH 6.0. Endogenous peroxidase activity was blocked with a 3% hydrogen peroxide for 10 minutes. Then, slides were incubated overnight at 4°C with respective primary antibodies. Visualization was performed using DAB (3,3'-diaminobenzidine). Tissue sections

were counterstained with hematoxylin, dehydrated, and mounted. An oligodendroglioma and hepatocellular carcinoma with immunoreactivity was used for positive control (Olig2 and YKL-40, respectively). As a negative control the primary antibodies were omitted.

Immunoreactivity for YKL-40 was evaluated by a three-tiered system (0 – negative; 1 – moderate/patchy staining in tumor cell; 3 – strongly positive) [26]. Staining for Olig2 was scored only in cells as positive (1), and negative or weak positive (0). The authors did the scoring independently. To obtain more accurate results, 2 independent observers evaluated all immunostaining experiments.

Statistical analysis

All statistical analyses were performed with SPSS Statistics version 20 (IBM) with a significance level of 5% ($p \leq 0.05$). The χ^2 test and the Fisher's exact test were used for the evaluation of the association between Olig2 and YKL-40 (positive vs. negative immunoexpression) and covariates. Karnofsky (KPS) from 3 months was included for analyses because at this time used to occur the most significant and lasting change in patient clinical status. Overall survival (OS) was determined from the date of diagnosis to the date of death. Progression-free survival (PFS) was determined from the date of diagnosis to the date of relapse. Kaplan-Meier method was used to investigate Olig2 and YKL-40 expression as univariate in prediction of the patient's survival related to SVZ. Multivariate survival analyses were performed by a stepwise Cox proportional hazards model used for univariate and multivariate analyses of PFS and OS.

Results

Patient demographics are presented in Table I. Expressions of Olig2 and YKL-40 in 152 GBs were investigated by IHC. Olig2 expressions were successfully detected in 12 (15.58%) of 77 SVZ type II GBs and 16 (21.3%) of 75 SVZ type III GBs, respectively. YKL-40 expression was observed in 45 (58.4%) of 77 SVZ type II GBs and in 17 (22.6%) of 75 SVZ type III GBs, respectively. Positive expression of YKL-40 was found in the cytoplasm of GB tumor cells (Fig. 1). Olig2+ GB cells showed strong nuclear immunoreactivity. For better understanding of the analytical results, YKL-40 expressions were classified as positive (1+, 2+) or negative (0).

Relationship between the immunoexpression of Olig2 and YKL-40 and clinico-pathological findings

The results of the pathologic findings are shown in Table II. Expression of Olig2 was not associated with the patient's age (≤ 65 years old versus > 65 years old), gender, Karnofsky at diagnosis (KPS at Dx), progression-free survival (PFS), overall survival (OS), and GB type. However, Olig 2 was associated with KPS at 3 months ($p = 0.035$). YKL-40 did not ($p > 0.05$) correlate with gender, and KPS at diagno-

Table I. Clinical characteristics of 152 patients with glioblastoma

Groups	Characteristics
Age	Years
≤ 65	93
> 65	59
Gender	N°
Male	79
Female	73
Karnofsky (KPS) at Dx, Score	N°
< 70	20
≥ 70	132
KPS at 3 months, Score	N°
< 70	47
≥ 70	105
Overall Survival, OS	Weeks
≤ 54	98
> 54	53
Progression-free survival, PFS	Weeks
≤ 54	131
> 54	21
Subventricular relationship	N°
Group II	77
Group III	75
Extent of tumor resection	N°
Gross total resection	40
Subtotal resection	86
Biopsy	26
First-line therapy	N°
Radiotherapy	26
Chemotherapy	1
Radiotherapy and chemotherapy	98
Therapeutic abstention	27

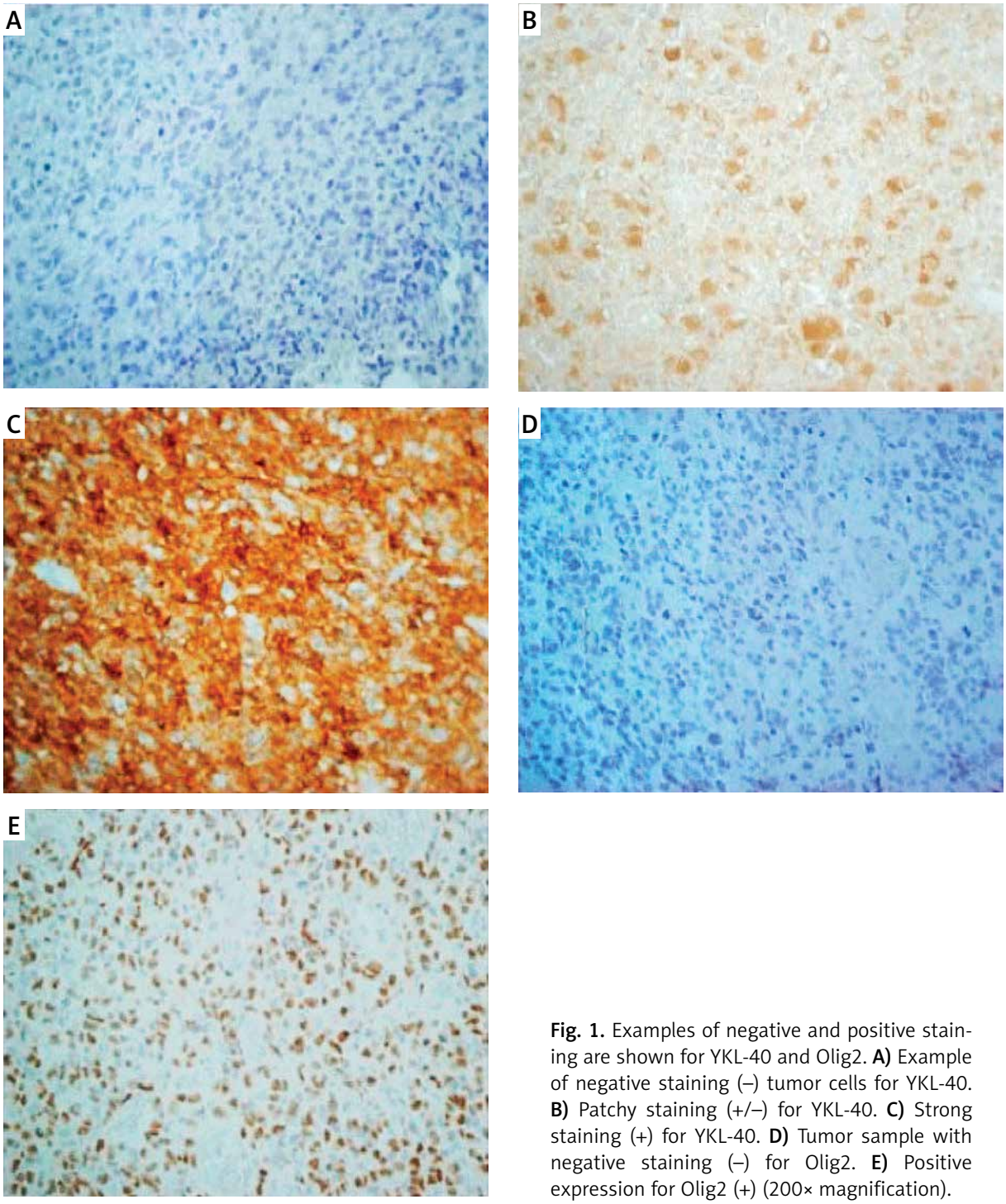

Fig. 1. Examples of negative and positive staining are shown for YKL-40 and Olig2. **A)** Example of negative staining (–) tumor cells for YKL-40. **B)** Patchy staining (+/–) for YKL-40. **C)** Strong staining (+) for YKL-40. **D)** Tumor sample with negative staining (–) for Olig2. **E)** Positive expression for Olig2 (+) (200× magnification).

sis. Interestingly, YKL-40 was significantly associated with age, KPS at 3 months, PFS, OS, and GB type. Kaplan-Meier analysis showed that YKL-40 (CHI3L1) expression was significantly different from Olig2 expression ($p > 0.05$) (Figs. 2 and 3).

Univariate and multivariate analysis of prognostic variables

To identify and evaluate the variables with potential prognostic significance in patients with GB, univariate and multivariate analysis using Kaplan-Meier

Table II. Correlations between CHI3L1 and Olig2 expression in tumor tissues and clinic pathological features of patients with glioblastoma

Variables	CHI3L1		*p* value	Olig2		*p* value
	Positive	Negative		Positive	Negative	
Age						
< 65	31	62	0.019*	20	73	0.218
>65	31	28	8	51		
Gender						
Male	34	45	0.557	13	66	0.516
Female	28	45	15	58		
KPS at Dx						
< 70	11	9	0.165	2	18	0.297
> 70	51	81	26	106		
KPS at 3 months						
< 70	26	21	0.015*	4	43	0.035*
> 70	36	69	24	81		
PFS						
< 54	58	73	0.013*	22	109	0.157
> 54	4	17	7	14		
OS						
< 54	52	46	0.00*	15	83	0.164
> 54	10	44	13	41		
GBMs						
SVZ II	45	32	0.00*	12	65	0.361
SVZ III	17	58	16	59		
Extent of tumor resection						
Gross total resection	9	31	0.02*	9	31	0.281
Subtotal resection	36	50	17	69		
Biopsy	17	9	2	24		
First-line therapy						
Radiotherapy	14	12	0.029*	1	26	0.023*
Chemotherapy	0	1	1	0		
Radiotherapy and chemotherapy	32	66	22	76		
Therapeutic absention	16	11	1	26		

*χ^2 tests, *p < 0.05*

and Cox proportional hazard model was performed. In a univariate proportional hazards regression analysis, the factors associated with survival were: age, KPS at 3 months, YKL-40 (CHI3L1), and Olig2. In addition, univariate analysis confirmed that neither the gender (p = 0.13) nor Olig2 immunoexpression (p = 0.86) affected OS.

We evaluated the potential prognostic factors following the Cox proportional hazards models using forward stepwise multivariate selection analysis (Table III). The variables significantly associated with OS were: PFS < 54 weeks (HR: 5.86; CI: 3.02-11.33; p = 0.00); radiotherapy (HR: 0.34; CI: 0.18-0.60; p = 0.00); radio- and chemotherapy (HR: 0.05; CI: 0.03-

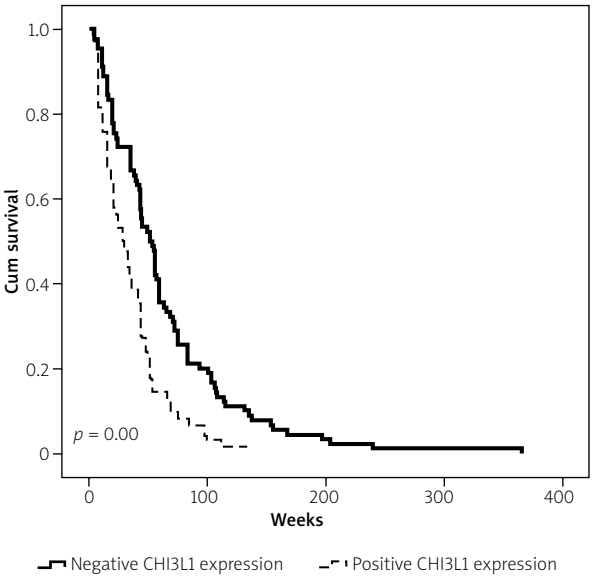

Fig. 2. Patients expressing YKL-40 (CHI3L1) in tumor tissues show a significantly worse overall survival. Kaplan-Meier analysis for overall survival in a series of glioblastomas according to YKL 40 expression.

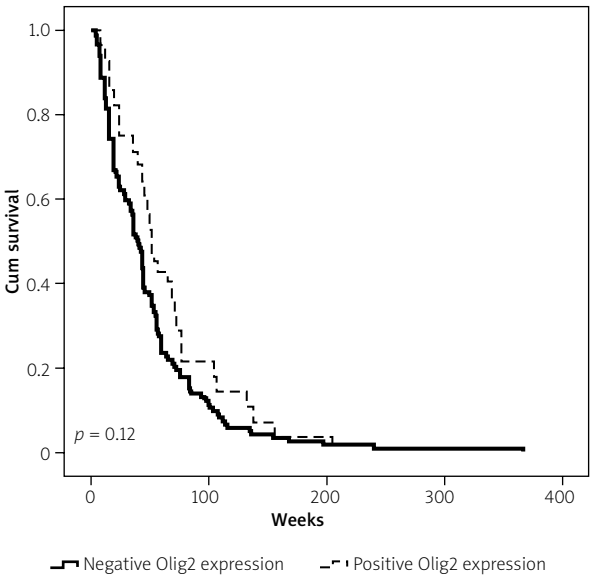

Fig. 3. Kaplan-Meier overall survival curves of the series of 152 glioblastomas with a different expression of Olig2. The difference in survival between Olig2+ and Olig2– is not statistically significant ($p = 0.12$).

Table III. Univariate and multivariate analyses of variables associated with survival

Variables	Univariate analysis			Multivariate analysis		
	HR	95% CI	*p* value	HR	95% CI	*p* value
Age, years (< 65 vs. > 65)	0.46	0.33-0.65	0.00*	0.76	0.52-1.12	0.17
Gender (male vs. female)	1.28	0.92-1.78	0.13	1.21	0.85-1.71	0.27
KPS at Dx (< 70 vs. > 70)	0.42	1.46-3.82	0.00*			
KPS at 3 months (< 70 vs. > 70)	3.95	2.72-5.73	0.00*	1.50	0.97-2.32	0.63
PFS, weeks (< 54 vs. > 54)	0.13	0.07-0.25	0.00*	5.41	2.78-10.54	0.00*
CHI3L1-GBM cells (pos. vs. neg.)	1.22	1.08-1.38	0.00*	1.61	1.12-2.31	0.01*
Olig2-GBM (pos. vs. neg.)	0.98	0.84-1.15	0.86			
Biopsy			0.00*			
Gross total resection	0.23	0.14-0.40	0.00*			
Subtotal resection	0.31	0.19-0.49	0.00*			
Radiotherapy			0.00*	0.34	0.18-0.60	0.00*
Chemotherapy	2.65	0.35-20.1	0.34	1.02	0.13-8.02	0.97
Radiotherapy and chemotherapy	0.10	0.05-0.17	0.00*	0.05	0.03-0.10	0.00*
Therapeutic absention	2.84	1.59-5.04	0.00*			

*Fisher's exact, *p < 0.05*
KPS – Karnofsky score, KPS at Dx – Karnofsky score at diagnosis, PFS – progression-free survival
CI – confidence interval, HR – hazard ratio, pos. – positive, neg. – negative

0.10; $p = 0.0$), and YKL-40+ GBs (HR: 1.61; CI: 1.28-2.31; $p = 0.01$). However, Olig2+ GBs were not included in multivariate analysis.

Discussion

Although the SVZ has been recognized for many years, its neurogenesis and gliomagenesis remains unclear. Subventricular zone may be a source of tumors with higher proliferative and invasive capacities [5]. Recent research efforts in neuro-oncology are focused in targeting the tumorigenesis theory and to find signal transduction pathways that influence the GB development and change its dismal prognosis, given that surgery and adjuvant chemotherapy with radiotherapy are insufficient due to a diffuse infiltration by tumor tissue into the brain [4,12,37]. Therefore, identifying molecular targets that could provide prognostic new data is needed and would be helpful for its therapy.

Olig2+ GBs are not significantly expressed in GB type II and III, against predictive and critical functions for Olig2 [32,34]. Under the stem cell hypothesis, Olig2 fulfills criteria of a lineage-restricted competence factor for gliogenesis [8,15] that is necessary for the development of neural progenitors and progeny cells in the CNS [12]. Like others, [22] we have suggested that Olig2 expression may be downregulated in mature astrocyte.

YKL-40 is a potent angiogenic factor that was recently identified to be one of the most expressed proteins in GB when compared to low-grade glioma and normal brain. YKL-40 protein expression was proposed as a potential serum marker for GB [10,16,26]. High YKL-40 expression in GB has been correlated with a short OS and a poor response to radiotherapy [14,16]. We found that GBs contacting the SVZ trended with shorter OS, although it is unclear if tumors contacting the SVZ have more aggressive behavior, allowing tumor stem cells and their progeny to rapidly proliferate and migrate. The main reasons for a less favorable outcome in GB patients with SVZ involvement are not yet completely understood. Interestingly, we have found a significantly greater YKL-40 expression among the subventricular zone contacting GBs than Olig2+ GBs. Previous work [27] has determined that YKL-40 was particularly linked to SVZ type IV and V. One of the limitations of this study was the small sample size of SVZ type II patients. According to our results, there was also a trend toward a worse OS among SVZ type II GBs when compared with SVZ type III GBs. Univariate, multivariate, and Kaplan-Meier analyses demonstrated that expression of YKL-40 was a significant negative indicator of the behavior of GB.

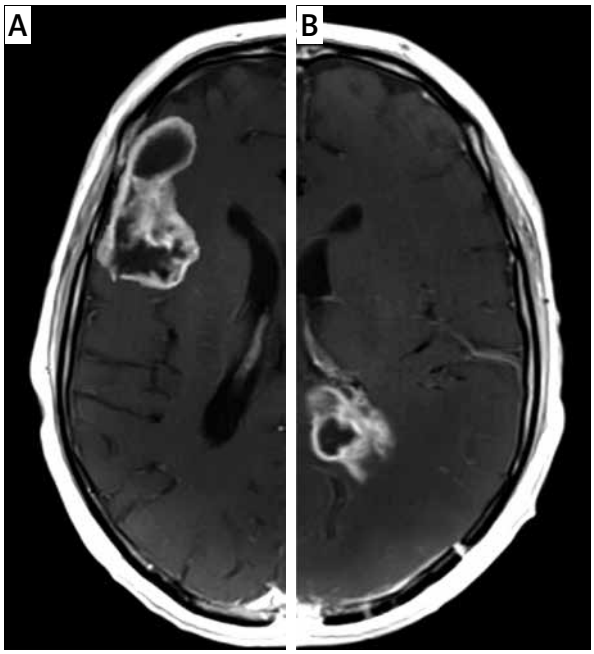

Fig. 4. MRI T1 weighted sequence after Gd-DTPA infusion shows the spatial relationship of glioblastomas related to the SVZ. **A**) SVZ III tumors involve only the cortex; **B**) SVZ II contacts only the SVZ.

The present study was performed on a heterogeneous population of GB patients, all of whom underwent total resection, subtotal resection or biopsy followed by the same adjuvant therapy (chemotherapy and radiotherapy). To date, the extent of resection has been an accepted prognostic factor [3,23,33]. Nevertheless, although it is well accepted that tumor resection may improve the symptoms we have found impact on OS only in the univariate analysis. However, extensive resection combined with adjuvant therapy could also explain the advantageous impact in terms of OS in a multivariate analysis.

The difference in survival among patients with GB has been seen to significantly depend on age, KPS at 3 months, extent of resection, and immunoexpression of YKL-40. We have found that there was a significant correlation between the expression of Olig2 and KPS at 3 months. Age at diagnosis and preoperative KPS score have been the most recognized predictors of OS [4]. KPS score at 3 months from diagnosis was a prognostic factor more valuable than KPS

score at diagnosis, which may be attributed to the influence of surgery. Most of YKL-40+ GBs had a PFS of less than 54 weeks. These data differ from the previous report [2] that found no prognostic association between YKL-40 expression and PFS. However, such disagreement may be because our study has a larger sample size and different age groups of patients.

Conclusions

Up to date, significant progress has been made in the understanding of GB regarding its topographical molecular expressions. The presence of GBs, which express prognostic markers in relationship to the subventricular zone, is of practical as well as theoretical interest. In fact, this information may be the road by which the most effective therapy can be focused. Our results demonstrated that dismal prognosis of GBs is significantly correlated to YKL-40 expression and linked to SVZ relationship. As YKL-40 has been found in serum and in brain tumor tissue, it has a potential as a therapeutic and prognosis marker for GB. Current insights will ultimately lead to a more individualized therapy for GB patients.

Our study suffers from the same limitations as other retrospective studies, with a biased selection of SVZ topographical locations, which influences the results. Therefore, further controlled studies are needed to validate our results in a prospective study with a greater number of GBs patients.

Disclosure

Authors report no conflict of interest.

References

1. Agnihotri S,Burrell KE, Wolf A, Jalali S, Hawkins C, Rutka JT, Zadeh G. Glioblastoma, a briefreview of history, molecular genetics, animal models and novel therapeuticstrategies. Arch Immunol Ther Exp 2013; 61: 25-41.
2. Antonelli M, Buttarelli FR, Arcella A, Nobusawa S, Donofrio V, Oghaki H, Giangaspero F. Prognostic significance of histological grading, p53 status, YKL-40 expression, and IDH1 mutations in pediatrichigh-grade gliomas. J Neurooncol 2010; 99: 209-215.
3. Bloch O, Han SJ, Cha S, Sun M, Aghi MK, McDermott MW, Berger MS, Parsa A. Impact of extent of resection for recurrent glioblastoma on overall survival. J Neurosurg 2012; 117: 1032-1038.
4. Bozdag S, Li A, Riddick G, Kotliarov Y, Baysan M, Iwamoto FM, Cam MC, Kotliarova S, Fine HA. Age-Specific Signatures of Glioblastoma at the Genomic, Genetic, and Epigenetic Levels. PLos One 2013; 8: e62982.
5. Chaichana KL, Pendleton C, Chambless L, Camara-Quintana J, Nathan JK, Hassam-Malani L, Li G, Harsh IV GR, Thompson RC, Lim M, Quinones-Hinojosa A. Multi-institutional validation of a preoperative scoring system which predicts survival for patients with glioblastom. J Clin Neurosci 2013; 20: 1422-1426.
6. Chen J, Li Y, Yu TS, McKay RM, Burns DK, Kernie SG, Parada LF. A restricted cell population propagates glioblastoma growth after chemotherapy. Nature 2012; 488: 522-526.
7. Cheng L, Bao S, Rich JN. Potential therapeutic implications of cancer stem cells in glioblastoma. Biochem Pharmacol 2010; 80: 654-665.
8. Colman H, Zhang L, Sulman EP, McDonald M, Shooshtari NL, Rivera a, Popoff S, Nutt CL, Louis DN, Cairncross JG, Gilbert MR, Phillips HS, Mehta MP, Chakravarti A, Pelloski CE, Bhat K, Feuerstein BG, Jenkins RB, Aldape K. A multigene predictor of outcome in glioblastoma. Neurooncol 2010; 12: 49-57.
9. Dahlrot RH, Kristensen BW, Hjelmborg J, Herrstedt J, Hansen S. A population-basedstudy of high-grade gliomas and mutated isocitrate dehydrogenase 1. Int J Clin Exp Pathol 2013; 6: 31-40.
10. Francescone RA, Scully S, Faibish M, Taylor SL, Oh D, Moral L, Yan W, Bentley B, Shao R. Role of YKL-40 in the angiogenesis, radioresistance, and progression of glioblastoma. J Biol Chem 2011; 286: 15332-15343.
11. Georgieva L, Moskvina V, Peirce T, Norton N, Bray NJ, Jones L, Holmans P, MacGregor S, Zammit S, Wilkinson J, Williams H, Nikolov I, Williams N, Ivanov D, Davis KL, Haroutunian V, Buxbaum JD, Craddock N, Kirov G, Owen MJ, O'Donovan MC. Convergent evidence that oligodendrocyte lineage transcription factor 2 (OLIG2) and interacting genes influence susceptibility to schizophrenia. Proc Natl Acad Sci USA 2006; 103: 12469-12474.
12. Ghazi SO, Stark M, Zhao Z, Mobley BC, Munden A, Hover L, Abel TW. Cell of Origin Determines Tumor Phenotype in anOncogenic Ras/p53 Knockout Transgenic Model of High-Grade Glioma. J Neuropathol Exp Neurol 2012; 71: 729-740.
13. Haskins WE, Zablotsky BL, Foret MR. Molecular characteristics in MRI-classifiedgroup 1 glioblastoma multiforme. Front Oncol 2013; 3: 1-8.
14. Horbinski C, Wang G, Wiley CA. YKL-40 is directly produced by tumor cells and is inversely linked to EGFR in glioblastomas. Int J Clin Exp Pathol 2010; 3: 226-237.
15. Ihrie RA, Alvarez-Buylla A. Lake-front property: a unique germinal niche bythe lateral ventricles of the adult brain. Neuron 2011; 70: 674-686.
16. Iwamoto FM, Hottinger AF, Karimi S, Riedel E, Dantis J, Jahdi M, Panageas KS, Lassman AB, Abrey LE, Fleisher M, DeAngelis LM, Holland EC, Hormigo A. Serum YKL-40 is a marker of prognosis and disease status in high-grade gliomas. Neurooncol 2011; 13: 1244-1251.
17. Jafri NF, Clarke JL, Weinberg V, Barani IJ, Cha S. Relationship of glioblatoma multiforme to the subventricular zone is associated with survival. Neurooncol 2013; 15: 91-96.
18. Karsy M, Gelbman M, Paarth S, Balumbu O, Moy F, Arslan E. Established and emergingvariants of glioblastoma multiforme: review of morphological and molecular features. Folia Neuropathol 2012; 50: 301-321.
19. Ku BM, Lee YK, Ryu J, Jeong JY, Choi J, Eun KM, Shin HY, Kim DG, Hwang EM, Yoo JC, Park JY, Roh GS, Kim HJ, Cho GJ, Choi WS,

Paek SH, Kang SS. CHI3L1 (YKL-40)is expressed in human gliomas and regulates the invasion, growth and survival of glioma cells. Int J Cancer 2011; 128: 1316-1326.
20. Ligon KL, Huillard E, Mehta S, Kesari S, Liu H, Alberta JA, Bachoo RM, Kane M, Louis DN, DePinho RA, Anderson DJ, Stiles CD, Rowitch DH. Olig2-regulated lineage-restricted pathway controls replication competence in neural stem cells and malignant glioma. Neuron 2007; 53: 503-517.
21. Lim DA, Cha S, Mayo MC, Chen M, Keles E, VandenBerg S, Berger M. Relationship of glioblastoma multiforme to neural stem cell regions predicts invasive and multifocal tumor phenotype. Neurooncol 2007; 9: 424-429.
22. Marshall CAG, Novitch BG, Goldman JE. Olig2 Directs Astrocyte and Oligodendrocyte Formation in Postnatal Subventricular Zone Cells. J Neurosci 2005; 25: 7289-7298.
23. McGirt MJ, Chaichana KL, Attenello FJ, Weingart JD, Than K, Burger PC, Olivi A, Brem H, Quinones-Hinojosa A. Extent of surgical resection is independently associated with survival in patients with hemispheric infiltrating low-grade gliomas. Neurosurgery 2008; 63: 700-708.
24. Michaelsen SR, Christensen IJ, Grunnet K, Stockhausen M, Broholm H, Kostaljanetz M, Poulsen HS. Clinical variables serve as prognostic factors in a model for survival from glioblastoma multiforme: an observational study of a cohort of consecutive non-selected patients from a single institution. BMC Cancer 2013; 13: 1-11
25. Park CK, Kim JH, Nam DH, Kim CY, Chung SB, Kim YH, Seol HJ, Kim TM, Choi SH, Lee SH, Heo DS, Kim IH, Kim DG, Jung HW. A practical scoring system to determine whether to proceed with surgical resection in recurrent glioblastoma. Neurooncol 2013; 15: 1096-1101.
26. Pelloski CE,Mahajan A, Maor M, Chang EL, Woo S, Gilbert M, Colman H, Yang H, Ledoux A, Blair H, Passe S, Jenkins RB, Aldape KD. YKL-40 Expression is Associated with Poorer Response to Radiation and Shorter OverallSurvival in Glioblastoma. Clin Cancer Res 2005; 11: 3326-3334.
27. Piña-Batista KM, Fernandez-Vega I, deEulate-Beramendi SA, Gutierrez-Morales JC, Kurbanov A, Asnel D, Meilán A, Astudillo A. Prognostic significance of the markers IDH1 and YKL40 related to the subventricular zone. Folia Neuropathol 2015; 53: 52-59.
28. Reya T, Morrison SJ, Clarke MF, Weissman IL. Stem cells, cancer, and cancer stem cells. Nature 2001; 414: 105-111.
29. Schiffer D, Mellai M, Annovazzi L, Caldera V, Piazzi A, Denysenko T, Melcarne A. Stem cell niches in glioblastoma: a neuropathological view. Biomed Res Int 2014: 2014: 1-7.
30. Shao R, Francescone RA, Ngernyuang N, Bentley B, Taylor SL, Moral L, Yan W. Anti-YKL-40 antibody and ionizing irradiation synergistically inhibit tumor vascularization and malignancy in glioblastoma. Carcinogenesis 2014; 35: 373-382.
31. Stupp R, Mason WP, van den Bent MJ, Weller M, Fisher B, Taphoorn MJ, Belanger K, Brandes AA, Marosi C, Bogdahn U, Curschmann J, Janzer RC, Ludwin SK, Gorlia T, Allgeier A, Lacombe D, Cairncross JG, Eisenhauer E, Mirimanoff RO; European Organisation for Research and Treatment of Cancer Brain Tumor and Radiotherapy Groups; National Cancer Institute of Canada Trials Group. Radiotherapy plus concomitant and adjuvant temozolomide for glioblastoma. N Engl J Med 2005; 352: 987-996.
32. Tabu K, Ohba Y, Suzuki T, Makino Y, Kimura T, Ohnishi A, Sakai M, Watanabe T, Tanaka S, Sawa H. Oligodendrocyte lineage transcription factor 2 inhibits the motility of a human glial tumor cell line by activating RhoA. Molecular Cancer Res 2007; 5: 1099-1109.
33. Urbanska K, Sokolowska J, Szmidt M, Sysa P. Glioblastoma multiforme- an overview. Contemp Oncol 2014; 18: 307-312.
34. Van Meir EG, Hadjipanayis CG, Norden AD, Shu HK, Wen PY, Olson JJ. Exciting new advances in neuro-oncology: the avenue to a cure for malignant glioma. Cancer J Clin 2010; 60: 166-193.
35. Yip S, Butterfield YS, Morozova O, Chittaranjan S, Blough MD, An J, Birol I, Chesnelong C, Chiu R, Chuah E, Corbett R, Docking R, Firme M, Hirst M, Jackman S, Karsan A, Li H, Louis DN, Maslova A, Moore R, Moradian A, Mungull KL, Perizzolo M, Qian J, Roldan G, Smith EE, Tamura-Wells J, Thiessen N, Varhol R, Weiss S, Wu W, Young S, Zhao Y, Mungall AJ, Jones SJ, Morin GB, Chan JA, Caincross JG, Marra MA. Concurrent CIC mutations, IDH mutations and 1p/19q loss distinguish oligodendrogliomas from other cancers. J Pathol 2012; 226: 7-16.
36. Zhang W, Kawanishi M, Miyake K, Kagawa M, Kawai N, Murao K, Nishiyama A, Fei Z, Zhang X, Tamiya T. Associationbetween YKL-40 and adult primary astrocytoma. Cancer 2010; 116: 2688-2697.
37. Zhu VF, Yang J, Lebrun DG, Li M. Understanding the role of cytokines in Glioblastoma Multiforme pathogenesis. Cancer Lett 2012; 316: 139-150.

Original article

Folia Neuropathologica

Angiocentric glioma from a perspective of A-B-C classification of epilepsy associated tumors

Dariusz Adamek[1], Grzegorz Przemysław Siwek[2], Adrian Andrzej Chrobak[2], Izabela Herman-Sucharska[3], Stanisław Kwiatkowski[4], Rafał Morga[5], Edyta Radwańska[1], Barbara Urbanowicz[6]

[1]Department of Neuropathology, Medical College, Jagiellonian University Krakow, [2]Students' Pathology Scientific Group, Medical College, Jagiellonian University, Krakow, [3]Department of Electroradiology, Medical College, Jagiellonian University, Krakow, [4]Department of Pediatric Neurosurgery, University Children's Hospital of Krakow, Medical College, Jagiellonian University, Krakow, [5]Department of Neurosurgery, University Hospital, Medical College, Jagiellonian University, Krakow, [6]Electron Microscopy Laboratory, University Children's Hospital of Kraków, Medical College, Jagiellonian University, Krakow, Poland

Folia Neuropathol 2016; 54 (1): 40-49 DOI: 10.5114/fn.2016.58914

Abstract

Angiocentric glioma (AG) is a newly-classified, very rare, WHO grade I central nervous system (CNS) lesion, occurring usually in children and young adults. Only 52 patients with AG have been reported so far, making it one of the rarest neuropathological entities. Hereby we present two new cases of AG in young subjects with detailed neuropathological investigations and a neuroradiological picture along with a brief summary of all already published literature reports of this tumor.

Histopathological examination of the resected tissue from both cases revealed similar changes characteristic of AG. The tumors were composed of spindle-like, elongated cells, forming characteristic pseudorosettes around vessels and diffusively infiltrating surrounding tissue, trapping neurons between tumor cells. Noticeably, some neoplastic cells encrusting vessels extended far beyond the main tumor mass. Hypothetically, this may be responsible for the recurrence of the tumor even in the case of apparently total excision. In immunohistochemistry, AG cells were glial fibrillary acidic protein (GFAP) and vimentin positive, also exhibiting a strikingly significant epithelial membrane antigen (EMA) dot-like staining pattern. In one of the cases, electron microscopy revealed ependymal differentiation features such as microvilli and cilia. Taken together, all these data strongly confirm a dual astroglial-ependymal nature of the tumor. Follow up corroborates benign character of this neoplasm. Both AGs reported here were immunonegative for the product of the mutated IDH-1 gene what, according to our best knowledge, has never been reported so far. It may suggest that in their pathogenesis AGs differ from grade II astrocytomas, which in most cases harbor a mutation of IDH-1. Noteworthy, neuroimaging in our cases was relatively characteristic but not conclusive, therefore biopsy (at least) is mandatory. A newly proposed so called "A-B-C" classification of long-term epilepsy-associated tumors (LEATs) places AG in a category named ANET. The authors shortly review the A-B-C classification of LEATs.

Key words: *angiocentric, glioma, electron microscopy, drug-resistant epilepsy, seizures, immunohistochemistry, LEATs, epileptomas.*

Communicating author

Dariusz Adamek, Department of Neuropathology, *Medical College*, Jagiellonian University, 3 Botaniczna St., 31-503 Krakow, Poland, e-mail: mnadamek@cyf-kr.edu.pl

Introduction

Angiocentric glioma (AG) is a very rare low-grade neoplasm, mainly affecting children and young adults. So far, to our best knowledge only 52 cases have been reported, with first literature reports dating back to 2005, when two different cases of central nervous system (CNS) lesions were described as a new pathological entity, due to their specific magnetic resonance imaging (MRI) appearance and glial and ependymal differentiation in histopathological examination [11,29]. Those findings were included in the 2007 World Health Organization (WHO) Classification of Tumours of the Central Nervous System, which classified AG as WHO I grade tumor [14]. Angiocentric glioma occurs in a broad age range, varying from 2 to 70 years of age, however it seems to affect more frequently children and young adults. Angiocentric glioma grows predominantly in supratentorial locations, usually in frontal and temporal cortex, however there are cases of lesions localized in mid-brain, amygdalae and hippocampus [13,17,19,23]. A typical symptom of AG is drug-resistant epilepsy. Some patients suffer also from headaches and vision impairments. In MRI examination, AG forms a well-demarcated lesion, hyperintense on T2 and hypointense on T1-weighted image, with "stalk-like" protrusions towards ventricle [11]. Calcifications are only rarely observed [24]. Most common treatment is surgical resection, which seems to be the most beneficial for the patients. In histopathological examination, tumor tissue exhibits a very characteristic growth pattern, in its most typical form composed of elongated, spindle like cells, arranged radially and longitudinally around vessels and forming palisade-like structures under pia. Angiocentric glioma cells exhibit a low proliferative rate, with reported labeling Ki-67 (MIB-1) indices ranging from 1 to 5%, what corroborates with benign clinical behavior observed in these tumors [12]. Notwithstanding some cases with higher mitotic rates were also reported [12,22]. In AG one can observe traits of both astroglial and ependymal-originated cells, what may suggest an origin from a hypothetical common progenitor cell. Angiocentric glioma proves to be a challenge, as the main symptom i.e. drug-resistant epilepsy and its complications e.g. cranial trauma can be misleading in the diagnostic process. Predilection to frontal and temporal cortex is also troublesome, therefore surgical resections need to be performed with extra caution, best – using neuronavigation methods, with the help of fMRI and diffusion tensor imaging (fibertracking). Due to relatively scarce information about the clinical course, optimal methods of treatment, and prognosis, every piece of information is valuable to establish valid, evidence-based methods of handling this condition. In this study, we present 2 cases of young patients with AG and a thorough functional and radiological examination, performed before the surgery.

Material and methods

Case 1

A girl aged 11 years was admitted to the regional hospital after an episode of generalized seizures. Electroencephalography (EEG) and MRI were performed. Electroencephalography examination revealed an abnormal pattern with numerous seizure spikes, registered bilaterally over frontal lobes, with the predominance of the left frontal lobe and the tendency of generalization. Magnetic resonance imaging revealed a T1 hypointense, T2 hyperintense lesion located in the left frontal lobe (Fig. 1A-E), sized 25 × 35 × 45 mm. The patient was transferred to the University Children's Hospital in Krakow with a diagnosis of brain tumor. Due to the vital site of the change (proximity to left motor and sensory cortex), additional methods of imaging: fMRI and tractography were performed to minimize the risk of collateral damage. Gross total resection of the tumor was achieved, the patient was released home with no signs of focal brain injury. During 16 months' post-operative period, neither further seizures nor other symptoms of tumor recurrence were noted.

Case 2

A male aged 25 years with no previous history of any health problems was admitted to the hospital after 3 episodes of seizures. As a result of the last epileptic episode, the patient suffered from facial trauma. In neurological examination, no signs of focal brain injury have been found. Computed tomography (CT) revealed a hyperdensive, well-demarcated mass, size of 21 × 8 mm, located in the left frontal lobe. The mass was surrounded by a zone of grade I edema. The ventricular system of the brain showed no pathological changes. Initially, the lesion was interpreted as a hemorrhagic focus of brain concussion. Due to the unknown origin of the two initial

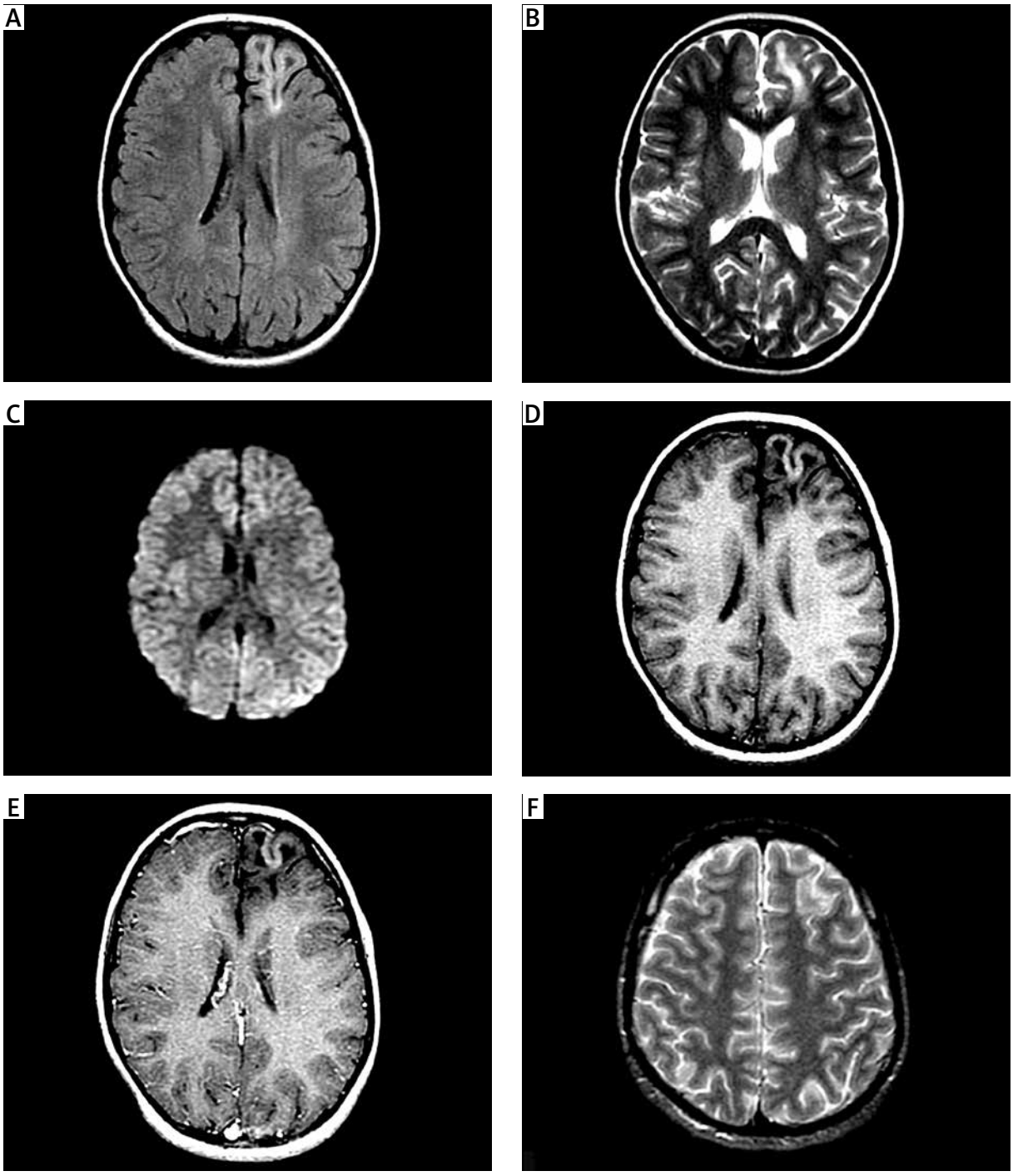

Fig. 1. Magnetic resonance imaging. Case No 1. **A)** Partially hyperintense cortically based lesion in the left frontal lobe. MRI; axial plain; FLAIR sequence. **B)** Hyperintense lesion with stalk-like extension toward the ventricle. MRI; axial plain; frFSET2 sequence. **C)** No evidence of restriction diffusion inside the lesion. MRI; axial plain; DWI sequence. **D)** Ribbon-like hyperintense rim. MRI; axial plain; SET1 sequence. **E)** No enhancement inside the tumor. MRI; axial plain; postcontrast SET1. **F)** Case No 2. Slightly bubbly hyperintense lesion in the frontal lobe, without evidence of expansion. MRI; axial plain; frFSET2.

seizures, the patient was qualified for MRI, which showed T2 hyperintense, T1 hypointense mass, located in the left frontal lobe, forming a cone-like structure (Fig. 1F), sized about 25 × 15 × 30 mm ranging from the pia up to 5 mm distance from the left lateral ventricle. The patient showed no neurological or neuropsychological abnormality. Left frontal craniotomy revealed a widened brain lobule, containing the whole mass of the tumor. The lesion was dissected with the help of neuronavigation based on brain MRI. Neurological status of the patient after the surgery did not deteriorate. On the seventh day after the surgery one episode of seizures was noted. During 40 months' follow-up repeated MRI and EEG excluded the recurrence of the tumor. Also no further seizures were observed.

Results

In both presented cases, histopathological and immunohistochemical examination of the resected tissue revealed an identical pattern (summary of immunohistochemical methods applied given in Table I). The tumors were composed of elongated cells (Fig. 2A), characteristically surrounding vessels and forming pseudorosette structures around them (Fig. 2B, C). A few delicate perivascular accumulations of glioma cells extended to some distance out of the main tumor mass (Fig. 2D). Tumor cells, adjacent to pia created a conspicuous palisading pattern (Fig. 2A). Inside of the tumor tissue, there were remaining Neu-N positive neurons, some of them trapped between AG cells, which all were immunonegative for Neu-N (Fig. 2E). Tumor cells were negative for synaptophysin, what contrasted with synaptophysin-positive neuropil background (Fig. 2F). Glioma cells were strongly immunopositive for GFAP, what indicates their astrocytic differentiation (Fig. 2G), noticeably showing conspicuous dot-like positivity for EMA, which is regarded as a signature of ependymoma (Fig. 2H). Ependymal traits were further confirmed by electron microscopy, which showed numerous microvilli, tight junctions and cilia (Fig. 2I) (electron microscopy was performed only in Case 1). In both cases tumor cells were strongly positive for vimentin and totally negative for cytokeratins (AE1/AE3). Moreover, both cases were immunohistochemically negative for mutated product of the isocitrate dehydrogenase (IDH-1) gene. Mitoses were absent and only exceptionally, single Ki-67 immunopositive nuclei were seen. Taken together, in both cases the morphological features and the pattern of immunoexpression were pathognomonic for AG.

Discussion

Considering many factors such as age, gender, localization and symptomatology of the disease, both cases present a typical course of AG. In the published cases (summarized in Table II), mean age of diagnosis was almost 18 years (mean = 17.7, SD = 16). So far, AG has been presented in 23 female and 29 male patients (total number: 52). Reported cases were located in temporal lobes (20 cases,

Table I. Summary of immunohistochemistry

Name	Company	Dillution	Unmasking	Incubation time	Detection
GFAP	DAKO	1/50	EDTA	30 min	EnVision
EMA	DAKO	1/100	–	30 min	EnVision
CD34	DAKO	1/50	Citrate buffer	60 min	EnVision
S-100	DAKO	1/400	–	30 min	EnVision
Vim	DAKO	Ready to use	–	30 min	EnVision
AE1/AE3	DAKO	1/50	Proteinase	30 min	EnVision
Ki-67	DAKO	25-Jan	EDTA	24 h	EnVision
Neu-N	Millipore	1/100	Citrate buffer	24 h	UltraVision HRP Polymer
Synaptophysine	DAKO	20-Jan	EDTA	30 min	Envision
IDH-1	Dianova	1/100	Citrate buffer	30 min	UltraVision HRP Polymer

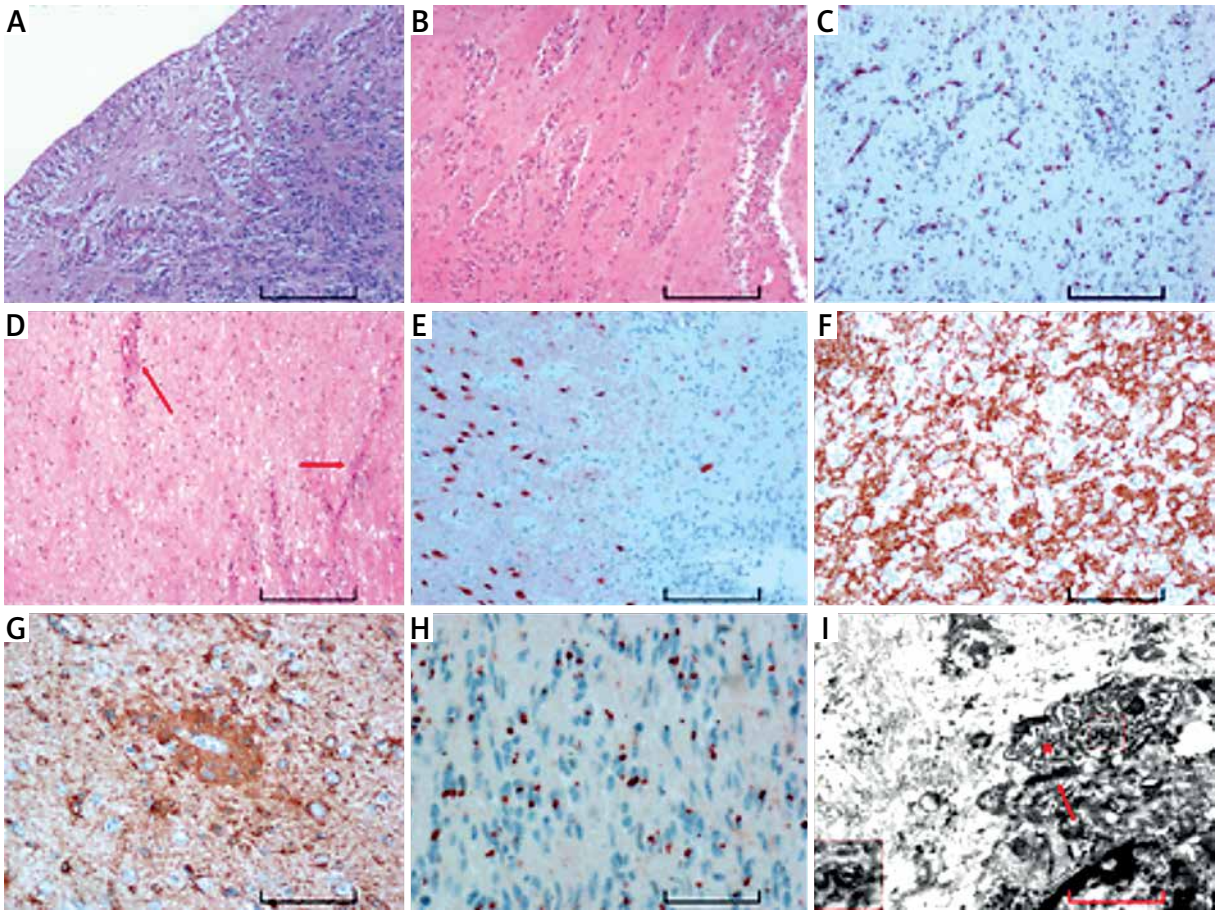

Fig. 2. Angiocentric glioma. Tumor outgrowth within the cortex, reaches pia, where it forms a palisade-like pattern **(A)** and characteristic pseudorosettes around vessels **(B)**. Perivascular arrangement is well observed in a slide stained immunohistochemically for CD34 – marker of endothelial cells **(C)**. Some vessels encrusted with single bona fide glioma cells (**D**, see arrows) extend relatively far away from the main tumor mass **(D)**. Within the invaded cortex, there are still numerous remaining neurons **(E)**. Synaptophysin-negative tumor cells contrast strongly with positive neuropil background **(F)**. Cells show strong immunopositivity for GFAP **(G)** and dot-like immunopositivity for EMA **(H)**. Electron microscopy revealed numerous microvilli (i, asterisk), cilia (i, marked with a quadrangle and enlarged in the inset), and tight junctions (i, arrowhead). Methods applied: **A, B, D** – hematoxylin-eosin, **C** – CD34, **E** – Neu-N, **F** – synaptophysin, **G** – GFAP, **H** – EMA immunostaining, **I** – electron microscopy. Case 1 represented in: **A, C, E, F, G, I,** case 2 represented in: **B, D, H**.

out of which 6 in hippocampus and 6 in amygdala), frontal lobes (18), parietal lobes (13), occipital lobes (5), insula (2) brainstem (1), thalamus (1) (the numbers do not add up to a total of 52, since in some reports locations overlap more than 1 lobe). 40/52 patients presented seizures which can be regarded as the most typical symptom of this tumor. Only a few patients suffered from focal neurological symptoms. Accordingly, in both presented cases the most prominent symptoms were also seizures, resistant to typical anti-epileptic treatment. In case 1 MRI has shown a well-demarcated lesion, with no signs of the mass effect (Fig. 1A-E). In case 2 the correct diagnosis was hindered by radiological signs of brain contusion, caused by trauma in the course of epileptic seizures. Consecutively MRI imaging revealed a lesion, suggestive of a benign/low-malignant tumor (Fig. 1F). According to WHO 2007 Classification of Tumours of the Central Nervous System, major differential diagnosis in the case of a well-delineated cortically based lesion in the frontal lobe in children with epilepsy is angiocentric glioma, oligodendroglioma, dysembryoplastic neuroepithelial tumor (DNT) and ganglioglioma [21]. Dysembryoplastic

Table II. Summary of the reported cases of AG

Authors	Year	Age of diagnosis	Gender	Localisation	Symptoms
Alexandru *et al.*	2013	12	F	Left frontotemporal	Seizures
Lu *et al.*	2013	15	M	Right frontal	Progressive left-sided weakness + headache
Aguilar *et al.*	2012	15	M	Right anterior frontal	Progressive left-sided weakness + umbness
Liu *et al.*	2012	14	M	Right posterior inferior temporal	Seizures
		22	M	Left temporal + amygdala + hippocampus	Seizures
		13	F	Anterior temporal + amygdala	Seizures
Koral *et al.*	2012	4	M	Right temporal	Development and speech delay
Grajkowska *et al.*	2011	15	F	Right temporal	Seizures
		14	M	Left occipito-parietal	Seizures
Miyahara *et al.*	2011	66	F	Right insula	Seizures
Takada *et al.*	2011	26	M	Right superior frontal	Seizures
Miyata *et al.*	2012	54	F	Left hippocampus + amygdala	Seizures
		37	M	Left uncus + amygdala	Seizures
Rho *et al.*	2011	10	F	Right medial frontal	Dizziness, otalgia, nystagmus
Marburger *et al.*	2011	10	F	Left parieto-occipital	Seizures
		15	M	Left temporal + amygdala + hippocampus	Seizures
		19	M	Left parietal	Seizures
		3	F	Left temporal + amygdala + hippocampus	Seizures
		15	M	Right thalamus	Headache + visual disturbances
Pokharel *et al.*	2011	3	M	Right posterior parietal	Seizures
Hu *et al.*	2010	19	M	Left frontal	Dizziness
Mott *et al.*	2010	57	F	Right frontal	Seizures, left hand tremor, headaches
Shakur *et al.*	2009	13	F	Left anterior temporal	Seizures + headaches
		10	M	Left posterior temporal	Hearing impairment, shortening attention span
		10	M	Left middle temporal	Seizures
Covington *et al.*	2009	5	F	Exophytic on brainstem	Severe cranial neuropathy + gait disturbance
Fulton *et al.*	2009	2	M	Right frontoparietal	Seizures
Lum *et al.*	2008	5	M	Right frontal	Seizures
Sugita *et al.*	2008	6	M	Right occipitoparietal	Seizures

Table II. Cont.

Authors	Year	Age of diagnosis	Gender	Localisation	Symptoms
Preusser *et al.*	2007	15	M	Precuneus	Seizures
		6	M	Medial temporal	Seizures
		17	M	Frontoparietal	Psychomotor disturbance
		9	F	Medial inferior temporal	Psychomotor disturbance
		37	F	Hippocampus	Seizures
		70	F	Hippocampus	Psychomotor disturbance
		35	M	Parietal	Psychomotor disturbance
		15	F	Precuneus	Seizures
Wang *et al.*	2005	3	M	Left occipital	Seizures
		14	M	Right inferior frontal	Seizures
		3	F	Left occipital	Seizures
		4	F	Right parietal	Seizures
		30	F	Left anterior temporal	Seizures
		26	M	Left frontal	Seizures
		37	M	Right frontal	Seizures
		15	F	Right medial temporal	Seizures
Lellouch-Tubiana *et al.*	2005	2	M	Right frontoparietal	Seizures
		4.5	M	Right parietal	Seizures
		6.5	M	Left frontoparietal	Seizures
		3	F	Left frontal	Seizures
		4	F	Left medial temporal	Seizures
		9.5	F	Left frontal	Seizures
		13	F	Right orbitofrontal, gyrus rectus, insula	Seizures

neuroepithelial tumor has more "bubbly" appearance on T2w images. Oligodendroglioma is a gray-white matter interface originated mass. Angiocentric glioma typically expands gyri, creates T1w hyperintense rim and stalk-like extension toward the ventricle [11]. The clue in proper diagnosis of this tumor may also be intrinsic ribbon-like T1 shortening [10]. Gangliogliomas often enhance, while angiocentric gliomas do not. The most typical findings of angiocentric glioma are presented in Case 1.

In Case 1 the operation was performed with the help of the neuronavigation, thus reducing the risk of complications. In this case, during so far 16 months' follow-up, no epileptic seizures have been observed, what is consistent with a typical course of the disease, according to the literature. In case 2, only one episode of the seizures was observed soon after surgery, but there were no seizures in the follow-up (42 months). One may speculate that this single episode of seizures reflected rather a side effect of post-operation damage, than the result of residual tumor tissue. Neuropathological investigation of resected tumors have shown a common characteristic picture of AG with especially conspicuous perivascular crowding of cells, subpial palisading, and a typical immunohistochemical staining pattern indicating shared astrocytic and ependymal properties of tumor cells.

In histopathological differential diagnosis of this tumor one needs to include low-grade neoplasms, such as DNT, which also occurs in children and manifests clinically by seizures. Literature theoretically indicates focal cortical dysplasia, low-grade astrocytoma [22], ependymoma, astroblastoma and papillary glioneuronal tumor, and even also subependymoma, pilocytic astrocytoma, and ganglion cell tumor as candidates for differential diagnosis [3]. The presence of tumor cells in distant regions from the original mass should be also noted, as it might contribute to the observed tendency for recurrence of this tumor. Neurosurgeons might contribute to these data, while planning secondary resection of the recurring tumor by further enlarging the operation area in proximity of the vessels.

In practice the most important options of differential diagnosis encompass astroblastoma, ependymoma and (less importantly) papillary glioneuronal tumor.

Given the twofold nature of AG (features of both glial and ependymal cells), it is plausible that the tumor itself could originate from the early progenitor cell. There are scarce data concerning pathophysiology of this tumor. In electron microscopy AGs exhibit signs of ependymal differentiation (microvilli, cilia, tight junctions) [29]. A diffuse infiltration pattern along with presence of immunopositivity for S100, GFAP, and vimentin is consistent with the glial (especially astrocytic) character of the tumor. Immunonegativity for synaptophysin and Neu-N helps to exclude the papillary glioneuronal tumor. The differentiation of AG with astroblastoma and ependymoma is more troublesome. Ependymoma (apart from the different location in most cases) microscopically seems to present with more slender cell nuclei and less distinct cell boundaries, and reactivity for GFAP also seems to be less pronounced than in AG. Even more disputable is to set guidelines for differentiation between AG and astroblastoma, since among others, an electromicroscopic picture may be similar to that of AG. Probably, the most helpful clue, speaking in favor of astroblastoma is the lack of subpial palisading and presence of vascular sclerosis and hyalinization [3]. Regarding its cellular composition AG, in contrast to diffuse astrocytoma, is much more monomorphic [16]. In most cases of AG, a low mitotic count is observed. However, if a high mitotic count is present it does not alter the benign character of growth [22].

According to new proposals of Blumcke *et al*., angiocentric gliomas make a separate entity (so called angiocentric neuroepithelial tumor – ANET), included in the group of tumors characteristically related to epilepsy and hence accordingly named "long-term epilepsy associated tumors" (LEATs). "Long-term epilepsy associated tumors" incorporate a large variety of neuronal and glial tumors that are encountered in patients, surgically treated for a long-time epilepsy (over 2 years). Typically, LEATs are benign tumors with presence of the neuronal component and predilection to neocortical regions, especially temporal lobes. They tend to acquire their epileptogenic potential in young age, thus in most cases, first symptoms of these neoplasms are focal seizures. "Long-term epilepsy associated tumors" present slow growth rates, therefore the prognosis for the patients, even without the radical surgery, are generally very good. However in a number of cases, progression of seizures or even anaplastic transformation to higher WHO grades have been observed [28]. Blumcke *et al*. proposed a new approach to diagnosing and treatment of a group of these tumors. This approach is applicable for both clinicians (that are responsible for weighing the risk and gains from surgery) and neuropathologists. While in the case of adult and elderly patients, diagnosis of a brain tumor is usually followed by the resection of the lesion, in LEATs patients this might not be the only conceivable way of proceeding. Children and young adults with the lesions located in typical locations for LEATs (e.g. temporal lobes) could be managed differently. At first, careful examination with the help of experienced neuroradiologists is mandatory. Due to a slow growth rate and benign behavior of the tumor, pharmacological treatment is to be introduced to achieve seizure control, however bearing in mind the adverse long-term effects of medication and impact of uncontrolled seizures on patients' cognition. When this option turns to be ineffective, surgical resection is advocated. During the surgery, one has to bear in mind that some types of LEATs tend to infiltrate the radiologically-unchanged tissue, therefore in a non-dominant lobe, gross resection of the tumor including adjacent tissues is advised. If the tumor is localized in the dominant lobe or in close proximity to vital brain regions, invasive electrocorticography is strongly advised to limit the damage, while allowing to achieve the best available effect. Regarding pathological examination of the lesion, Blumcke *et al*. proposed a new A-B-C classification of epilepsy-associated tumors, that is focused on immunochem-

istry markers (MAP2, CD34). In the case of AG, the authors proposed returning to the original term of "angiocentric neuroepithelial tumor" (ANET) [11]. Other items of A-B-C nomenclature include: BNET, CNET, DNET, ENET, GNET, INET. BNETs, regarded as "basic" oncofetal neuroepithelial tumors, are positive for CD34, and as for now are typically diagnosed as gangliogliomas. In contrast, CD34-negative tumors so far also typically diagnosed as gangliogliomas are named GNETs ("gangliocytic" neuroepithelial tumors). CNET and DNET refer to a complex (CNET), and simple ("typical") respectively form of dysembryoplastic neuroepithelial tumor (DNET = DNT). ENET, in turn, is a sort of an imprecisely defined category for tumors, negative for CD34 (ENET standing for "epileptogenic NET not otherwise specified"). Lastly, INET is to be referred to tumors so far termed as "isomorphic astrocytomas" – a variant of diffuse astrocytoma, characterized by very low cellularity and strikingly uniformed, regular morphology. Supposedly, though being diffused, they deserve rather WHO grade I than II [4].

Our results confirm the proposed diagnostic criteria of ANET (as an equivalent of AG): tumor cells in both samples were CD34 and IDH-1 negative, EMA immuno-staining showed a dot-like pattern as well as palisade-like growth pattern around the vessel. The presence of tumor cells in distant regions from the original mass should be also noted, as it might contribute to the observed tendency for recurrence of this tumor. Neurosurgeons might contribute to these data, while planning secondary resection of the recurring tumor by further enlarging the operation area in proximity of the vessels.

There are attempts to characterize the genetic signature of AGs, Preusser *et al*. using comparative genetic hybridization did not find any specific gene marker for AG: genetic aberrations in tumor cells were sparse and heterogeneous, however in 1 out of 8 cases a severe genetic imbalance was found. This aberration was a loss of chromosomal bands 6q24-q25. Imbalance on 6q is observed in many neoplasms, more interestingly, it has been described as frequent in intracranial ependymomas. Preusser states that a potential candidate gene located on 6q24.1 is PLAGL1/ZAC1 gene, which is an important transcription factor receptor, involved in regulation of the cell cycle and apoptosis. Even more interesting is that the features of neuronal degenerations (neurofibrillary tangles and Aβ plaques) in "trapped neurons" were found [23]. Vast majority of the cases presented a benign course of the disease – some patients with a history of the seizures counted in decades [20,23]. Despite that, supposedly malignant variants of AG (possibly WHO III), characterized by a higher mitotic index, vascular proliferation and necroses were also observed [1,15]. The elective method of treatment is gross total resection, but subtotal resection and chemotherapy and radiotherapy had also been used, especially in more difficult locations or to handle rare, high grade variants [1,5,16,20]. One has to acknowledge that the neuroradiological picture, though characteristic, is not definitely specific therefore at least biopsy is mandatory. The aforementioned presence of tumor cells well beyond the main tumor mass speaks in favor of the necessity of gross total resection (if possible). This approach not only should lower the risk of recurrence, but also might be of importance in treatment of epilepsy. Prognosis after gross total resection is very good, with a low incidence of recurrence of the seizures in long-term follow up and only 2 registered cases of death in the post-operative period [22]. According to Pokharel *et al*., thanks to the benign character of AG (confirmed by biopsy), some patients may live without the need of gross removal of tumor (radiotherapy only), what can be vital, especially for elderly patients [22]. New technologies like MRI, MRI-spectroscopy, diffusion tensor MRI have enabled neurosurgeons to limit collateral damage and precisely remove even diffusely infiltrating AG masses thus eliminating the origin of epileptic seizures. Our observations indicate that the vessels surrounded by tumor cells extend relatively far away from the main tumor mass (Fig. 2D), and that implies the risk of regrowth even if such event happens relatively long after surgery. We have found both AGs reported here to be immunonegative for the product of the mutated IDH-1 gene, which according to our best knowledge has never been reported so far. We are aware that it does not necessarily indicate a universal characteristic of AG, however at least in the reported cases IDH-1 negativity provides evidence that in their pathogenesis AGs differ from grade II astrocytomas, which in most cases harbor a mutation of IDH-1 [9].

Acknowledgments

The paper has been supported by Jagiellonian University in Kraków grant: No. KZDS/003862 and partially by Dariusz Adamek Specjalistyczna Prak-

tyka Lekarska Patomorfologia – Neuropatologia, ul. Zachodnia 8/3 30-350 Kraków NIP 6571874155.

Disclosure

Authors report no conflict of interest.

References

1. Aguilar HN, Hung RW, Mehta V, Kotylak T. Imaging characteristics of an unusual, high-grade angiocentric glioma: a case report and review of the literature. J Radiol Case Rep 2012; 6: 1-10.
2. Alexandru D, Haghighi B, Muhonen MG. The treatment of angiocentric glioma: case report and literature review. Perm J 2013; 17: e100-2.
3. Burger PC, Scheithauer BW, Kleinschmidt-DeMasters BK, Ersen A, Rodriguez FJ, Tihan T, Rushing EJ. Diagnostic Pathology – Neuropathology. 1st ed. AMIRSYS Inc., Salt Lake City 2012, pp. 126-131.
4. Blumcke I, Aronica E, Urbach H, Alexopoulos A, Gonzalez-Martinez JA. A neuropathology-based approach to epilepsy surgery in brain tumors and proposal for a new terminology use for long-term epilepsy-associated brain tumors. Acta Neuropathol 2014; 128: 39-54.
5. Covington DB, Rosenblum MK, Brathwaite CD, Sandberg DI. Angiocentric glioma-like tumor of the midbrain. Pediatr Neurosurg 2009; 45: 429-433.
6. Fulton SP, Clarke DF, Wheless JW, Ellison DW, Ogg R, Boop FA. Angiocentric glioma-induced seizures in a 2-year-old child. J Child Neurol 2009; 24: 852-856.
7. Grajkowska W, Matyja E, Daszkiewicz P, Roszkowski M, Peregud-Pogorzelski J, Jurkiewicz E. Angiocentric glioma: a rare intractable epilepsy-related tumour in children. Folia Neuropathol 2014; 52: 253-259.
8. Hu XW, Zhang YH, Wang JJ, Jiang XF, Liu JM, Yang PF. Angiocentric glioma with rich blood supply. J Clin Neurosci 2010; 17: 917-918.
9. Ichimura K, Pearson DM, Kocialkowski S, Bäcklund LM, Chan R, Jones DT, Collins VP. IDH1 mutations are present in the majority of common adult gliomas but rare in primary glioblastomas. Neuro Oncol 2009; 11: 341-347.
10. Koral K, Koral KM, Sklar F. Angiocentric glioma in a 4-year-old boy: imaging characteristics and review of the literature. Clin Imaging 2012; 36: 61-64.
11. Lellouch-Tubiana A, Boddaert N, Bourgeois M, Fohlen M, Jouvet A, Delalande O, Seidenwurm D, Brunelle F, Sainte-Rose C. Angiocentricneuroepithelial tumor (ANET): a new epilepsy-related clinicopathological entity with distinctive MRI. Brain Pathol 2005; 15: 281-286.
12. Li JY, Langford LA, Adesina A, Bodhireddy SR, Wang M, Fuller GN. The high mitotic count detected by phospho-histone H3 immunostain does not alter the benign behavior of angiocentric glioma. Brain Tumor Pathol 2012; 29: 68-72.
13. Liu CQ, Zhou J, Qi X, Luan GM. Refractory temporal lobe epilepsy caused by angiocentric glioma complicated with focal cortical dysplasia: a surgical case series. J Neurooncol 2012; 110: 375-380.
14. Louis DN, Ohgaki H, Wiestler OD, Cavenee WK, Burger PC, Jouvet A, Scheithauer BW, Kleihues P. The 2007 WHO classification of tumours of the central nervous system. Acta Neuropathol 2007; 114: 97-109.
15. Lu JQ, Patel S, Wilson BA, Pugh J, Mehta V. Malignant glioma with angiocentric features. J Neurosurg Pediatr 2013; 11: 350-355.
16. Lum DJ, Halliday W, Watson M, Smith A, Law A. Cortical ependymoma or monomorphousangiocentric glioma? Neuropathology 2008; 28: 81-86.
17. Marburger T, Prayson R. Angiocentric glioma: a clinicopathologic review of 5 tumors with identification of associated cortical dysplasia. Arch Pathol Lab Med 2011; 135: 1037-1041.
18. Miyahara H, Toyoshima Y, Natsumeda M, Uzuka T, Aoki H, Nakayama Y, Okamoto K, Fujii Y, Kakita A, Takahashi H. Anaplastic astrocytoma with angiocentric ependymal differentiation. Neuropathology 2011; 31: 292-298.
19. Miyata H, Ryufuku M, Kubota Y, Ochiai T, Niimura K, Hori T. Adult-onset angiocentric glioma of epithelioid cell-predominant type of the mesial temporal lobe suggestive of a rare but distinct clinicopathological subset within a spectrum of angiocentric cortical ependymal tumors. Neuropathology 2012; 32: 479-491.
20. Mott RT, Ellis TL, Geisinger KR. Angiocentric glioma: a case report and review of the literature. Diagn Cytopathol 2010; 38: 452-456.
21. Osborn AG, Salzman KL, Thurnher MM, Rees JH, Castillo M. The new World Health Organization Classification of Central Nervous System Tumors: what can the neuroradiologist really say? AJNR Am J Neuroradiol 2012; 33: 795-802.
22. Pokharel S, Parker JR, Parker JC Jr, Coventry S, Stevenson CB, Moeller KK. Angiocentric glioma with high proliferative index: case report and review of the literature. Ann Clin Lab Sci 2011; 41: 257-261.
23. Preusser M, Hoischen A, Novak K, Czech T, Prayer D, Hainfellner JA, Baumgartner C, Woermann FG, Tuxhorn IE, Pannek HW, Bergmann M, Radlwimmer B, Villagrán R, Weber RG, Hans VH. Angiocentric glioma: report of clinico-pathologic and genetic findings in 8 cases. Am J Surg Pathol 2007; 31: 1709-1718.
24. Rho GJ, Kim H, Kim HI, Ju MJ. A case of angiocentric glioma with unusual clinical and radiological features. J Korean Neurosurg Soc 2011; 49: 367-369.
25. Shakur SF, McGirt MJ, Johnson MW, Burger PC, Ahn E, Carson BS, Jallo GI. Angiocentric glioma: a case series. J Neurosurg Pediatr 2009; 3: 197-202.
26. Sugita Y, Ono T, Ohshima K, Niino D, Ito M, Toda K, Baba H. Brain surface spindle cell glioma in a patient with medically intractable partial epilepsy: a variant of monomorphousangiocentric glioma? Neuropathology 2008; 28: 516-520.
27. Takada S, Iwasaki M, Suzuki H, Nakasato N, Kumabe T, Tominaga T. Angiocentric glioma and surrounding cortical dysplasia manifesting as intractable frontal lobe epilepsy – case report. Neurol Med Chir (Tokyo) 2011; 51: 522-526.
28. Thom M, Blümcke I, Aronica E. Long-term epilepsy-associated tumors. Brain Pathol 2012; 22: 350-379.
29. Wang M, Tihan T, Rojiani AM, Bodhireddy SR, Prayson RA, Iacuone JJ, Alles AJ, Donahue DJ, Hessler RB, Kim JH, Haas M, Rosenblum MK, Burger PC. Monomorphous angiocentric glioma: a distinctive epileptogenic neoplasm with features of infiltrating astrocytoma and ependymoma. J Neuropathol Exp Neurol 2005; 64: 875-881.

Original article

Folia Neuropathologica

Time-related morphometric studies of neurofilaments in brain contusions

Mariusz Kobek[1], Zbigniew Jankowski[2], Jakub Szala[3], Zbigniew Gąszczyk-Ożarowski[4], Artur Pałasz[5], Rafał Skowronek[1]

[1]Department of Forensic Medicine and Toxicology, School of Medicine in Katowice, Medical University of Silesia in Katowice, [2]Department of Forensic Medicine, Medical University of Gdańsk, [3]Institute of Materials Science, Silesian University of Technology, Gliwice, [4]Department of Forensic Medicine, Wrocław Medical University, Wrocław, [5]Department of Histology, Chair of Histology and Embryology, School of Medicine in Katowice, Medical University of Silesia in Katowice, Poland

Folia Neuropathol 2016; 54 (1): 50-58 DOI: 10.5114/fn.2016.58915

Abstract

In forensic pathology age determination of injuries is of key importance. The purpose of the study was to analyze morphometrically changes in neurofilaments following the brain contusion and relate them to the length of the time of survival. To do this, the authors analyzed specimens of brains collected during medicolegal autopsies. According to the available literature, no such study involving material from deceased humans was conducted. The researched material was divided into nine subgroups (10 cases each) according to the time of death of persons: immediately at the crime site, 12 hours, 24 hours, 2 days, 3 days, 4 days, 5 days, 6 days and 7 days after head trauma. Neurofilaments were immunohistochemically stained and evaluated quantitatively using the Met-Ilo computer application. The initial results were then analyzed statistically with the one way analysis of variance (ANOVA) and the least significant difference (LSD) tests. It was calculated that there are significant differences in numbers and area fractions of neurofilaments within 7 days after head trauma. It must be concluded that morphometric analysis of neurofilaments is a promising method but further studies are required.

Key words: *brain contusion, neurofilaments, morphometry, survival time.*

Introduction

In medicolegal traumatology determination of the age of injuries is extremely important, as it allows to establish the time of trauma. Basing on this knowledge, in the course of legal investigation the public prosecutor can substantiate his allegations that the offense being inquired was committed at a given date.

The issue of age determination of brain contusions has been within the scope of interest of forensic pathologists and neuropathologists since the beginning of the twentieth century. The usual study method consists in analysis of morphological changes within the site of contusion which follow from complicated processes of resorption and organization of the contused nerve tissue.

Communicating author

Rafał Skowronek, MD, Department of Forensic Medicine and Toxicology, School of Medicine in Katowice, Medical University of Silesia in Katowice, 18 Medyków St., 40-752 Katowice, Poland, e-mail: rafal-skowronek@wp.pl

In everyday practice it is posttraumatic changes in the nerve tissue with concomitant cell-mediated reactions that are analyzed. Apart from classic histologic stainings immunohistochemical procedures are utilized as well. They allow for univocal identification of cells which have migrated to the site of contusion [8,30].

The literature offers tabular comparisons of morphological changes with regard to the age of brain contusion, i.e. the time that has lapsed since the trauma [2,13,17]. However, laboratory practice has shown that these methods are not accurate enough and therefore pose a danger of diagnostic errors.

Study of several different morphologic elements within the site of brain contusion increases the accuracy of analysis and, as a consequence, decreases the range of uncertainty of evaluations. Nowadays, progress in immunohistochemistry makes it possible to study structural elements of cells, including nerve tissue cells.

The authors have attempted to determine the applicability of histopathologic examination of posttraumatic changes of morphologic structures of nerve cells in victims of fatal intracranial injuries.

Because of postmortem changes, mainly autolysis, which usually obscure pathological findings, alterations in neurofilaments (NF) – structural proteins of nerve cells, which are more resistant to autolysis than other cell proteins, e.g. enzymes – have been chosen for study [11,23].

What is worth emphasizing, the available literature lacks any data on temporal changes in the neuronal cytoskeleton after brain trauma which could be used for forensic wound age estimation. This observation has been made by neuropathologists as well [8].

Material and methods

The researched material comprised specimens of sites of contusions in cortical-subcortical regions of cerebral hemispheres of 90 deceased persons whose corpses have undergone medicolegal autopsies in the Department of Forensic Medicine of the Medical University of Gdańsk in accordance with proper rulings of local public prosecutors. The comparative material consisted of specimens collected during medicolegal autopsies of 10 deceased persons who died immediately after the head trauma. This time specimens were collected from brain regions that showed neither macroscopic nor microscopic posttraumatic changes. The presence of diffuse axonal injury (DAI) was excluded by an experienced neuropathologist.

There was no need to obtain any prior approval for human subjects' research from a local bioethics committee due to the judgment of the Supreme Court which ruled that both paraffin blocks and microscopic slides comprise health records (case no. V CSK 256/10, judgment of 9 February 2011).

Circumstances of head traumas were as follows: car accidents (pedestrians, drivers and passengers), falls from height, uncontrollable falls from erect position, and assaults.

The researched material was divided into nine subgroups (10 cases each) according to the time of death of a person: immediately at the site, 12 hours, 24 hours, 2 days, 3 days, 4 days, 5 days, 6 days and 7 days after head trauma. All people who did not die immediately at the site and were treated in hospital got a similar pattern of treatment, typical for craniocerebral injuries (antiedematous drug – mannitol; steroid – dexamethasone; general anesthetic – thiopental; antitetanic anatoxin; antibiotics). One of the above-mentioned drugs – dexamethasone has a potential protective influence on neurofilament degradation what is discussed below.

The specimens were being fixed in 4% neutral buffered formaldehyde solution for 48 to 72 hours and the basic histologic tissue preparation method was applied with the use of the Shandon-Citadel 2000 autotechnicon tissue processor. Afterwards, the specimens were embedded in paraffin blocks (paraffin melting point being 56°C) and sliced in the Leica microtome into 4-micron-thick sections which were routinely stained with hematoxylin and eosin. Immunohistochemical reaction was performed using the Dako FLEX Monoclonal Mouse Anti-Human Neurofilament Protein Clone 2F11 without labelling of subunits. This antibody is specific for high-weight neurofilaments, which are considered to be the most resistant to degradation of all neurofilament types because of their highest degree of phosphorylation and ability to bind calmodulin [11,23]. The specimens were then mounted on glass slides and treated in the Dako FLEX Target Retrieval Solution High pH for demascation of the antigen. Deparaffinization and epitope revealing procedures were carried out in the PT-LINK machine for 20 minutes at 97°C. Staining was performed in the Dako Autostainer

Link 48 automaton. The specimens were dehydrated through a series of alcohol solutions of ascending concentration, passed through xylene and enclosed in Canada balsam.

In screening studies, highly fragmented and chaotically arranged NF and diversely stained background were observed which prevented from quantitative (morphometric) evaluation of changes. To circumvent this problem, in the study morphometric analysis was performed using "Met-Ilo", the image analysis application written in the Institute of Materials Science of the Silesian University of Technology [27]. Full color photomicrographs, taken at 400-fold magnification with the Axio Cam Erc 5s camera attached to the Carl Zeiss Scope A1 light microscope, were analyzed. To facilitate the analysis of biostructural image of NF additional modules were introduced.

In every histologic specimen of the nerve tissue, apart from NF there are other structures usually accompanied by information noise which is due to image artifacts produced in the course of tissue preparation and image digitalization. Therefore, before morphometric analysis is carried out it is necessary to select only such pixels that represent the analyzed structures. The end result of data processing is a binary image in which pixels of the analyzed structures are assigned a value of 1 and pixels of the background (not to be analyzed) are assigned a value of 0. The binary image is displayed as an overlay of the input image in such a way that pixels with value 0 are transparent and pixels with value 1 have a color which is determined by a user beforehand (Fig. 1).

The procedure of binarization can be carried out either manually, by a researcher, or automatically, basing on the data contained in the gray level histogram of the analyzed image. It is only in few cases that binarization immediately yields a correct binary image of analyzed objects. Therefore, the detection process has certain stages:

- modification of the input image,
- binarization,
- modification of the binary image.

Neurofilaments, which can be seen in images, are morphologically diverse as to their brightness,

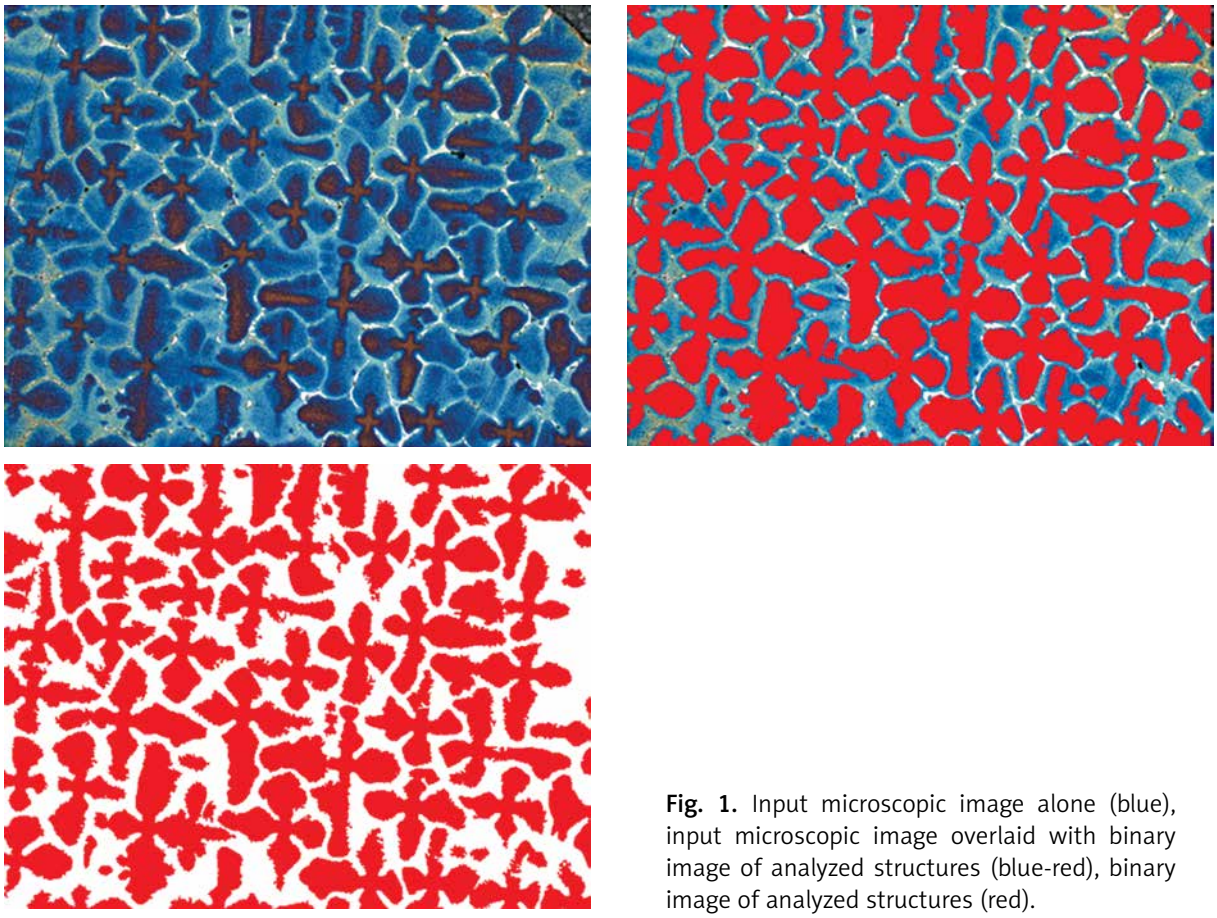

Fig. 1. Input microscopic image alone (blue), input microscopic image overlaid with binary image of analyzed structures (blue-red), binary image of analyzed structures (red).

color and area fraction (i.e. the proportion of the surface area of the detected neurofilaments to the surface area of all images). To minimize the impact of diverse brightness on results of quantitative analysis of the NF structure, the gray-scale histograms of the channels R, G and B were normalized in input images. The visual effect (Fig. 2) of this procedure is not breathtaking, but the procedure itself is critically important for correct binarization and morphometry.

Analyzed structures variably bind labelled NF antibodies. To objectify evaluation, it has been decided that only those structures would be assessed quantitatively which are intensely stained. Initial analyses have suggested that binarization of NF is most effective if performed in two stages.

In the first stage, an initial binary image, the so-called mask, is produced using the Ridler and Calvard *k*-means method [21]. In this method a histogram is divided into two areas. One area is made of pixels of the gray level lower than the threshold value *k*, the other comprises pixels of the gray level higher than the threshold value *k*. Output value of this threshold equals the arithmetic mean of minimal and maximal gray levels of the analyzed image. Each of these two areas is assigned a mean gray level (g_1 and g_2, respectively) and a new threshold value *k* is calculated from the formula $k = (g_1 + g_2)/2$. This value is used to divide the histogram into two separate areas. The procedure repeats with thresholds *k* computed in subsequent measuring loops till the threshold value *k* becomes constant.

In the second stage the *k*-means method is applied again. At this point the gray level histogram is constructed on the basis of those pixels whose value in the mask equals 1 (Fig. 3C). This kind of binarization is called geodesic binarization.

Neurofilaments and their fragments which had become visible in the course of binarization were selected with respect to their size. Structures which counted less than 10 pixels were removed from binary images, because they were most likely artifacts.

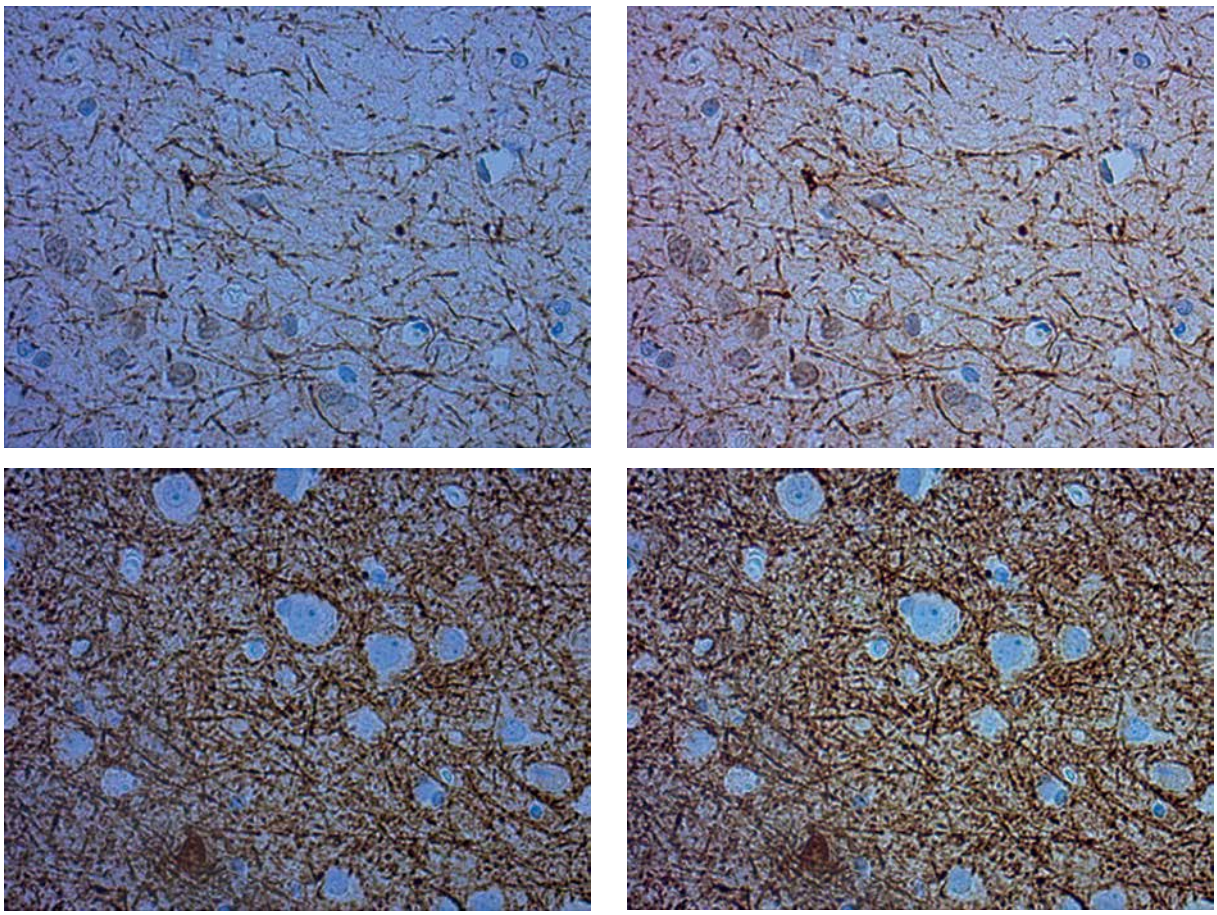

Fig. 2. Input images (left) and input images after R, G and B channel histogram normalization (right).

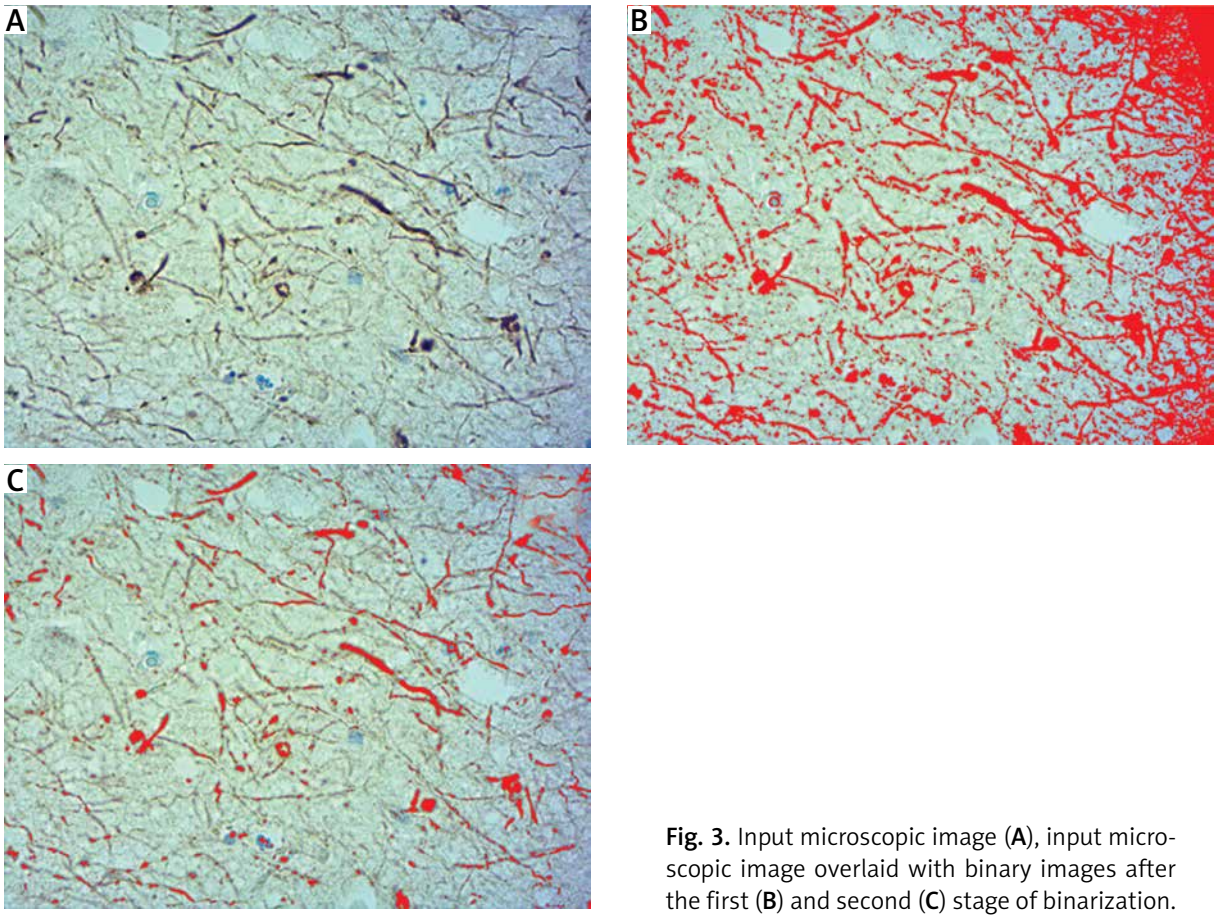

Fig. 3. Input microscopic image (**A**), input microscopic image overlaid with binary images after the first (**B**) and second (**C**) stage of binarization.

All of the above procedures were fully automated and, once initialized, operated without any participation of researchers.

Measurement was made using the Met-Ilo surface method, all available magnitudes were calculated.

Quantitative characteristics of NF comprised two features: the area fraction and the number in an analyzed field. In order to verify hypotheses that both features are normally distributed, the Shapiro-Wilk test was conducted. As the results were positive, one way analysis of variance was applied. The results are presented in Figures 4 and 5. As in both cases there were significant differences of average values ($p < 0.05$), the least significant difference test was applied.

We have compared postmortem brains of deceased individuals with and without evidence of head trauma. The test results for the two means (Student's *t*-test) showed no statistically significant differences between these two kinds of controls, both for the average of the NF area fraction ($p = 0.185$), as well as to NF number ($p = 0.517$), so the distant (non-contused) area from the same brain may be a sufficient control for the analysis of changes in the NF architecture following brain contusion.

Results

Examples of neurofilament structures after application of the Met-Ilo method are presented in Figure 6.

The results of statistical analysis of morphometric studies of NF in the researched groups are presented in Figures 4 and 5. The results of the application of the least significance difference test (value of *p* significance level) are presented in the aforementioned figures at the base of 3D bar charts. Statistically significant differences are bolded (in Figs. 4 and 5, values 0.001 actually mean $p \leq 0.001$).

Figure 4 presents the relationship between the area fraction (i.e. the density of NF) and the time

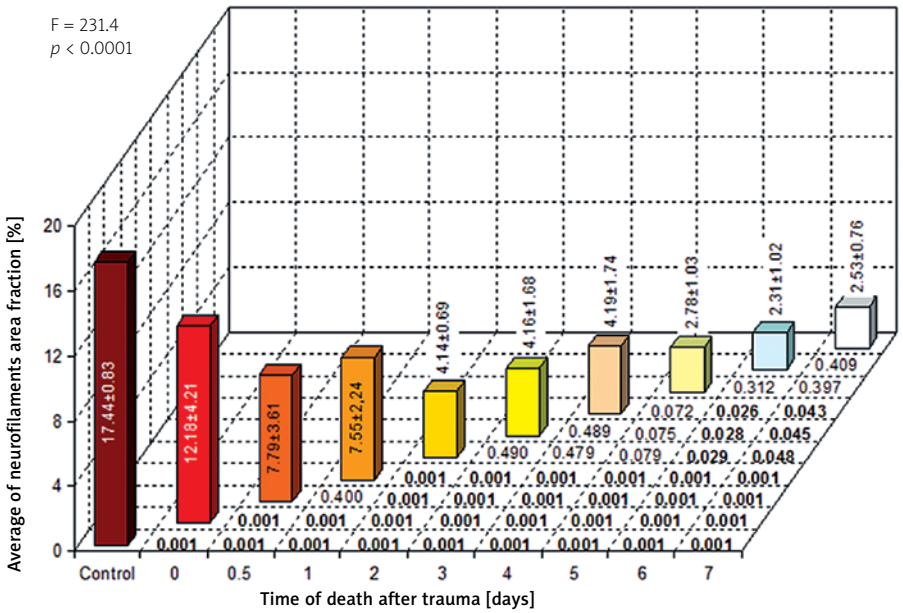

Fig. 4. The relationship between the area fraction (i.e. the density of neurofilaments) and the time lapsed after head trauma.

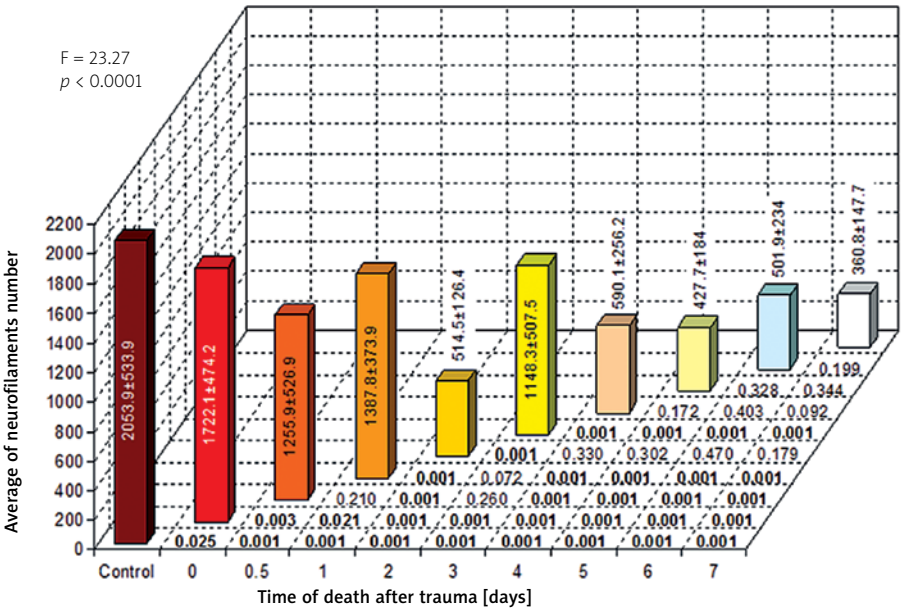

Fig. 5. The relationship between the number of neurofilaments and the time lapsed after head trauma.

lapsed after head trauma. The results of one way analysis of variance (Fig. 4) have shown that the average area fraction of NF is significantly different ($F = 231.4$; $p < 0.001$) within the period of seven days after head trauma. Calculations carried out with the least significant different method have yielded the following results:

- in the researched groups there was a statistically significant constant decrease of the area fraction of NF when compared to the control group,
- average values of the area fraction of NF after 12 and 24 hours (there were no statistically significant differences between these two) have significantly lower values than the values in the con-

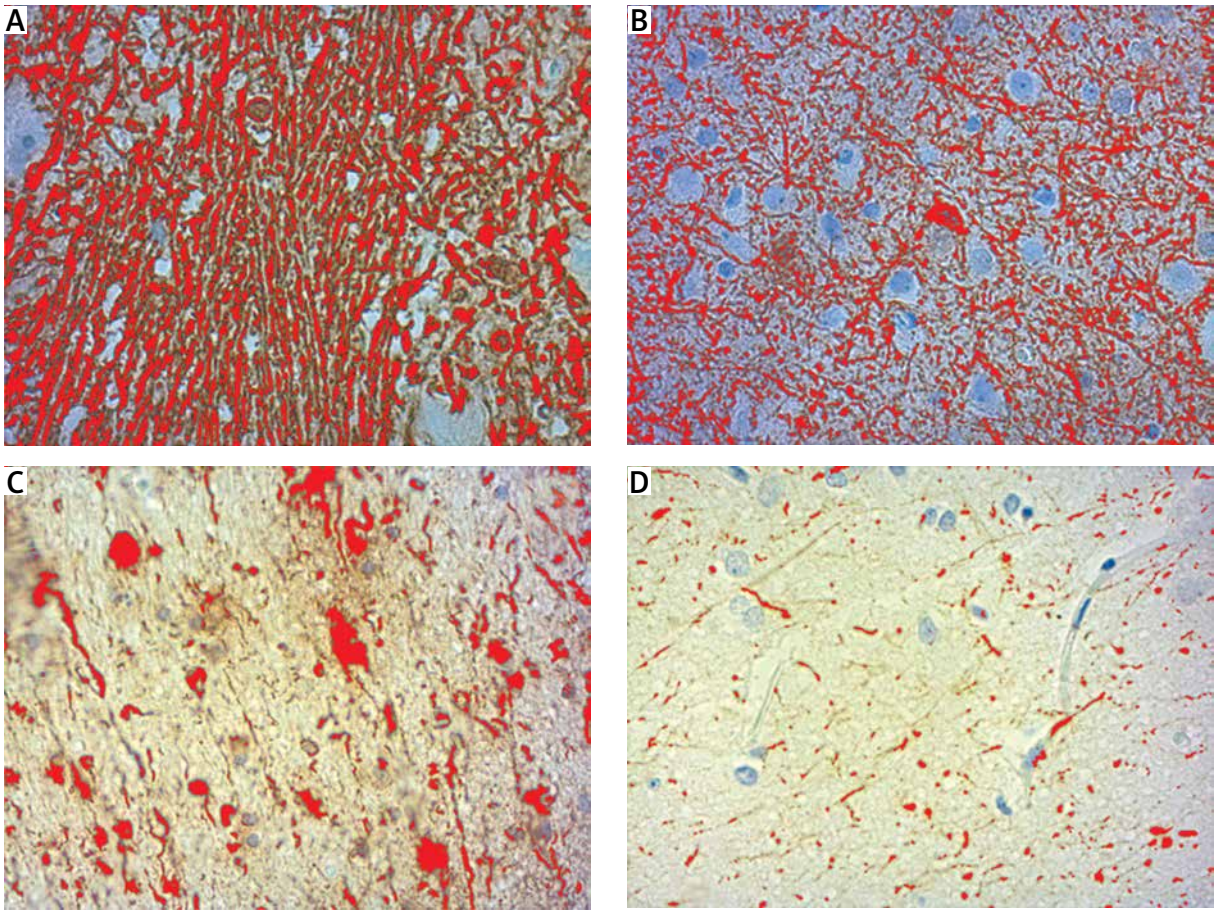

Fig. 6. Neurofilament structures: **A**) brain region remote from trauma with no damage, immediate death; **B**) contusion site, immediate death; **C**) contusion site, death 2 days after head trauma; **D**) contusion site, death 7 days after head trauma.

trol group and the initial values in the researched groups,

- from 2 to 4 days after head trauma, the average values are not significantly different, but they are significantly lower than the values in the preceding periods,
- from 5 to 7 days after trauma, there is a further decrease in the average area fraction. The average values are not significantly different, but they are lower than in the preceding periods. In spite of the lack of significance with regard to the period of 2 to 4 days after trauma, the differences are so large that they are almost statistically significant.

Figure 5 presents the relationship between the number of NF and the time lapsed after head trauma.

The results of one way analysis of variance (Fig. 5) have revealed that the average numbers of NF are statistically different ($F = 23.27$; $p < 0.001$) within the period of seven days after head trauma. Levels of significance, as calculated from the least significant different method, show that:

- the distribution of differences of average numbers of NF, when related to time after trauma, is similar to the distribution of the area fraction,
- a distinct deviation from this regularity occurs on day 3 after trauma – there is a statistically significant increase in the average number which is probably due to defragmentation,
- the average number of neurofilaments in later stages of observation decreases to a lesser extent than the area fraction.

Discussion

Neurofilaments are structural proteins which comprise the cytoskeleton of the nerve cell. The cytoskeleton is present in the perikaryon and extends into the dendrite and axons. Three kinds of proteins of different molecular weights form low-weight (NF-L),

medium-weight (NF-M) and high-weight (NF-H) neurofilaments. Neurofilaments together with cytokeratins, lamins, vimentin and vimentin-like filaments constitute intermediate filaments which scaffold the nerve cell [6,26]. NF-L, NF-M and NF-H are uniformly dispersed in the perikaryon and processes both in the central and peripheral nervous systems [28]. In the brain NF can be shown by means of immunohistochemical methods with labelled antibodies, in the cerebrospinal fluid with ELISA or Western-blotting [6,28].

Traumatic brain injuries (TBI) cause mechanical deformation of the nerve tissue, including the NF cytoskeleton, which may play a key role in the posttraumatic cessation of axonal transport [7]. Experiments have shown that TBI results in the loss of cytoskeleton proteins, including NF, such as NF68, NF200, NF300, spectrin and microtubule-associated protein 2 (MAP2). In the rat nerve tissue those changes are observed as soon as three hours after trauma. Correct reconstruction of NF and, more broadly speaking, of cytoarchitecture facilitates convalescence, but increased disarrangement of NF can cause the death of neurons, often preceded by the dysfunction of the central nervous system. Changes in NF were observed both in acute ischemia and TBI in studies involving animal experiments [1,18]. In humans as well as in animals morphologic changes in NF occur in DAI following TBI. In animals those changes are observed in sites of contusions, accompanied by selective necrosis of neurons in the brain cortex, especially in the hippocampus which is exceptionally susceptible to hypoxia and several other damaging factors [3,5,10,16,19,20,22-26].

Evaluation of quantitative alterations in NF in the site of TBI is in fact impossible due to their specific structure, size and number which can be observed only after specially-targeted staining with labelled antibodies. The morphometric method the authors have employed allows for thorough evaluation of changes in NF in the sites of contusion with respect to the time flow. Two parameters were used: the number and area fraction of NF (see above), but it appears that the relationship between the area fraction of NF and the time after injury seems more valuable.

It has been reported previously that dexamethasone – the drug given to the patients who did not die immediately at the site and were treated in hospital – has been used to prevent NF degradation and suppress vasogenic edema and inflammatory responses following brain insult [9]. There are also additional data that dexamethasone treatment maintains NF integrity following intracerebral hemorrhage damage [14]. However even with this potential protective influence of dexamethasone authors were able to see significant differences (decrease) in numbers and area fractions of NF between the studied groups.

As already mentioned, the available literature suggests that all previous studies of posttraumatic changes in NF have involved animal experimental models (rats, mice, pigs). In majority of studies, NF-H and NF-L were researched [3-5,7,10,12,15,16, 19,20,23,28]. Neurofilaments at the site of the brain contusion disintegrate, their complete disappearance was observed 1 to 2 weeks following trauma [10,20,22,26]. These results are not inconsistent with ours. In our study the last group of the deceased consists of patients who died on day 7 after trauma and at that point of time both the number and area fraction of NF have the lowest values.

Our results are consistent with results of a Czech team [29] who stained S-100B, GFAP and hyperphosphorylated NF with immunohistochemical (tissues) and biochemical (blood plasma) methods. The material they worked on had been collected from living patients with DAI who survived 10 days after trauma and from patients who died. NF-H concentration in the blood plasma was increasing with the lapse of time, which implies there is a continuous disintegration of the cytoskeleton and leakage of NF-H to the blood. Throughout the whole ten-day period the blood plasma NF-H concentration was higher in patients with DAI than in patients with limited brain injuries.

It must be noted, however, that some works have shown an increase in immunoreactivity of NF after trauma. Li et al. observed a statistically significant gradual time-dependent increase in immunoreactivity (average density) of NF-L (up to 72 hours) in certain structures of the rat brain: the corpus callosum, internal and external capsule and pyramidal tracts [15].

To sum up, we think that the morphometric analysis of NF in the sites of the brain contusion can become a valuable method for determination of the age of brain contusions. However, this promising method should be further verified by prospective studies of specimens collected from human corpses.

Disclosure

Authors report no conflict of interest.

References

1. Aronowski J, Cho KH, Strong R, Grotta JC. Neurofilament proteolysis after focal ischemia; when does cells die after experimental stroke. J Cereb Blood Flow Metab 1999; 19: 652-660.
2. Dettmeyer RB. Forensic histopathology. Springer-Verlag, Berlin Heidelberg 2011.
3. DiLeonardi AM, Huh JW, Raghupathi R. Impaired axonal transport and neurofilament compaction occur in separate populations of injured axons following diffuse brain injury in the immature rat. Brain Res 2009; 1263: 174-182.
4. Geddes JW, Bondada V, Tekirian TL, Pang Z, Siman RG. Perikaryal accumulation and proteolysis of neurofilament proteins in the post-mortem rat brain. Neurobiol Aging 1995; 16: 651-660.
5. Grady MS, McLaughlin MR, Christman CW, Valadka AB, Fligner CL, Povlishock JT. The use of antibodies targeted against the neurofilament subunits for the detection of diffuse axonal injury. J Neuropathol Exp Neurol 1993; 21: 143-152.
6. Gresle MM, Butzkueven H, Shaw G. Neurofilament proteins as body fluid biomarkers of neurodegeneration in multiple sclerosis. Mult Scler Int 2011; 2011: 315406.
7. Hamberger A, Huang YL, Zhu H, Bao F, Ding M, Blennow K, Olsson A, Hansson HA, Viano D, Haglid KG. Redistribution of neurofilaments and accumulation of beta-amyloid protein after brain injury by rotational acceleration of the head. J Neurotrauma 2003; 20: 169-178.
8. Hausmann R. Timing of cortical contusions in human brain injury. morphological parameters for a forensic wound-age estimation. In: Tsokos M (ed.). Forensic Pathology Reviews. Vol. 1. Humana Press Inc, Totowa, New Jersey 2004; pp. 53-75.
9. Holmin S, Mathiesen T. Dexamethasone and colchicine reduce inflammation and delayed oedema following experimental brain contusion. Acta Neurochir (Wien) 1996; 138: 418-424.
10. Huh JW, Laurer HL, Raghupathi R, Helfaer MA, Saatman KE. Rapid loss and partial recovery of neurofilament immunostaining following focal brain injury in mice. Exp Neurol 2002; 175: 198-208.
11. Johnson GV, Greenwood JA, Costello AC, Troncoso JC. The regulatory role of calmodulin in the proteolysis of individual neurofilament proteins by calpain. Neurochem Res 1991; 16: 869-873.
12. King CE, Canty AJ, Vickers JC. Alterations in neurofilaments associated with reactive brain changes and axonal sprouting following acute physical injury to the rat neocortex. Neuropathol Appl Neurobiol 2001; 27: 115-126.
13. Kobek M, Skowronek R, Jankowski Z, Pałasz A. Neurofilaments and traumatic brain injury. Arch Med Sadowej Kryminol 2014; 64: 268-279.
14. Lee IN, Cheng WC, Chung CY, Lee MH, Lin MH, Kuo CH, Weng HH, Yang JT. Dexamethasone reduces brain cell apoptosis and inhibits inflammatory response in rats with intracerebral hemorrhage. J Neurosci Res 2015; 93: 178-188.
15. Li S, Sun Y, Shan D, Feng B, Xing J, Duan Y, Dai J, Lei H, Zhou Y. Temporal profiles of axonal injury following impact acceleration traumatic brain injury in rats – a comparative study with diffusion tensor imaging and morphological analysis. Int J Legal Med 2013; 127: 159-167.
16. Markos S. Neurofilament dephosphorylation and microglial activation following traumatic brain injury in the immature rat. TCNJ J Student Scholarship 2011; 13: 1-10.
17. Oemichen M, Auer RN, Konig HG. Forensic neuropathology and associated neurology. Springer-Verlag, Berlin Heidelberg 2006.
18. Ogata N, Yonekawa Y, Taki W, Kannagi R, Murachi T, Hamakubo T, Kikuchi H. Degradation of neurofilament protein in cerebral ischemia. J Neurosurg 1989; 70: 103-107.
19. Posmantur R, Hayes RL, Dixon CE, Taft WC. Neurofilament 68 and neurofilament 200 protein levels decrease after traumatic brain injury. J Neurotrauma 1994; 11: 533-545.
20. Posmantur RM, Newcomb JK, Kampfl A, Hayes RL. Light and confocal microscopic studies of evolutionary changes in neurofilament proteins following cortical impact injury in the rat. Exp Neurol 2000; 161: 15-26.
21. Ridler TW, Calvard S. Picture thresholding using an iterative selection method. SMC 1978; 8: 629-632.
22. Saatman KE, Graham DI, McIntosh TK. The Neuronal cytoskeleton is at risk after mild and moderate brain injury. J Neurotrauma 1998; 15: 1047-1058.
23. Serbest G, Burkhardt MF, Siman R, Raghupathi R, Saatman KE. Temporal profiles of cytoskeletal protein loss following traumatic axonal injury in mice. Neurochem Res 2007; 32: 2006-2014.
24. Sherriff FE, Bridges LR, Gentleman SM, Sivaloganathan S, Wilson S. Markers of axonal injury in post mortem human brain. Acta Neuropathol 1994; 88: 433-439.
25. Smith DH, Meaney DF. Axonal damage in traumatic brain injury. Neuroscientist 2000; 6: 483-495.
26. Smith DH, Uryu K, Saatman KE, Trojanowski JQ, McIntosh TK. Protein accumulation in traumatic brain injury. Neuromolecular Med 2003; 4: 59-72.
27. Szala J. Application of computer-aided image analysis methods for quantitative evaluation of material structure (in Polish). Silesian University of Technology, Gliwice 2001.
28. Trojanowski JQ, Walkenstein N, Lee VM. Expression of neurofilament subunits in neurons of the central and peripheral nervous system: an immunohistochemical study with monoclonal antibodies. J Neurosci 1986; 6: 650-660.
29. Vajtr D, Benada O, Linzer P, Sámal F, Springer D, Strejc P, Beran M, Průša R, Zima T. Immunohistochemistry and serum values of S-100B, glial fibrillary acidic protein, and hyperphosphorylated neurofilaments in brain injuries. Soud Lek 2012; 57: 7-12.
30. Wang Q, Michiue T, Maeda H. Immunohistochemistry of neuronal apoptosis in fatal traumas: the contribution of forensic molecular pathology in medical science. In: Ntuli TM (ed.). Apoptosis and Medicine. InTech, Rijeka, Croatia, 2012; pp. 247-276.

Original paper

Folia Neuropathologica

Pelizaeus-Merzbacher disease in patients with molecularly confirmed diagnosis

Hanna Mierzewska[1], Ewa Jamroz[2], Tomasz Mazurczak[1], Dorota Hoffman-Zacharska[3], Elżbieta Szczepanik[1]

[1]Clinic of Child and Adolescence Neurology, Institute of Mother and Child, Warsaw, [2]Department and Clinic of Paediatrics and Neurology of Developmental Age, Upper Silesia Centre of Child's Health, Katowice, [3]Department of Medical Genetics, Institute of Mother and Child, Warsaw, Poland

Folia Neuropathol 2016; 54 (1): 59-65 DOI: 10.5114/fn.2016.58916

Abstract

Pelizaeus-Merzbacher disease (PMD) is X-linked hypomyelinating leukodystrophy caused by mutations of the PLP1 gene, which codes the proteolipid protein 1. The result of mutations is abnormal myelination – hypomyelination and dysmyelination of cerebral white matter, and in some form of the disease hypomyelinating peripheral neuropathy. DNA samples from 68 patients suspected of PMD due to the clinical course and hypomyelination at magnetic resonance imaging (MRI) were analyzed. Medical history and detailed clinical course of PMD patients were also analyzed. Different mutations of the PLP1 gene were detected in 14 boys from 11 families (~20%). Amongst the molecularly confirmed patients, 13 presented classical PMD forms but clinical phenotypes varied in the severity even amongst siblings. One patient presented a severe connatal form. One mother, obligate carrier, presented complicated SPG2 (spastic paraparesis). There was no phenotype-genotype correlation in our material. In many cases PMD was suspected with a delay of many years, sometimes only after birth of another affected child in the family. Pelizaeus-Merzbacher disease was most frequently misdiagnosed as cerebral palsy.

Key words: *Pelizaeus-Merzbacher disease, hypomyelination, dysmyelination, leukodystrophy, PLP1 gene mutations, MRI.*

Introduction

Pelizaeus-Merzbacher disease (PMD) is X-linked recessive hypomyelinating leukodystrophy resulting from mutations in the *PLP1* gene. The disease is allelic with spastic paraplegia type 2 (SPG2). The gene codes two protein isoforms, PLP1, the major component of myelin in the central nervous system and DM20 present in the peripheral nervous system [2,8]. Until now four phenotypes of PMD/SPG2 have been described. They include the severe inborn, classical, PLP1-null (with peripheral neuropathy) form of PMD, and the uncomplicated or complicated SPG2 [1-3]. Neuropathological findings in PMD include widespread lack or reduction of myelin sheets, sometimes with patchy appearance of perivascular areas (tigroid pattern) and with relatively preserved neurons and their processes [2]. In our material various pathogenic PLP1 gene mutations were detected in 15 patients.

Thirteen cases have been classified as the classical form according to international clinical, electrophysiological and brain magnetic resonance imaging

Communicating author

Hanna Mierzewska, MD, PhD, Clinic of Child and Adolescence Neurology, Institute of Mother and Child, 17A Kasprzaka St., 01-211 Warsaw, Poland, e-mail: h.mierzewska@gmail.com

(MRI) criteria of hypomyelination. They manifested variable clinical course, which could be observed even in siblings. One patient presented with the severe connatal form. One mother who was the obligate carrier manifested signs and symptoms of a complicated form of SPG2. Diagnosis of PMD was established with a delay of several years, most frequently after delivery of another affected child in the family. Most frequently PMD was misdiagnosed as cerebral palsy (CP). Below, we present a clinical pattern of the disease in patients with molecularly confirmed PMD and analyze causes of the delay in the appropriate diagnosis.

Material and methods

The analyzed material included DNA samples from 68 boys and their 58 mothers, from different centers in Poland from 2007. The inclusion criteria were hypomyelination at MRI according to R. Schiffmann and van der Knaap, including a hyperintensity of the white matter in T2 and Flair [8], characteristic brain auditory evoked potentials (decreased or absent brainstem auditory evoked potentials of waves III-V) as well as the clinical pattern and medical history. Clinical PMD phenotypes were established according to international clinical criteria as classic (onset within the first 5 years of life with the nystagmus occurring within 1-2 months of age, initial hypotonia followed by spastic quadriparesis, ataxia, titubation, dystonia, athetosis, and cognitive decline), connatal (constant nystagmus, general hypotonia, preserved deep tendon reflexes microcephaly, severe developmental delay, marked pre- and postnatal growth retardation) and complicated SPG2 (spastic paraparesis, incontinence, dementia) [1,2,8]. Pedigree analyses of all families were conducted [4,5].

Analysis of DNA samples taken from peripheral blood was performed as described in the earlier paper [4]. At first, investigation for deletion/duplication was performed by MLPA technique and in cases without PLP1 duplications we looked for the presence of the point mutations [4].

Results

Diagnosis of PMD was established in 14 boys from 11 families. Ten mothers proved to be carriers, including one symptomatic carrier with signs of a complicated spastic paraparesis. The familial cases included two sets of siblings, each with two affected brothers, in one family two first cousins were affected. Respective clinical and molecular data are listed in Table I.

Clinical data

The classical form of PMD of different severity has been diagnosed in 13 patients. One patient manifested a severe connatal form. In patients with the classical PMD the first signs and symptoms were noted between the 1st and the 8th month of life. They included nystagmus, axial hypotonia and a delayed psychomotor development, particularly concerning motor skills. Gradually, with maturation of their nervous system they developed tremor of the head and/or oscillating movements of the head (titubation), linked to nystagmus. Permanent stridor was present in some patients; in most severely affected children it was evident only while crying. In the second half-a-year or the second year of life, cerebellar ataxia became obvious within the trunk and extremities, as well as dyskinesias (mainly choreoathetoid movements), overlapping with intentional movements. In one of the patients, cerebellar ataxia persisted till the 8th year of life. Deep tendon reflexes were constantly present but elevated reflexes were noted most frequently after the 12th month of life. Spasticity did not appear until the second up to fourth year of life; in older children it was more pronounced in lower extremities. Older children manifested mainly focal or multifocal dystonia overlapping with the pyramidal signs. All the thirteen patients had psychomotor retardation, but an emotional and mental development was relatively better preserved than motor activities. One of the patients manifested normal intelligence in Leiter International Performance Scale. Ophthalmological examination detected small, pale optic discs in all patients. Nevertheless, vision was relatively well preserved. A clear neurological deterioration and regress in the development were observed after a few years, and in one case, after more than ten years.

The patient with the connatal form was delivered with signs of intrauterine growth retardation. His psychomotor development was profoundly retarded and failure to thrive was evident. His clinical pattern involved a mild, constant nystagmus, extreme muscular axial and limbs hypotonia with preserved deep tendon reflexes and slight involuntary movements of hands and feet [5]. The mother affected of SPG2 had slowly progressing spasticity of lower limbs, urine incontinence and cognitive decline. Her brain MRI revealed abnormal diffuse hypomyelination/dysmyelination.

Table I. Clinical and molecular data of patients affected by Pelizaeus-Merzbacher disease, molecularly confirmed. For detailed information of molecular data see also [4]

Family No.	Patient No.	Age of first signs (In affected children: nystagmus, axial and limbs hypotony, head tremor, developmental delay, stridor, dyskinesias)	Tentative diagnosis	Age of diagnosis (years)	Signs and symptoms when PMD was suspected Pyramido-extrapyramidal syndrome	Brain MRI: hypomyelination (hyperintensity at T2 and FLAIR)	Leiter scale IQ	Type of mutation [4]
I	1 proband	8-9 months	Cerebral palsy	13	+++	+	49	Point nonsense p. Glu129* (c.385C>T)
	2	3 months	Familial progressive encephalopathy	11	+++	+	41	
II	3 proband	3 months	Cerebral palsy	10	+++	+	30	Point missense p. Ile47Thr (c140T>C)
	4	1 month	Familial progressive encephalopathy	8	+++	+	68	
	Mother – symptomatic	21 years paraparesis	SPG2	26	Spastic paraparesis, urine incontinence, cognitive decline (SPG2)	Hypo- and diffuse dysmyelination	71	
III	5 proband	8 months	Cerebral palsy	9 (molecular confirmation at 21 years)	++	+	99	Duplication of 1-7 exons
IV	6 proband	3 months	Cerebral palsy	1.5	+	+	85	Duplication of 1-7 exons
V	7 proband	7 months	Cerebral palsy	14	+++	+	53	Duplication of 1-7 exons
	8	4 months	Familial progressive encephalopathy	10	+++	+	45	
VI	9 proband	2 months	PMD	11	+++	+	75	Point missense p.Ala88Asp (c.263C>G)
VII	10 proband	6 months	Cerebellar malformation?	4	+	+		Point missense p.Val209Asp (c.626T>A)
VIII	11 proband	Neonatal period	Spinal muscular atrophy	1	Severe developmental delay with severe hypotonia, reflexes (+); hypotrophy	+	30	Duplication of 1-7 exons

Table I. Cont.

Family No.	Patient No.	Age of first signs (In affected children: nystagmus, axial and limbs hypotony, head tremor, developmental delay, stridor, dyskinesias)	Tentative diagnosis	Age of diagnosis (years)	Signs and symptoms when PMD was suspected Pyramido-extrapyramidal syndrome	Brain MRI: hypomyelination (hyperintensity at T2 and FLAIR)	Leiter scale IQ	Type of mutation [4]
IX	12 proband	Infancy < 12 months	Cerebral palsy	17	+++	+	67	Duplication of 1-7 exons
X	13 proband	Infancy < 12 months	Cerebral palsy	1.5	++	+	75	Duplication of 1-7 exons
XI	14 proband	Infancy < 12 months	Cerebral palsy	16	+++	+	65	Duplication of 1-7 exons

In 11 out of the 14 boys (family I, II, V – see Table I), PMD was preceded by diagnosis of cerebral palsy, including three patients diagnosed with its cerebellar form and one patient suspected of cerebellar malformation. All of them were probands (the first affected family members). Just only after a few up to more than ten years, when the disorders deteriorated, or after delivery of similarly affected second child, the patients were referred to geneticists as familial progressive encephalopathy. In 4 patients, PMD was diagnosed in infancy: three brothers of an affected patient and an 11-month-old proband consulted by an experienced physician. In all the cases the decision to perform molecular testing was taken following detection of hypomyelination on MRI imaging (Fig. 1).

Molecular finding

The molecular analysis demonstrated duplication of the entire gene but of a slightly different range in seven cases (family III, IV, VII, IX, X, XI), and four point mutations of missense (family I) and nonsense types (family II, V, VI) in exons 2, 3 and 4 (see Table I) [4].

Discussion

Pelizaeus-Merzbacher disease is the best known leukodystrophy with hypomyelination. In the Czech Republic and in Germany its incidence is estimated at 1 : 90,000 to 1 : 100,000 live births [2,8]. Thus, we may conclude that in Poland many cases of PMD/SPG2 remain undiagnosed. The small group of 15 patients presented above, referred from various pediatric Polish centers since 2007 necessitates considering the reasons for such a low diagnostic efficacy. The first contributing factor may be unspecific character of clinical signs and symptoms. A similar clinical pattern can be found in several inborn and acquired diseases, of which the most frequently encountered is cerebral palsy. The "labelled" patient is referred to rehabilitation centers. In the early period of the disease the increasing muscular tonus is thought to reflect positive effects of rehabilitation. So the progress of the disease is falsely taken for improvement. Additionally some other disturbances alleviate or are modified by the maturation of the nervous system. This also makes the physicians blind to the possibility of another diagnosis. Further development of spasticity is thought to be related to evolution of cerebral palsy and the affected children probably may not return to diagnostic centers.

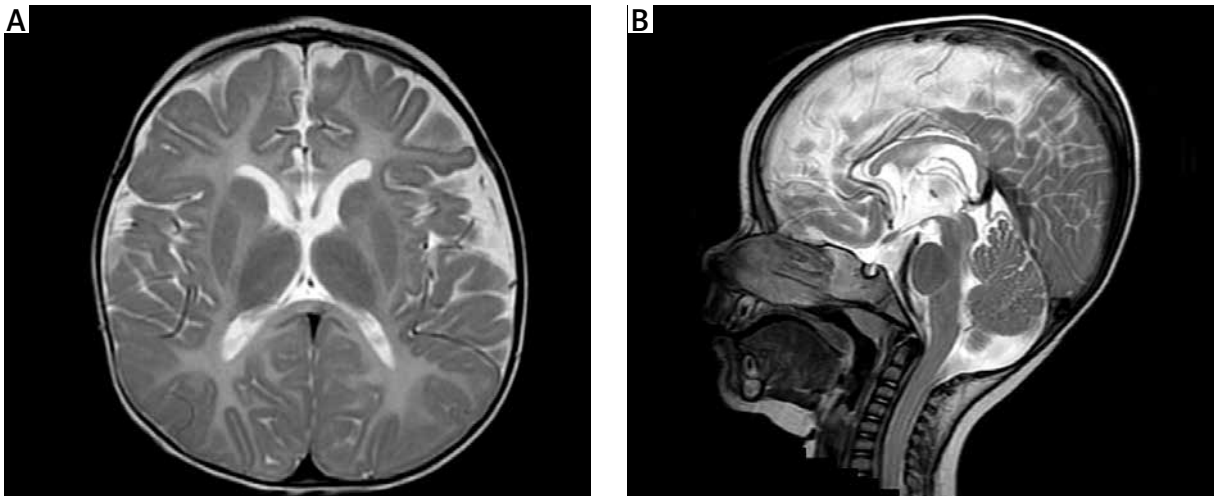

Fig. 1. A) T2-weighted magnetic resonance imaging of the brain of a 1.5-year-old patient affected by Pelizaeus-Merzbacher disease. Transverse section – mild hyperintensity (as compared to cortex) of whole white matter is visible, also in posterior limb of internal capsules. **B)** Sagittal T2-weighted magnetic resonance imaging – see very thin corpus callosum due to the decreased white matter volume.

A "red flag" does not appear until the day when another boy in the patient's family is delivered with similar signs and symptoms. As a result, the former diagnosis is revised and the child is referred to a geneticist.

The delays and errors in diagnosis of PMD are probably caused also by the currently prevalent view that all neurodegenerative diseases always manifest a gradual progressive deterioration. In contrast, the majority of children with PMD, despite neurological disturbances, show progress of various range in their psychomotor, emotional and intellectual development. They frequently acquire a number of abilities due to the enormous developmental potential of the young organism. Most of our patients started to demonstrate evident, gradual deterioration, not before a few, up to ten, years. This is confirmed by literature data [1-3,8].

The vast majority of our patients presented the classical form of PMD but of variable clinical severity even within the same family and the same mutation. This observation together with the small number of patients means that we cannot conclude about any genotype-phenotype correlations. Moreover, the patient with the connatal form of PMD also carried the duplication of the entire gene just as the patients with the classic form, which additionally confirmed the absence of such a correlation.

Differences in the clinical picture were rather related to the time when certain signs appeared as well as their intensity rather than their type. They were neither characteristic nor significant, so they did not result in any new elements in the diagnostic criteria. The variability of the disease course observed in siblings was also seen by other authors [1-3,8]. It can be explained by influence of the remaining genetic material, as well as epigenetic and environmental factors [2,8].

The diagnosis in all probands but one, just as in other rare genetic disorders, was established late, after a few up to over ten years after the appearance of the first symptoms of the disease [2,7]. Due to its X-linked inheritance, the diagnosis of PMD in familial cases may be enhanced by pedigree analysis if males are affected along the feminine line of inheritance. A proportion of PMD cases may develop de novo, which is not always acknowledged by specialists other than geneticists.

The detection of hypomyelination of the central nervous system is an indispensable element to suspect PMD or other hypomyelinating leukodystrophy (HLD). It can be demonstrated exclusively by magnetic resonance imaging (MRI) with analysis of individual time sequences, particularly at T2 and FLAIR [3]. Unfortunately, some of the probands initially had only computed tomography (CT) performed, most frequently for economic reasons. CT does not allow for correct differentiation of the lesion type (hypo-, dys- or demyelination).

Brain auditory evoked potentials (BAEP) are a second medical test which may detect hypomye-

lination but only differentiates this type of abnormality from the other white matter lesions. So the examination is not helpful and additionally available in just a few diagnostic centers.

Fundoscopic examination showed in PMD patients small, hypoplastic optic discs or their pallor, related to hypoplasia or atrophy, but not characteristic of the disease. It can be detected in several inborn or acquired diseases of the white matter [11]. It should be underlined that despite this lesion patients preserve vision for a long time.

The only investigation that can confirm the diagnosis of PMD is molecular analysis, demonstrating mutations in the *PLP1* gene [2,8]. In our material molecular confirmation of PMD was obtained in 15 cases per 68 DNA samples (around 20%) submitted for testing. Duplications encompassing 7 exons (the entire gene) were found in 7 cases, whereas point mutations of missense or nonsense type (see also the Table) were demonstrated in the remaining cases [4,5]. The duplication results in overproduction of PLP and DM20 proteins while the remaining mutations result in their abnormal (missense) or truncated (nonsense) form [2,8].

In the remaining 39 patients mutations have not been detected. It might be due to still insufficient molecular investigative techniques or to the fact that a similar clinical picture may result from other genetic causes. For the last two decades molecular genetics development have allowed to demonstrate heterogeneity of HLD [8,11,12]. Apart from PMD, more than ten HLD were established, manifesting various types of the inheritance pattern [6,8,11]. The clinical course of these diseases may be similar to that of PMD or sometimes additional signs are present e.g. hypodontia, cataract or atrophy of basal ganglia on MRI [9-12]. Moreover, world experts in the white matter diseases state that unclassified leukodystrophies with hypomyelination still exist [9,11]. These new findings may be accessed by available online international internet data bases, such as OMIM or www.genereview.org, that are regularly updated.

Conclusions

The classical PMD form represents a slowly progressing leukodystrophy, with apparent clinical improvement in the first years and deterioration not observed until the later period of life. The MRI is an essential method for detection and differentiation of white matter lesion types. The diagnosis of PMD can be confirmed only with molecular analysis. Genetic confirmation of the diagnosis allows to cover the family with genetic counselling and to suggest an appropriate supportive therapy. It also terminates a long-standing and very expensive diagnostic process, which in addition can be emotionally very painful for all the family members.

It is highly probable that a considerable number of PMD patients remain undiagnosed, so boys with a "label" of cerebral palsy should be watched carefully for alternative diagnosis.

Acknowledgements

We are sincerely grateful to our patients and their parents for their participation in the study as well for their informed consent to DNA analysis and publication. We are also grateful to doctors Antoni Kierdaszuk, Jolanta Wierzba and Anna Jakubiuk-Tomaszuk who referred the patients to our center.

Disclosure

Authors report no conflict of interest.

References

1. Cailloux F, Gauthier-Barichard F, Mimault C, Isabelle V, Courtois V, Giraud G, Dastugue B, Boespflug-Tanguy O. Genotype-phenotype correlation in inherited brain myelination defects due to proteolipid protein gene mutations. Eur J Hum Genet 2000; 8: 837-845.
2. Garbern JY, Krajewski K, Hobson G. PLP1-related disorders. Gene Reviews 2010; available at: http://www.ncbi.nlm.nih.gov/books/NBK1182 [Accessed February 2015].
3. Grossi S, Regis S, Biancheri R, Mort M, Lualdi S, Bertini E, Uziel G, Boespflug-Tanguy O, Simonati A, Corsolini F, Demir E, Marchiani V, Percesepe A, Stanzial F, Rossi A, Vaurs-Barrière C, Cooper DN, Filocamo M. Molecular genetic analysis of the PLP1 gene in 38 families with PLP1-related disorders: identification and functional characterization of 11 novel PLP1 mutations. Orphanet J Rare Dis 2011; 6: 40.
4. Hoffman-Zacharska D, Mierzewska H, Szczepanik E, Poznański J, Mazurczak T, Jakubiuk-Tomaszuk A, Mądry J, Kierdaszuk A, Bal J. The spectrum of PLP1 gene mutations in patients with the classical form of the Pelizaeus-Merzbacher disease. Med Wieku Rozwoj 2013; 17: 293-300.
5. Hoffman-Zacharska D, Mierzewska H, Mazurczak T, Derwińska K, Górka K, Kłyszejko J, Szkudlińska-Pawlak S, Szczepanik E. Connatal Pelizaeus-Merzbacher disease caused by Xq21-22 submicroscopic duplication including the PLP1 gene – case report. Neurol Dziec 2013; 45: 73-77 [in Polish].

6. Lyons G, Kolodny EH, Pastores GM. Neurology of hereditary metabolic disorders of children. 3rd ed. McGraw-Hill, New York 2006.
7. Mądry J, Hoffman-Zacharska D, Królicki L, Jakuciński M, Friedman A. PLP1 gene duplication as a cause of the classic form of Pelizaeus-Merzbacher disease – case report. Neurol Neurochir Pol 2010; 44: 511-515.
8. OMIM. Available online at www.ncbi.nlm.nih.gov/omim [Accessed February 2015].
9. Schiffmann R, van der Knaap MS. Invited Article: an MRI-based approach to the diagnosis of white matter disorders. Neurology 2009; 72: 750-759.
10. Steenweg ME, Vanderver A, Blaser S, Bizzi A, de Koning TJ, Mancini GM, van Wieringen WN, Barkhof F, Wolf NI, van der Knaap MS. Magnetic resonance imaging pattern recognition in hypomyelinating disorders. Brain 2010; 133: 2971-2982.
11. Vanderver A, Tonduti D, Schiffmann R, Schmidt J, Van der Knaap MS. Leukodystrophy overview. In: Pagon RA, Adam MP, Ardinger HH, Bird TD, Dolan CR, Fong CT, Smith RJH, Stephens K (eds.). GeneReviews® [Internet]. Seattle (WA): University of Washington, Seattle; 1993-2014. http://www.ncbi.nlm.nih.gov/books [Accessed February 2015].
12. Wolf NI, Vanderver A, van Spaendonk RM, Schiffmann R, Brais B, Bugiani M, Sistermans E, Catsman-Berrevoets C, Kros JM, Pinto PS, Pohl D, Tirupathi S, Strømme P, de Grauw T, Fribourg S, Demos M, Pizzino A, Naidu S, Guerrero K, van der Knaap MS, Bernard G; 4H Research Group. Clinical spectrum of 4H leukodystrophy caused by POLR3A and POLR3B mutations. Neurology 2014; 83: 1898-1905.

Original paper

Folia Neuropathologica

Application of molecular imaging combined with genetic screening in diagnosing MELAS, diabetes and recurrent pancreatitis

Wang Zhiping[1#], Li Quwen[2#], Zhou Hai[1], Zhou Jian[1], Gao Peiyi[1]

[1]Department of Radiology, Beijing Tian Tan Hospital, Capital Medical University, Beijing, [2]Department of Priority Laboratory for Zoonoses Research, Fujian Central for Disease and Prevention, Fuzhou, China

[#]These authors contributed equally to this manuscript.

Folia Neuropathol 2016; 54 (1): 66-71

DOI: 10.5114/fn.2016.58917

Abstract

Aim: *We report molecular imaging combined with gene diagnosis in a family with 7 members who carried an A3243G mutation in mitochondrial tRNA and p.Thr 137 Met in cationic trypsinogen (PRSS1) gene presented with mitochondrial encephalomyopathy, lactic acidosis, and stroke-like episodes (MELAS), diabetes, and recurrent pancreatitis.*

Material and methods: *DNA sequencing was used to detect and validate mitochondrial DNA and PRSS1. We also verified that mitochondrial heterozygous mutations and c.410 C>T mutation causing p.Thr 137 Met could be detected in oral epithelial cells or in urine sediment cells. In addition, molecular imaging was carried out in the affected family members.*

Results: *In this pedigree, MELAS syndrome accompanied by pancreatitis was an important clinical feature, followed by diabetes. Heteroplasmy of the mtDNA A3243G and c.410 C>T mutation of PRSS1 was found in all tissue samples of these patients, but no mutations were found in 520 normal control and normal individuals of the family. However, based on molecular imaging observations, patients with relatively higher lactate/pyruvate levels had more typical and more severe symptoms, particularly those of pancreatic disease (diabetes or pancreatitis).*

Conclusions: *MELAS syndrome may be associated with pancreatitis. For the diagnosis, it is more reasonable to perform molecular imaging combined with gene diagnosis.*

Key words: *MELAS, pancreatitis, PRSS1 mutation, molecular imaging, clinical features.*

Introduction

Mitochondrial myopathy, encephalopathy, lactic acidosis, and stroke-like episodes syndrome (MELAS) are established phenotypes of mitochondrial encephalomyopathy. MELAS has been reported worldwide in recent decades [10,20,22]. It has been confirmed that a mitochondrial DNA (mtDNA) 3243A>G transition was associated with MELAS in most of these patients and that mutations in mtDNA could be useful for revealing the nature of MELAS. However, reports of MELAS combined with pancreatitis are uncommon and its pathogenesis remains unclear. In addition, a misdiagnosis or a missed diagnosis of pancreatitis combined with MELAS could be

Communicating author

Dr. Wang ZP, Department of Radiology, Beijing Tian Tan Hospital, Capital Medical University, Beijing 100050, China, e-mail: ping1023@139.com

fatal [1,5]. In this paper, we report on a Chinese family afflicted by MELAS combined with diabetes and recurrent pancreatitis.

MELAS, which forms a major clinical subgroup of the mitochondrial encephalomyopathies, is caused by any of several different single base replacements in the mt $tRNA^{Leu(UUR)}$ gene, which is responsible for the translation of UUR (R = A or G) leucine codons in mitochondrial genes [1-5]. It has been reported that 15% of patients with mitochondriopathies have symptoms of digestive disorders [3,7,14]. In contrast, mitochondrial dysfunction in the pancreas frequently results in diabetes mellitus and exocrine insufficiency, but only rarely leads to acute or chronic pancreatitis. Therefore, it was necessary to study the differences between the patients from this pedigree, particularly with regard to the differential diagnosis of pancreatitis.

In recent years, scientific advances have provided us with more comprehensive and objective insights into the pathophysiology of pancreatitis. Since the first discovery of the trypsinogen gene (*PRSS1*) mutations in hereditary pancreatitis, a variety of gene defects associated with pancreatitis have been reported. Mutations that lead to the generation of more trypsin, or reduce the activity of trypsin inhibitors or trypsin degradation, have been reported to be associated with pancreatitis, either alone or in epistasis. This has broadened the horizon to understand the mechanisms of the disease, and has helped to identify those who are at risk of developing pancreatitis. For many years, inappropriate intra-acinar trypsinogen activation has prevailed as a key initiator of pancreatitis, although the evidence is not direct or concrete [13,17]. Continued experimental studies are necessary to determine the specific relations of trypsin-antitrypsin imbalance and genetic heterogeneity in MELAS.

Material and methods

Patients

This study was approved by the Capital Medical University Committee and Fujian Central for Disease and Prevention Committee and all study participants gave informed consent to DNA analyses. Clinical information for the proband and 4 other family members was obtained by personal interviews using a structured questionnaire and/or clinical trials.

Materials

Mutant loads from the female carriers were assessed using peripheral blood samples and, if possible, urine and/or oral mucosa samples. In addition, hair follicles and muscle tissue were taken from the proband and his mother.

Clinical data

A total of 5 members from the maternal pedigree were included in this survey (Fig. 1): 2 males (II3, III1) and 3 females (I2, II2, II5). We recorded age, height, body weight, and other physiological conditions for the maternal pedigree. Any history of seizures and stroke-like episodes were recorded. Subjects took a Mini-Mental State Examination (MMSE) to evaluate their cognitive function. A standard vision chart, and pure tone and audiometry were used to determine vision and hearing conditions. We also tested ECG, EEG, and EMG. All family members also had tests for plasma lactate while in a resting state and at 15 minutes after a stepping exercise.

DNA extraction and molecular genetic analysis

Genomic DNA was extracted from peripheral blood and other tissue specimens using a QIAamp DNA mini kit (Qiagen, Germany). Three genes involved in pancreatitis – *PRSS1, SPINK1*, and *CFTR* – were sequenced according to references [11,12,18]. The mtDNA3243 A>G and PRSS1 c.410 C>T mutations (p.Thr 137 Met) were examined by polymerase chain reaction (PCR) and direct sequencing. For sequencing, a Perkin Elmer Big Dye Sequencing kit (Perkin-Elmer,

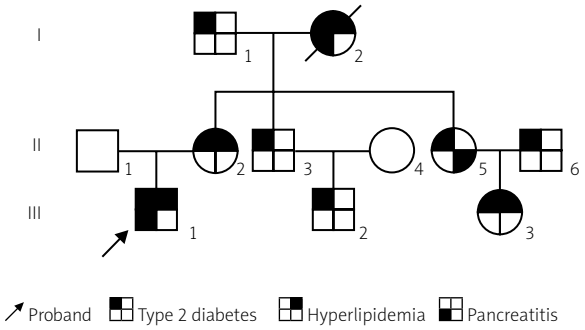

Fig. 1. Pedigree of the family carrying the mitochondrial DNA A3243G and *PRSS1* p.Thr 137 Met mutation.

Shelton, CT, USA) and an ABI PRISM7700 sequencer (Perkin-Elmer ABI, Foster City, CA) were used.

Results

Clinical data and ancillary test

Patient III1, a man born in 1992, had non-insulin-dependent (type 2) diabetes mellitus that began at the age of 16 and pancreatitis that first time occurred at the age of 10. Recent hospitalization was because of paroxysmal unconsciousness, convulsions limbs for 9 days and repeated vomiting for 7 days. The patient was diagnosed with emaciation, memory, computing and understanding power decreased significantly, tendon reflexes slowly and meningeal irritation-positive. CSF pressure was 80 mm H_2O, lactic acid was 3.5 mmol/l (normal < 2.1 mmol/l) and sugar, protein and Cl^- were normal. Plasma lactate (L) was 3.18 µmol/l, pyruvate (P) was 0.154 µmol/l and the ratio of L/P is 20.60, serum amylase fluctuations were 258-602 U/l. The proband was given control of epilepsy, gastrointestinal decompression and parenteral nutrition and high doses of coenzyme Q and symptoms were improved after treatment. The man strictly follows doctor's orders and is followed up every 3 months and acquisition of peripheral blood, hair follicle and urine sediment samples from the patients was under the approval of Fujian Medical Ethics Committee.

PCR-RFLP and molecular genetic analysis results are shown in Figure 2 and 3. Heteroplasmy for the A3243G mutation in mtDNA was found in all samples from the affected patients (II2, II3, II5, III1). The proportion of mutated mtDNA varied from 36 to 73%, depending on the tissue analyzed. In selected patients of non-disease state, there were no significant differences in heteroplasmy for the A3243G mutation in mtDNA. In addition, in the affected patients, no mutations were found in the genes coding for *PRSS1, SPINK1*, and *CFTR*.

Molecular genetic analysis

Heteroplasmy for the A3243G mutation in mtDNA was found in all samples from the affected patients. The proportion of mutated mtDNA varied from 36 to 73%, depending on the tissue analyzed. In selected patients of non-disease state, there were no significant differences heteroplasmy for the A3243G mutation in mtDNA. In addition, in the affected patients, no mutations were found in the genes coding for *PRSS1, SPINK1*, and *CFTR*.

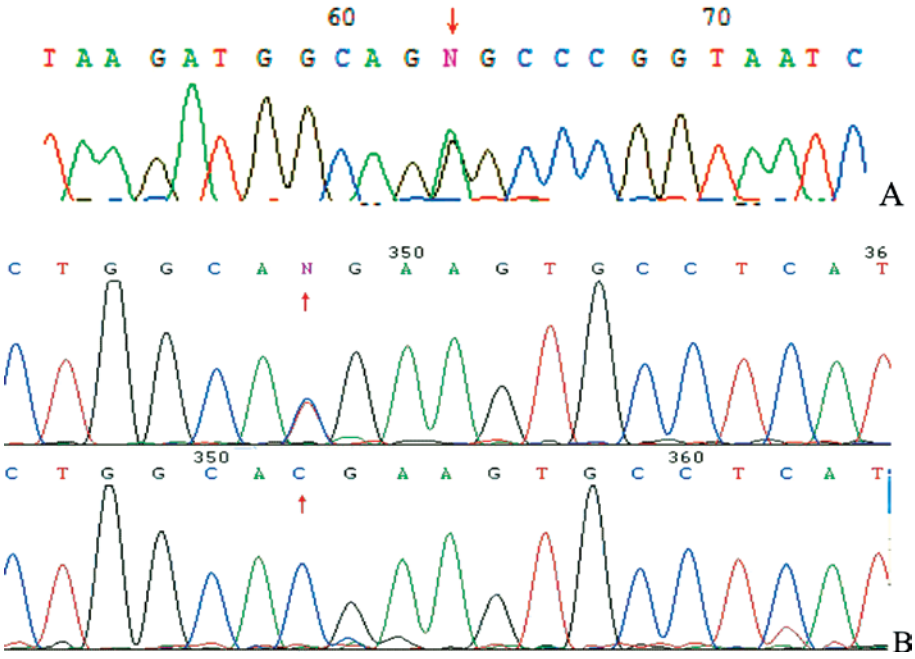

Fig. 2. Mutations of mtDNA and the *PRSS1* gene. **A**) A3243G mutation in mtDNA. **B**) c.410 C>T (p.T137M) mutation in the *PRSS1* gene.

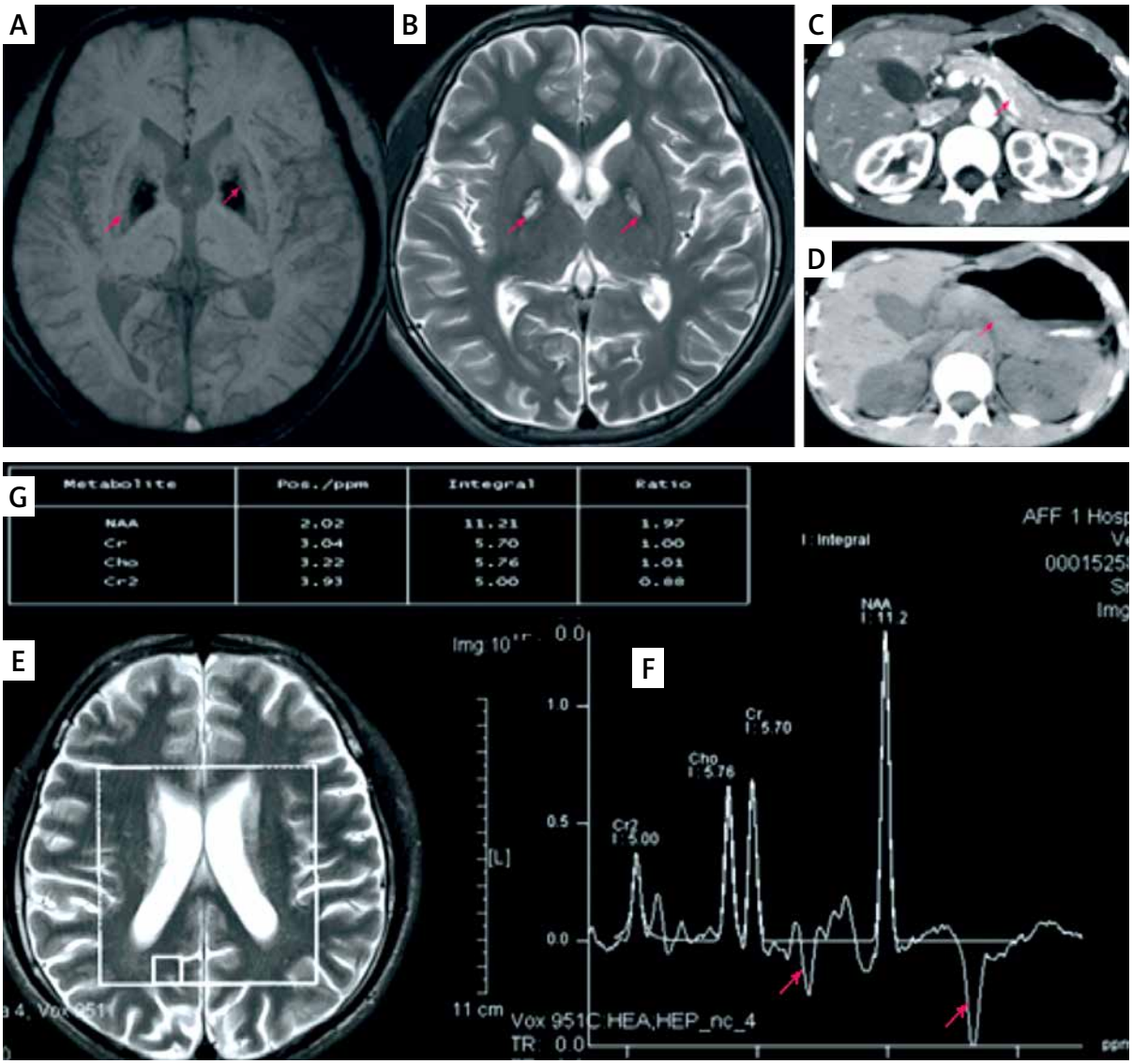

Fig. 3. Proband imaging findings. **A**) and **B**) Brain MRI findings. **C**) Enhanced CT findings of pancreas. **D**) CT findings of pancreas. **E-G**) Molecular imaging findings.

Imaging data

Imaging showed bilateral malacia limb internal capsule, surrounding hemosiderin deposition, symmetry of abnormal signal intensity in the bilateral caudate nucleus, brain atrophy, an inverted lactate peak could be seen in bilateral basal ganglia, bilateral dorsal thalamus and parietal white matter, and the NAA/Cho ratio was not reduced suggesting the local accumulation of lactic acid. His pancreas was fully formed and had a small amount of leakage around it. It had a dilated descending part, considered to be due to an obstruction.

Discussion

The A3243G transition in the *MTTL1* mitochondrial gene is the most common pathogenetic mutation found in mtDNA [2,11,12,18]. This mutation is associated with a broad spectrum of clinical manifestations, including mitochondrial encephalomyopathy, lactic acidosis, stroke-like episodic syndrome (MELAS) and maternally inherited diabetes and deafness syndrome (MIDD) [4,8,15,21]. Diabetes mellitus and exocrine insufficiency are the most common pancreatic features of mitochondriopathy. In contrast, to date there have been only six reports of patients with

acute or chronic pancreatitis associated with mtDNA mutations. Four of these cases involved the A3243G mutation. Therefore, clinicians should be aware of the possibility of a missed diagnosis or a misdiagnosis of MELAS accompanied by pancreatitis [9]. The molecular diagnostic accuracy of MELAS is directly related to the choice of samples as the mitochondrial mutation load is quite different in different tissues and the mutation load is usually low in peripheral blood [16]. This is because mitochondrial DNA is divided randomly among daughter cells during mitosis and the daughter cells have different proportions of mutant or wild-type mitochondrial DNA.

In this study, urinary sediment cells and oral epithelial cells were collected, which have good diagnostic performance and are convenient samples to be collected for non-invasive screening of the family members of patients. The hair follicle is also a sensitive tissue that has the A3243G point mutation in its mitochondrial DNA. During aging, this mutation will disappear in blood cells, while hair follicles will maintain this mutation and have the advantages of ease of collection and storage, and can also be used to screen asymptomatic family members for genetic counseling.

The diagnosis and differential diagnosis of MELAS should be based on clinical symptoms, molecular biology, iconography, and other comprehensive analyses. The standard for detection is the sequencing of nuclear gene mutations. However, in the field of molecular diagnostics for mitochondrial diseases, owing to the considerably high frequency of mtDNA polymorphisms, which often is the variation due to homogeneity, and the limitations of sequencing, it is considered that those cases with mutation rates of 0-20% or 80-100% can easily be mistaken as homogeneity. Therefore, for the screening of heterogeneous cases, the sequencing method should be used in conjunction with other methods, such as restriction enzyme digestion, PCR primer mismatch, and other methods that can, to some extent, compensate for the disadvantages of sequencing for predicating possible heterozygous mutations. In addition, the proportions of different genotypes can be obtained when using gel scanning technology.

In the clinical diagnosis of mitochondrial disease, because of a variety of internal and external factors, the functional status of mitochondria is enormously diverse and it is difficult to confirm a precise definition of encephalomyopathy from any single aspect of clinical symptoms, pathological or biochemical. MtDNA mutation testing is helpful for diagnosing mitochondrial diseases, but it is not the only means. In recent years, with the rapid development of molecular imaging technology (spectroscopy), the direct finding of a lactate peak (areas of lactic acid accumulation) in the pineal body region using computer integration of data has contributed to the diagnosis of MELAS [19].

Pancreatitis may also be explained by a similar mitochondrial energy defect or vascular dysfunction. Although there is no direct evidence for vascular involvement in the pancreas of patients with the A3243G mutation, it is known that this organ is susceptible to ischemic injury, and perturbations of the systemic and pancreatic micro-vascularization play a significant role in the pathogenesis of pancreatitis [6]. In addition, mitochondrial diseases, including MELAS, are associated with an excess production of reactive oxygen species (ROC), which mostly occurs in the mitochondria as byproducts of oxidative phosphorylation, and has been described as an important factor in the pathogenesis and progression of pancreatitis [23].

In patients with MELAS, non-specific gastrointestinal symptoms, including constipation, stomach upset, liver disease, recurrent vomiting or recurrent pancreatitis, are being increasingly recognized. Different diseases share the same point base mutation leading to an “overlap syndrome” and the same clinical phenotypes can be caused by mutations at multiple sites. This means that it remains unknown whether the clinical symptoms of mitochondrial diseases are caused by a single gene mutation or by the interaction of mutations at different sites and heterogeneity. Thus, there are many problems that remain to be explored.

Disclosure

Authors report no conflict of interest.

References

1. Bouchet C, Steffann J, Corcos J, Monnot S, Paquis V, Rötig A, Lebon S, Levy P, Royer G, Giurgea I, Gigarel N, Benachi A, Dumez Y, Munnich A, Bonnefont JP. Prenatal diagnosis of myopathy, encephalopathy, lactic acidosis, and stroke-like syndrome: contribution to understanding mitochondrial DNA segregation during human embryofetal development. J Med Genet 2006; 43: 788-792.
2. Brandon MC, Lott MT, Nguyen KC, Spolim S, Navathe SB, Baldi P, Wallace DC. MITOMAP: a human mitochondrial genome database – 2004 update. Nucleic Acids Res 2005; 33: 611-613.

3. Burim RV, Canalle R, Martinelli Ade L, Takahashi CS. Polymorphisms in glutathione S-transferases GSTM1, GSTT1 and GSTP1 and cytochromes P450 CYP2E1 and CYP1A1 and susceptibility to cirrhosis or pancreatitis in alcoholics. Mutagenesis 2004; 19: 291-298.
4. Canafoglia L, Franceschetti S, Antozzi C. Epileptic phenotypes associated with mitochondrial disorders. Neurology 2001; 56:1340-1346.
5. Craven L, Tuppen HA, Greggains GD, Harbottle SJ, Murphy JL, Cree LM, Murdoch AP, Chinnery PF, Taylor RW, Lightowlers RN, Herbert M, Turnbull DM. Pronuclear transfer in human embryos to prevent transmission of mitochondrial DNA disease. Nature 2010; 465: 82-85.
6. Cuthbertson CM, Christophi C. Disturbances of the microcirculation in acute pancreatitis. Br J Surg 2006; 93: 518-530.
7. Debray FG, Drouin E, Herzog D, Lortie A, Lambert M, Garel L, Mitchell GA, Michaud JL. Recurrent pancreatitis in mitochondrial cytopathy. Am J Med Genet A 2006; 140: 2330-2335.
8. de Vries MC, Rodenburg RJ, Morava E, van Kaauwen EP, ter Laak H, Mullaart RA, Snoeck IN, van Hasselt PM, Harding P, van den Heuvel LP, Smeitink JA. Multiple oxidative phosphorylation deficiencies in severe childhood multi-system disorders due to polymerase gamma (POLG1) mutations. Eur J Pediatr 2007; 166: 229-234.
9. DiMauro S, Schon EA. Mitochondrial respiratory-chain diseases. N Engl J Med 2003; 348: 2656-2668.
10. Fragaki K, Procaccio V, Bannwarth S, Serre V, O'Hearn S, Potluri P, Augé G, Casagrande F, Caruba C, Lambert JC, Paquis-Flucklinger V. A neonatal polyvisceral failure linked to a de novo homoplasmic mutation in the mitochondrially encoded cytochrome b gene. Mitochondrion 2009; 9: 346-352.
11. Gao F, Li Y, Wang C, Zhuang Z, Liu QC, Chen J, Hong G, Xu Z. Identification of a Novel Frame-Shift Mutation in PRSS1 Gene in Han Patients with Autoimmune Pancreatitis. Curr Mol Med 2014; 14: 340-348.
12. Gao F, Li YM, Hong GL, Xu ZF, Liu QC, He QL, Lin LQ, Weng SH. PRSS1_p.Leu81Met mutation results in autoimmune pancreatitis. World J Gastroenterol 2013; 19: 3332-3338.
13. Giulivi C, Zhang YF, Omanska-Klusek A, Ross-Inta C, Wong S, Hertz-Picciotto I, Tassone F, Pessah IN. Mitochondrial dysfunction in autism. JAMA 2010; 304: 2389-2396.
14. Hom XB, Lavine JE. Gastrointestinal complications of mitochondrial disease. Mitochondrion 2004; 4: 601-607.
15. Iizuka T, Sakai F, Endo M, Suzuki N. Response to sumatriptan in headache of MELAS syndrome. Neurology 2003; 61: 577-578.
16. Kishnani PS, Van Hove JL, Shoffner JS, Kaufman A, Bossen EH, Kahler SG. Acute pancreatitis in an infant with lactic acidosis and a mutation at nucleotide 3243 in the mitochondrial DNA tRNALeu (UUR) gene. Eur J Pediatr 1996; 155: 898-903.
17. Lebre AS, Rio M, Faivre d'Arcier L, Vernerey D, Landrieu P, Slama A, Jardel C, Laforêt P, Rodriguez D, Dorison N, Galanaud D, Chabrol B, Paquis-Flucklinger V, Grévent D, Edvardson S, Steffann J, Funalot B, Villeneuve N, Valayannopoulos V, de Lonlay P, Desguerre I, Brunelle F, Bonnefont JP, Rötig A, Munnich A, Boddaert N. A common pattern of brain MRI imaging in mitochondrial diseases with complex I deficiency. J Med Genet 2011; 48: 16-23.
18. Liu QC, Gao F, Ou QS, Zhuang ZH, Lin SR, Yang B, Cheng ZJ. Novel mutation and polymorphism of PRSS1 gene in the Chinese patients with heredity pancreatitis and chronic pancreatitis. Chin M J 2008; 121: 108-111.
19. Möllers M, Maniura-Weber K, Kiseljakovic E, Bust M, Hayrapetyan A, Jaksch M, Helm M, Wiesner RJ, von Kleist-Retzow JC. A new mechanism for mtDNA pathogenesis: impairment of post-transcriptional maturation leads to severe depletion of mitochondrial tRNASer (UCN) caused by T7512C and G7497A point mutations. Nucleic Acids Res 2005; 33: 5647-5658.
20. Moraes CT, Ciacci F, Bonilla E, Ionasescu V, Schon EA, DiMauro S. A mitochondrial tRNA anticodon swap associated with a muscle disease. Nat Genet 1993; 4: 284-288.
21. Schaefer AM, McFarland R, Blakely EL, He L, Whittaker RG, Taylor RW, Chinnery PF, Turnbull DM. Prevalence of mitochondrial DNA disease in adults. Ann Neurol 2008; 63: 35-39.
22. Suzuki T, Suzuki T, Wada T, Saigo K, Watanabe K. Taurine as a constituent of mitochondrial tRNAs: new insights into the functions of taurine and human mitochondrial diseases. EMBO J 2002; 21: 6581-6589.
23. Tsai K, Wang SS, Chen TS, Kong CW, Chang FY, Lee SD, Lu FJ. Oxidative stress: an important phenomenon with pathogenetic significance in the progression of acute pancreatitis. Gut 1998; 42: 850-855.

Folia Neuropathologica

Late dissemination via cerebrospinal fluid of papillary tumor of the pineal region: a case report and literature review

Elżbieta Nowicka[1], Barbara Bobek-Billewicz[2], Janusz Szymaś[3], Rafał Tarnawski[1]

[1]3rd Radiotherapy and Chemotherapy Department, Maria Sklodowska-Curie Memorial Cancer Center and Institute of Oncology, Gliwice Branch, [2]Department of Radiology, Maria Sklodowska-Curie Memorial Cancer Center and Institute of Oncology, Gliwice Branch, [3]Pathology Department, Poznan University of Medical Science, Poznan, Poland

Folia Neuropathol 2016; 54 (1): 72-79 DOI: 10.5114/fn.2016.58918

Abstract

Papillary tumor of the pineal region (PTPR) represents a recently described entity and was included in the 2007 World Health Organization (WHO) classification of central nervous system tumors. The biological and clinical behavior of PTPR is variable and may correspond to WHO grades II or III. Papillary tumor of the pineal region can show aggressive biological behavior with local relapses and dissemination via the cerebrospinal fluid. Several cases of PTPR with leptomeningeal seeding and multiple lesions or spinal metastasis have been reported. We present an unusual clinical history of papillary tumor of the pineal region with ventricular and spinal dissemination five years after primary surgical treatment.

Key words: *papillary tumor of the pineal region, cerebrospinal fluid dissemination.*

Introduction

Pineal tumors account for less than 1.0% of all intracranial tumors [2]. Papillary tumor of the pineal region (PTPR) was for the first time described in 2003 by Jouvet *et al.* [5]. Papillary tumor of the pineal region was included in the 2007 World Health Organization (WHO) classification of central nervous system tumors [8]. The diagnosis of this neoplasm is often difficult because of its similarity to other primary or secondary papillary lesions of the pineal region, including parenchymal pineal tumors, papillary ependymoma, papillary meningioma, choroid plexus papilloma and metastatic papillary carcinoma [2]. The cell of origin is thought to be specialized ependymocytes of the subcommissural organ [3]. The biological and clinical behavior of PTPR is variable and may correspond to WHO grades II or III, but there are no precise histological grading criteria defined [8,9]. Papillary tumor of the pineal region can show aggressive biological behavior with local relapses and dissemination via the cerebrospinal fluid. Several cases of PTPR with leptomeningeal seeding and multiple lesions or spinal metastasis have been reported [1,2,4,6,7,10,11]. The optimal therapeutic approach of PTPR has not been well defined [1].

We present an unusual clinical history of papillary tumor of the pineal region with ventricular and spinal dissemination five years after primary surgical treatment.

Communicating author

Elżbieta Nowicka, 3rd Radiotherapy and Chemotherapy Department, Maria Sklodowska-Curie Memorial Cancer Center and Institute of Oncology, Gliwice Branch, 16 Wybrzeże Armii Krajowej St., 44-100 Gliwice, Poland, e-mail: enowicka@io.gliwice.pl

Case report

A 62-year-old Caucasian man who was admitted to the Center of Oncology MCS Memorial Institute in April 2013 after neurosurgical intervention due to the tumor of the foramen magnum region. He had his first neurosurgical intervention in the Neurosurgery Department in 2007. The first neurological symptoms were headache, loss of memory, psychosomatic retardation and vertigo in 2007. The magnetic resonance (MR) showed signs of significant hydrocephalus due to well circumscribed 20 × 13 mm large tumor in the pineal region. The tumor showed high intensity in T1 weighted images as well hyperintensity in T2 weighted images (Fig. 1A-B).

The patient did not accept a contrast injection so examination was performed without intravenous contrast and the data concerning contrast enhancement are not available. The patient underwent the suboccipital craniotomy and the tumor was totally removed. Histological examination of this tumor (Fig. 2, Appendix 1) had revealed cellular epithelioid tumor with papillary areas which did not demonstrate sufficiently well formed pseudorosettes supporting the diagnosis of ependymoma. At this time (2007) due to lack of sufficient experience with PTPR, this tumor was classified as pineocytoma, grade II. Craniospinal axis magnetic resonance imaging (MRI) scans were not recommended at that time. The patient did not receive any adjuvant therapy and was referred to regular MRI brain scans once a year. In October 2012, MRI revealed the pathological mass in the foramen magnum region which met the radiological criteria of meningioma, which was not seen in the MR scan performed after surgery in 2007 (Fig. 3A-B). At that time there was no tumor mass in the pineal region The suboccipital craniotomy, laminectomy and total tumor removal was performed in February 2013.

The pathologic examination of the operation specimen was performed in the Pathology Department of Poznań Medical University (Fig. 4, Appendix 2). The tumor was 14 × 9 mm large. The tumor was solid, infiltrative, white-gray in color. Microscopic evaluation did not confirm the expected meningioma diagnosis. Histological examination showed a subtly epithelial partly papillary morphology. The papillae were closely-packed and covered by layers of large polygonal columnar cells with oval nuclei, fine stippled chromatin, and a moderate amount of clear, vacuolated or pale eosinophilic cytoplasm. Mitosis, tumor necrosis or microvascular proliferation was lacking. Preliminary diagnosis was a papillary tumor of the pineal region. Immunohistochemical stains revealed diffuse

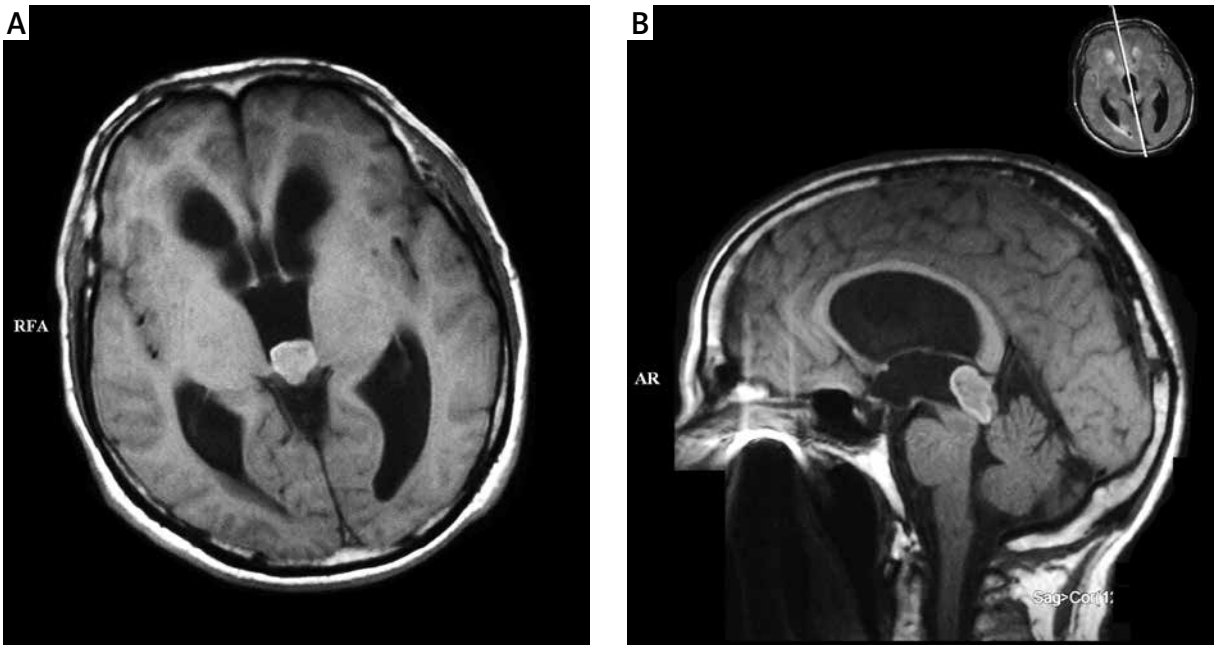

Fig. 1. T1-WI without contrast enhancement demonstrates well-delineated, slightly hyper intense mass in the pineal region. The lateral ventricles are enlarged with surrounding low-intensity interstitial edema as well as marked widening of the third ventricle are seen. No other tumors were found. **A**) Axial, **B**) sagittal.

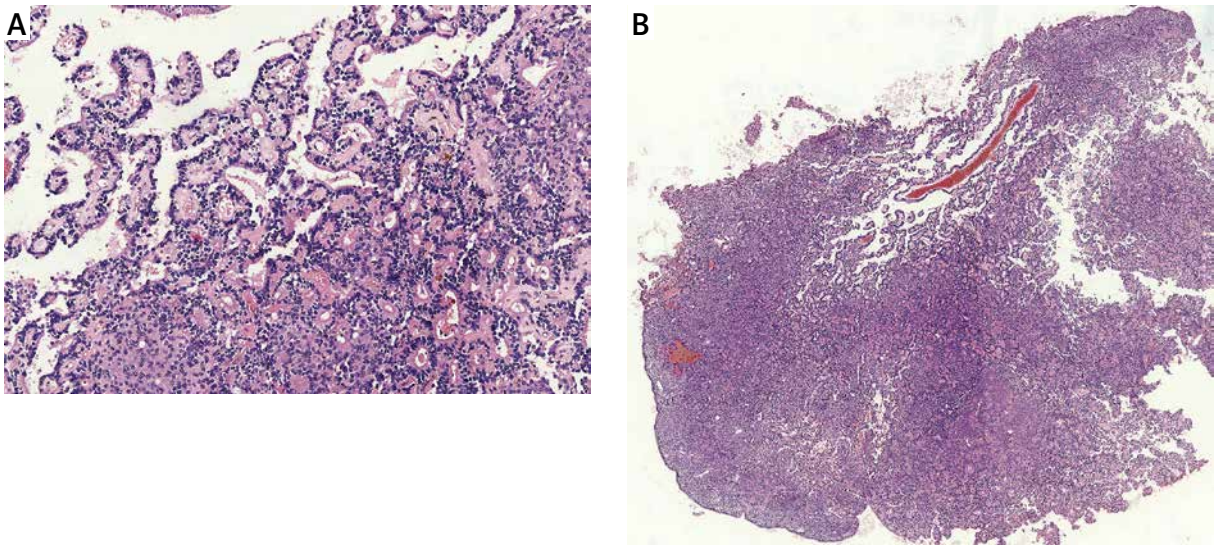

Fig. 2. At 2007 histological examination of this tumor has revealed cellular epithelioid tumor with papillary areas which did not demonstrate sufficiently well-formed pseudorosettes supporting the diagnosis of ependymoma. Due to lack of sufficient experience with PTPR, this tumor was classified as pineocytoma, grade II (Lab. number 201963 **A** and **B**).

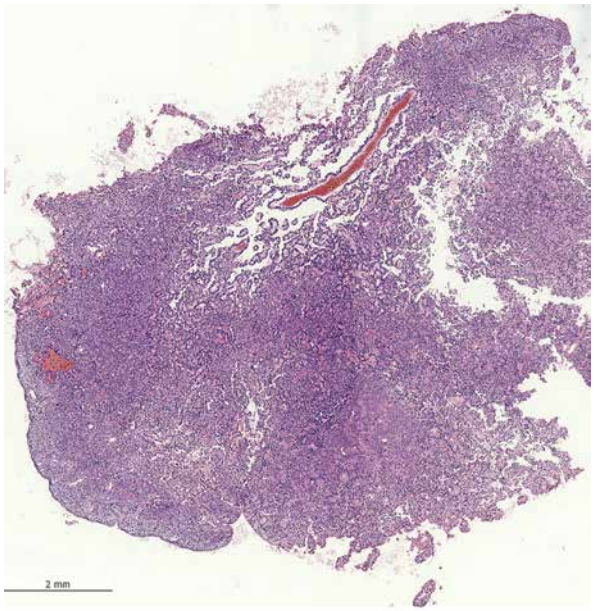

Appendix 1. Primary tumor 201963
http://150.254.71.142/vff.aspx?mo=1&im=3872&type=SlideIndex&sid=xr2exl3l2vmjuwhr2tlwccrp&d=VmpBeGFGcEhNWEJpYWtVOStO#/overlay/vectoroverlay

positivity for neuronal specific enolase, vimentin, cytokeratin 18 and the lack of neurofilament protein. Positive reaction for synaptophysin was seen only in a few neoplastic cells, whereas the expression of chromogranin A was negative. The tumor tissue did not exhibit GFAP expression. Proliferation index (Ki67) by immunostaining for MIB-1 was estimated to be about 10%. (Fig. 5A-D). An extra comparative histological and immunohistochemical examination was done with the material from the first surgery in 2007. The primary tumor which was originally classified as pineocytoma WHO II, after subsequent comparative analysis presented the same morphology and immunohistological profile as the second tumor. Based on the clinical behavior of the tumor, histopathological and immunohistochemical analyses, the final pathological diagnosis was a papillary tumor of the pineal region (PTPR), grade III.

The patient was referred to an oncology consultation in the Center of Oncology in Gliwice in April 2013. He was in good performance and neurological status. Clinical examination did not reveal any variations. An independent review and reanalysis of postoperative tissue blocks from the first and the latter surgical intervention were performed in the Department of Tumor Pathology in the Center of Oncology in Gliwice. The pathological consultation of paraffin embedded tissue confirmed primary diagnosis of the papillary tumor of the pineal region.

The MRI data were reviewed by radiologists and extra MRI scans of the cerebrospinal axis were done. The radiological examination revealed no tumor mass in the pineal region and total tumor resection of the foramen magnum region tumor (Fig. 6), but

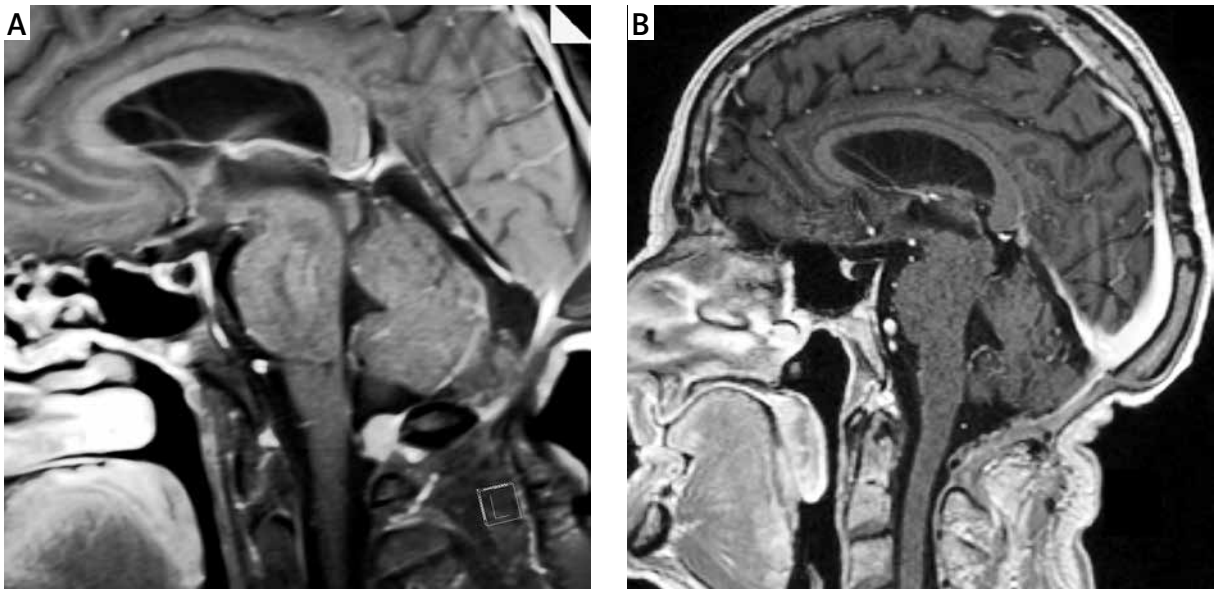

Fig. 3. Sagittal T1-WI C+. **A**) Well-circumscribed, homogeneously enhancing intradural extramedullary mass with a broad dorsal dural attachment in the foramen magnum (at the craniovertebral junction) (2012). The tumor is not seen in the scan performed after surgery in 2007 (**B**).

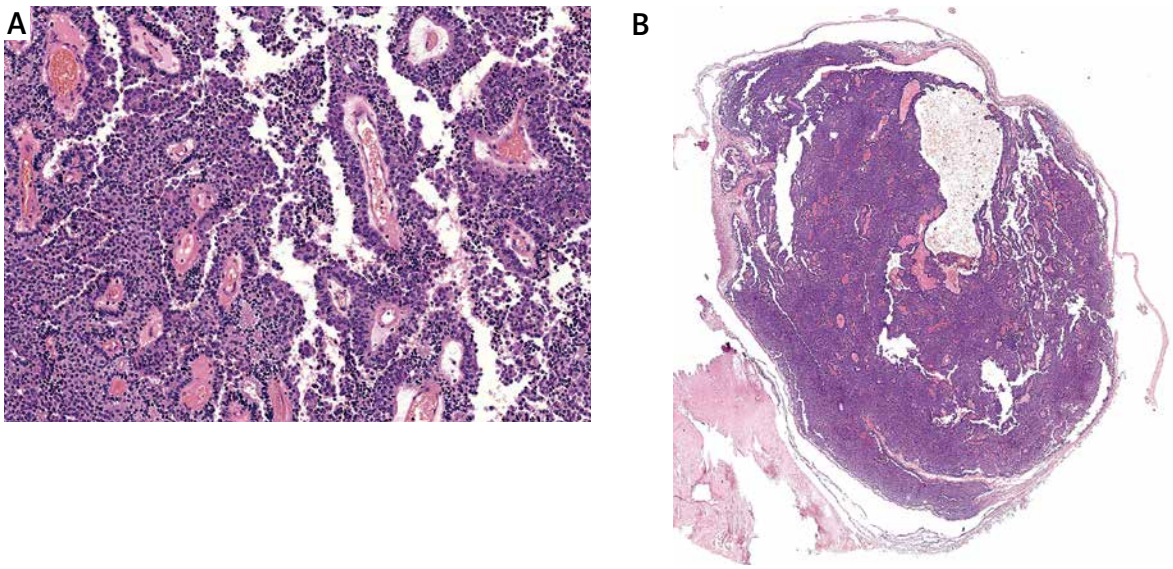

Fig. 4. At 2013 histological examination showed a subtly epithelial partly papillary morphology. The papillae were closely-packed and covered by layers of large polygonal columnar cells with oval nuclei, fine stippled chromatin, and moderate amount of clear, vacuolated or pale eosinophilic cytoplasm (Lab. number 499969 **A** and **B**).

a few small contrast enhancing foci up to 7 mm in diameter in the subependymal region of frontal (anterior) horns and stem of lateral ventricles with radiological image of metastases were diagnosed (Fig. 7A-C). The dissemination in the spinal axis was excluded. The patient was referred to radiotherapy and the decision was made to perform the craniospinal irradiation. From 26.06.2013 to 29.07.2013 the patient was irradiated with tomotherapy. The conventional fractionation was used with 1.8 Gy/g per fraction to the total dose of 36 Gy/g. The treatment was completed with good general and neu-

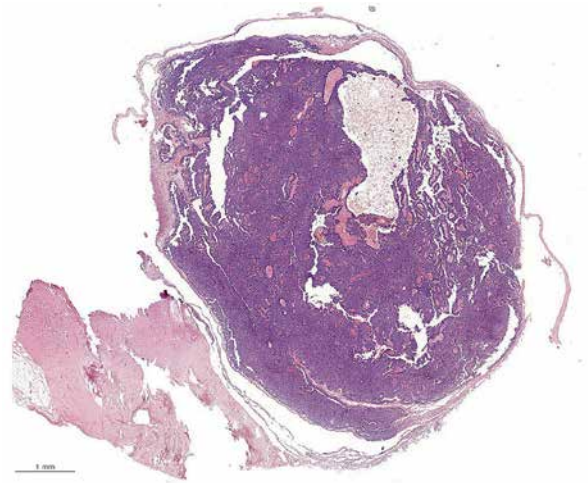

Appendix 2. Metastatic tumor 499969
http://150.254.71.142/vf1.aspx?&mo=1&im=3874&-type=SlideIndex&sid=xr2exl3l2vmjuwhr2tlwccrp&d=Vmp-BeGFGcEhNWEJpYWtVOStO#/overlay/vectoroverlay

rological tolerance. In the second and third week of treatment, a moderate decline of leucocytes and platelets: WHO II and WHO I respectively, was observed, which restored to the normal range after pharmacological intervention. There were no treatment breaks due to treatment complications. The patient was referred to follow up in the Outpatient Clinic. The first visit was three months after completion of treatment. The patient did well. There was no decline in general and neurological status. Hematological analyses did not reveal any decline in platelets and leucocytes. The last control diagnostic MRI in November 2014 revealed the stable status of small foci of the subependymal region of frontal (anterior) horns of lateral ventricles (Figure 7B and 7D). There were no radiological signs of local relapse. The close follow up is warranted. The next diagnostic MRI is planned in May 2015.

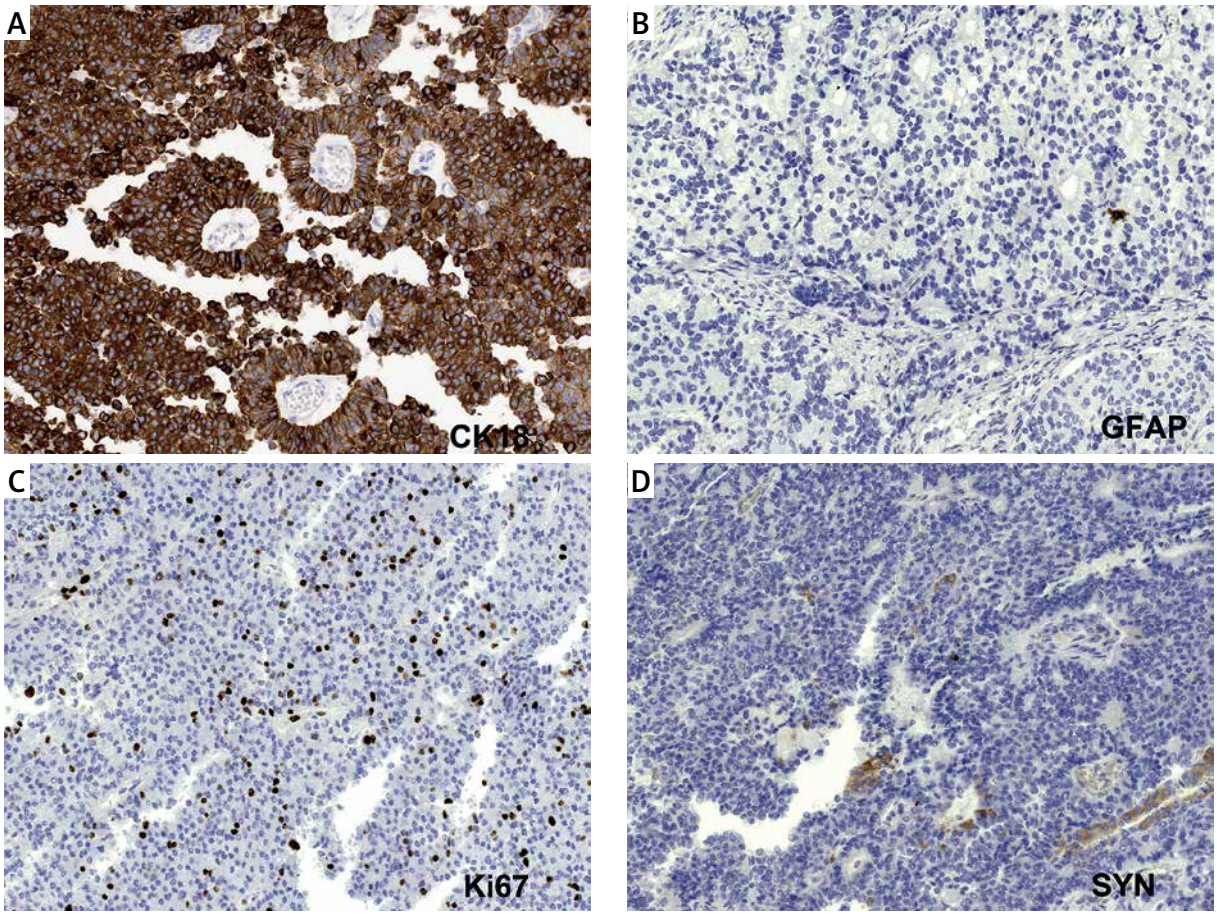

Fig. 5. Immunohistochemical stains revealed diffuse cytokeratin 18 positivity. The tumor tissue did not exhibit GFAP expression. Proliferation index (Ki67) by immunostaining for MIB-1 was estimated to be about 10%. Positive reaction for synaptophysin was seen only in a few neoplastic cells.

Discussion

Primary papillary tumor of the pineal region is a rare neoplasm. It was first described by Jouvet in 2003 and was finally included in WHO 2007 classification of tumors of the nervous system [2,8]. Only 72 cases have been described in the literature to date [10].

These rare tumors of the pineal region manifest in children and young adults (mean age 32 years) [4,11]. Histologically, papillary tumors of the pineal region are characterized by a papillary architecture and cellular epithelioid morphology. Crucial for differential diagnosis is specific immunohistochemical profile with strong reactivity to cytokeratin CK18, S-100, neuronal specific enolase (NSE), vimentin and focal or low glial fibrillary acidic protein (GFAP) [2,3,5,8,9]. The biological behavior of PTPR is variable and may correspond to WHO grades II or III [8]. Although there are more and more clinical data accumulated over last years on treatment modalities and outcomes, the treatment strategies are not well described. Surgical resection with subsequent local radiotherapy is current standard of care [8]. There are some data on chemotherapy use especially when local recurrence or spinal dissemination is diagnosed [1]. In the largest series of 44 patients with PTPR, the role of surgery, radiotherapy, and chemotherapy was analyzed by Fauchon *et al*. Median follow-up was 63.1 months. Median overall survival (OS) was not achieved. Median progression-free survival (PFS) was 58.1 months. Only gross total resection and younger age were associated with a longer OS, radiotherapy with chemotherapy having no significant impact. Progression-free survival was not influenced by gross total resection. Radiotherapy and chemotherapy had no significant effect. This retrospective series confirms the high risk of recurrence in PTPR: 58% at five years and 70% at six years [1]. Three out of 44 reported patients had the evidence of spinal cord seeding: one initially and the remaining while recurrence [1].

PTPR might display local recurrences and CSF dissemination despite surgical resection and radiotherapy [1,3,6]. Due to their localization the PTPR cells may spread via the cerebrospinal fluid [4,6]. In the series of 31 patients analyzed by Fèvre-Montagne *et al.*, the majority experienced recurrences: 5-year overall survival and progression-free survival were 73% and 27%, respectively [3].

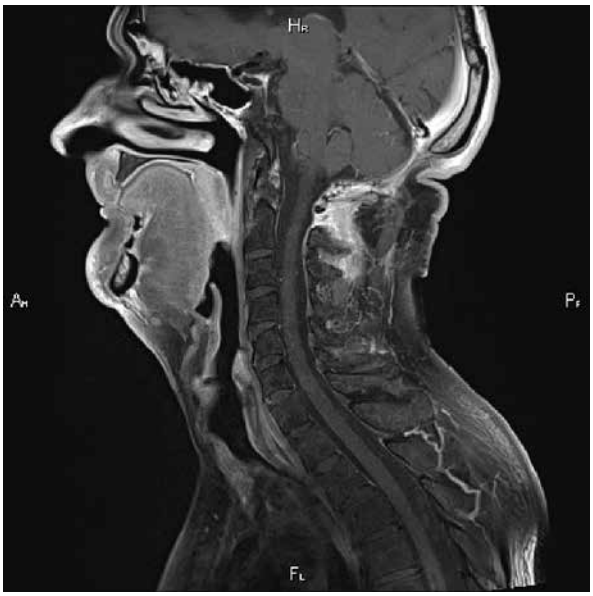

Fig. 6. Sagittal T1-WI C+ revealed no tumor mass in the pineal region and total tumor resection of the foramen magnum region tumor in 2013.

There are a few case reports of spinal dissemination [1,4-7]. Hong *et al.* reported a case of a 39-year-old woman who underwent four craniotomies for resection of the tumors in the pineal region. The primary histological diagnosis was pineoblastoma. She had three series of stereotactic radiotherapy following surgical interventions. After the definition of PTPR, the specimens were re-investigated and the diagnosis of papillary tumor of the pineal region was done. Even without clinical signs and symptoms the craniopsinal MRI was performed and the pathological mass at the level of L3 was presented. The resection was performed and the pathological examination showed the same morphological features as seen in the papillary pineal tumor. The patient was referred to follow-up, but four months later she relapsed locally again and irrespectively of surgical treatment she died three months later [4].

Poulgrain *et al*. described the clinical history of a 25-year-old woman who was diagnosed with the pineal region tumor and after subtotal surgical excision the histopathology diagnosis of PTPR was done. She was referred to adjuvant radiotherapy to 54 Gy/g in conventional fractionation and 23 months after treatment she developed an ataxia, vomiting and headache. The MRI presented a large recurrent pineal region infiltrating forth ventricle with additional tumor in the cerebellar hemisphere along with an increased cerebral blood flow [10].

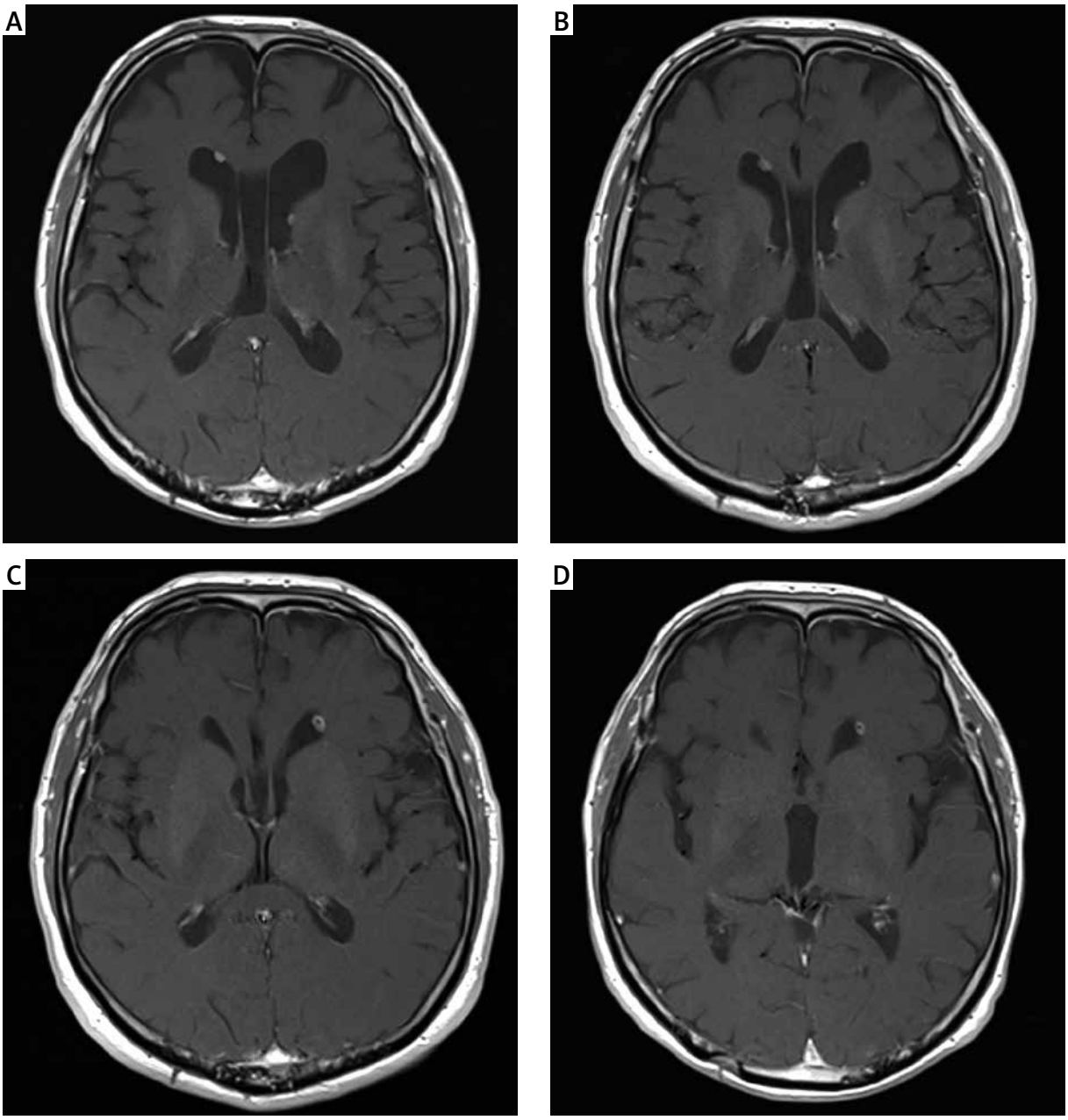

Fig. 7. Axial T1-WI C+ FS shows contrast enhancing subependymal nodules in the frontal horn of the left lateral ventricle before (**A**) and 5 months after RT (**B**); in the frontal horn of the right lateral ventricle before RT (**C**) and 5 months after RT (**D**). The small enhancing subependymal nodules in the lateral ventricles remain essentially unchanged on the post treatment MRI scan performed 6 and 10 months following completion of radiotherapy.

Another clinical report of leptomeningeal seeding by Kim *et al*. is the case of a 39-year-old woman who presented a history of headache and decreased visual acuity. Magnetic resonance imaging showed solid and cystic, contrast enhancing mass at the pineal region with associated ventriculomegaly. Smaller and contrast enhancing nodular lesions were also found at the pituitary stalk and bilateral internal acoustic canals. After endoscopic ventriculostomy the partial resection was performed. The pathological examination of the specimen revealed the features of PTPR. Despite the radiotherapy of the lesions through

gamma knife radiosurgery and a decrease in size of the primary lesions on MRI six months afterwards, new enhancing lesions occurred. The case presented is a proof that PTPR can disseminate to other sites distant from the original lesion [6].

We report the case of a 61-year-old man who was first operated in 2007 with the initial pathological diagnosis of pineocytoma. During the follow-up period the MRI scans showed the tumor in the foramen magnum region resembling meningioma, which was not seen in the MR scan performed after surgery in 2007. After surgery and histopathology examination of the specimen, the final diagnosis established in 2013 was PTPR. After re-examination of the tissue blocks from the first operation, the same morphology was presented. The immunochistochemical reactivity confirmed the diagnosis of PTPR. Magnetic resonance imaging showed the dissemination to the subependymal region of frontal (anterior) horns and stem of lateral ventricles. Our clinical data as well as already published series of PTPR patients indicate that the pattern of cerebrospinal fluid dissemination is possible. Concurring with other authors we strongly encourage the primary cerebrospinal axis MR imaging, after the PTPR is diagnosed [4,10]. Obvious cerebrospinal fluid dissemination in our patient led to a decision of craniospinal irradiation in order to treat visible dissemination in the brain and to prevent spinal seeding. The radiotherapy plan was similar to our protocol in patients with PNET or medulloblastoma. In a report of Fauchon *et al*., the radiotherapy to neuraxis was also performed in patients with craniospinal dissemination [1]. At the moment the follow-up is very short so we should wait for the outcome.

Papillary tumors of the pineal region are rare tumors with a strong propensity for local recurrences and which may disseminate via the craniospinal fluid. The clinical data on behavior of those tumors should still be followed and accumulated in a prospective, multi-center manner to enable the evaluation of the same diagnostic and treatment guideline consensus. What is important now from a practical point of view is the need for serial radiological examination of the entire cerebrospinal axis while the PTPR is diagnosed. It is not clear if cerebrospinal irradiation should be considered during the initial adjuvant therapy of PTPR.

Disclosure

Authors report no conflict of interest.

References

1. Fauchon F, Hasselblatt M, Jouvet A, Champier J, Popovic M, Kirollos R, Santarius T, Amemiya S, Kumabe T, Frappaz D, Lonjon M, Fèvre Montange M, Vasiljevic A. Role of surgery, radiotherapy and chemotherapy in papillary tumors of the pineal region: a multicenter study. J Neurooncol 2013; 112: 223-231.
2. Fèvre-Montange M, Vasiljevic A, Champier J, Jouvet A. Histopathology of tumors of the pineal region. Future Oncol 2010; 6: 791-809.
3. Fèvre-Montange M, Hasselblatt M, Figarella-Branger D, Chauveinc L, Champier J Saint-Pierre G, Taillandier L, Coulon A, Paulus W, Fauchon F, Jouvet A. Prognosis and histopathologic features in papillary tumors of the pineal region: a retrospective multicenter study of 31 cases. J Neuropathol Exp Neurol 2006; 65: 1004-1011.
4. Hong B, Nakamura M, Brandis A, Becker H, Krauss JK. Spinal metastasis of papillary tumor of the pineal region. Clin Neurol Neurosurg 2011; 113: 235-238.
5. Jouvet A, Fauchon F, Liberski P, Saint-Pierre G, Didier-Bazes M, Heitzmann A, Delisle MB, Biassette HA, Vincent S, Mikol J, Streichenberger N, Ahboucha S Brisson C, Belin MF, Fèvre-Montange M. Papillary tumor of the pineal region. Am J Surg Pathol 2003; 27: 505-512.
6. Kim YH, Kim JW, Park CK, Kim DG, Sohn CH, Chang KH, Park SH. Papillary tumor of pineal region presenting with leptomeningeal seeding. Neuropathology 2010; 30: 654-660.
7. Lechapt-Zalcman E, Chapon F, Guillamo JS, Khouris S, Menegalli-Boggelli D, Loussouarn D, Fèvre-Montange M, Jouvet A. Long term clinicopathological observations on papillary tumor of pineal region. Neuropathol Appl Neurobiol 2011; 37: 431-435.
8. Louis DN, Ohgaki H, Wiestler OD, Cavenee WK, Burger PC, Jouvet A, Scheithauer BW, Kleihues P. The 2007 WHO classificatoion of tumors of central nervous system. Acta Neuropathol 2007; 114: 97-109.
9. Matyja E, Grajkowska W, Nauman P, Bonicki W. Histopathological patterns of papillary tumor of pineal region. Folia Neuropathol 2011; 49: 181-190.
10. Poulgrain K, Gurgo R, Winter C, Ong B, Lau Q. Papillary tumor of pineal region. J Clin Neurosci 2011; 18: 1007-1017.
11. Sato TS, Kirby PA, Buatti JM, Moritani T. Papillary tumor of the pineal region: report of a rapidly progressive tumor with possible multicentric origin. Pediatr Radiol 2009; 39: 188-190.

Folia Neuropathologica

Rosette-forming glioneuronal tumour of the fourth ventricle: case report and review of the literature

Tayfun Hakan[1], Fügen Vardar Aker[2]

[1]Memorial Ataşehir Hospital, Ataşehir/İstanbul, [2]Haydarpaşa Numune Teaching and Research Hospital, Ataşehir/İstanbul, Turkey

Folia Neuropathol 2016; 54 (1): 80-87 DOI: 10.5114/fn.2016.58919

Abstract

Rosette-forming glioneuronal tumour (RGNT) of the fourth ventricle is one of the newly described primary tumours of the central nervous system. These tumours have two components of both neurocytic and glial areas but usually the glial component of the tumour predominates. They have biphasic cytoarchitecture with two elements; neurocytic rosettes resembling Homer-Wright rosettes, and astrocytic component resembling a pilocytic astrocytoma. They are low-grade tumours with lack of histopathological signs of malignancy. Here, clinical, magnetic resonance, computed tomography (CT) and pathological features of rosette-forming glioneuronal tumour of posterior fossa are presented. A 29-year-man was admitted with an acute neurological deterioration. A three ventricular hydrocephalus and a hypo-density around vermis in the posterior fossa were seen in his CT scans. He did well after an emergency external ventricular drainage. He had an elective operation and a mass that was reported to be a rosette-forming glioneuronal tumour of the fourth ventricle was excised.

Key words: *cerebellum, fourth ventricle, glioneuronal tumour, neuropathology, rosette-forming glioneuronal tumour.*

Introduction

Rosette-forming glioneuronal tumour (RGNT) of the fourth ventricle is one of the newly described primary tumours of the central nervous system [12]. Komori *et al*. [18] were the first who described this entity. They explained the characteristics of these tumours in terms of location, distinctive histological appearance with formation of neurocytic component and indolent biologic behaviour in a series of 11 cases report in 2002 [19]. Rosette-forming glioneuronal tumour was confirmed as a new type in the newly updated World Health Organization (WHO) classification of tumours of the central nervous system in 2007 [12]. Previously, these tumours assumed to be only infratentorial and located around fourth ventricle. Different locations of RGNT as chiasma [31], suprasellar region [30] and pineal region [10,13,19,32], septum pellucidum [36], intraventricular dissemination [35] and two spinal cord [5,28] were published later.

Although the histopathological features of these tumours are regarded as distinct and typical, they can show wide spectral clinical symptoms (Table I). We aimed to make a case addition to the limited clinical, radiological and pathological experience of this kind of rare and "poorly" described tumours.

Communicating author

Tayfun Hakan, MD, Assoc. Prof., Memorial Ataşehir Hospital, Vedat Günyol Caddesi No:30 Küçükbakkalköy 34758 Ataşehir/İstanbul, Turkey, e-mail: tayfunhakan@yahoo.com

Table I. Review of the literature of cases of rosette-forming glioneuronal tumour

Author	No.	Sex, age	Presenting symptom	Location	Treatment	Postoperative morbidity
Komori *et al.*	1	25, M	Headache, 4th nerve palsy	4. V, aquaduct, pineal region	Biopsy	–
	2	59, M	Ataxia	4. V, aquaduct	ST + RT	+
	3	24, F	Headache, ataxia, dysartria	4. V, aquaduct, vermis, pons	PR	–
	4	18, M	Seizure	4. V, aquaduct	GTR	–
	5	40, F	Headache	4. V, vermis	GTR	+
	6	38, F	Headache	4. V	GTR	–
	7	39, F	Headache, neck pain, blurred vision	4. V, aquaduct	GTR	+
	8	27, M	Headache, confusion, ataxia	4. V	PR	+
	9	18, F	Incidental, headache, ataxia	4. V, aquaduct	PR	+
	10	46, M	Headache, blurred vision, ataxia	4. V, vermis, cerebellum	PR	+
	11	12, F	Headache, ataxia	Tectum, aquaduct, pineal r.	PR	–
Preusser *et al.**	12	35, M	Incidental	4. V, vermis	Surgery!	Not known
Adachi *et al.*	13	18, F	Incidental, slight ataxia	4. V	PR	+
Albanese *et al.*	14	32, F	Headache, cervical pain, neck rigidity	4. V	GTR	+
Jacques *et al.*	15	39, M	Vertigo, headache, diplopia, nystagmus	4. V	GTR	–
	16	33, F	Headache, diplopia, ataxia, dysarthria, lethargy	4. V	GTR	Not known
	17	42, M	Headache	4. V	GTR	Not known
Johnson *et al.*	18	29, F	Headache, vertigo	4. V	NGTR	Not known
Rickert *et al.*	19	16, F	Therapy resistant back pain	Spinal cord (C7-T2)	GTR	–
Vajtai *et al.*	20	16, F	Vertigo, nausea, tinnitus, ataxia	Roof of 4. V	GTR	+
	21	30, F	Vertigo, vomiting, headache, clumsy walking	Roof of 4. V	GTR	–
Pimentel *et al.*	22	38, F	Headache	4. V	NGTR	+
	23	51, F	Dizziness	Cerebellum	GTR	–
Marhold *et al.*	24	20, M	Somnolence, anisocoria, ataxia	Pineal region, vermis, 4. V	GTR	+
	25	47, F	Headache, ataxia, hemiparesthesia	Inferior vermis	GTR	+
	26	39, F	Headache, vertigo, nausea, tinnitus	Foluculus, lateral (CPA)	GTR	–
Tan *et al.*	27	42, M	Headache, feeling "odd"	Upper cerebellar aquaduct	Biopsy	+
	28	38, F	Lightheadedness	Cerebellar vermis	Biopsy	–

Table I. Cont.

Author	No.	Sex, age	Presenting symptom	Location	Treatment	Postoperative morbidity
Joseph *et al.*	29	38, F	Headache, vomiting	Cereballar vermis	GTR	–
	30	24, F	Worsening of gait, anisocoria	4. V	PR	–
Scheithauer *et al.*	31	23, M	Eye pain, blurred vision, headache	Chiasma	PR	–
Anan *et al.*	32	44, F	Tetraparesis, dysesthesia, neurogenic bladder	Spinal cord, cervicothoracic	GTR	+ (slight aggravation)
Wang *et al.*	33	16, F	Seizure, loss of consciousness	ventricle	Biopsy	–
Kinno *et al.***	34	18, M	Gait disturbance, ataxia	Cerebellar vermis	PR	–
Li *et al.*	35	27, M	Headache, vomiting, clumsy walking	4. V	GTR	–
Arai *et al.*	36	15, F	Headache	4. V, ventricle, vermis	GTR	+
Luan *et al.*	37	30, F	Headache	Right cerebellar hemisphere	GTR	–
Ghosal *et al.*	38	22, M	Headache, diplopia (3rd nerve palsy)	Pineal gland & tectum	Decompression?	–
Frydenberg *et al.*	39	29, M	Headache, vomiting, decrease in the level of consciousness	Pineal gland	GTR	–
Matyja *et al.*	40	20, F	Headache, nausea, balance disturbance	4. V	PR	?
Sharma *et al.*	41	16, F	Headache, diplopia	Midbrain	Biopsy + RT	–
	42	17, M	Loss of consciousness	Suprasellar, 3rd ventricle	Biopsy	–
Gessi *et al.*	43	18, M	Not known	Vermis	GTR	–
Fushimi *et al.*	44	28, F	Intermittent headache	Cerebellar midline	PR	–
Ellezam *et al.*	45	29, F	Not known	Inf vermis/4. V	Not known	Not known
	46	23, F	Not known	Inf vermis/4. V	Not known	Not known
	47	12, M	Not known	Inf vermis/4. V	Not known	Not known
	48	50, M	Not known	Inf vermis/4. V	Not known	Not known
	49	45, M	Not known	Midbrain/tectal	Not known	Not known
	50	18, F	Not known	Inf vermis/4. V	Not known	Not known
	51	30, F	Not known	3rd V	Not known	Not known
	52	15, M	Not known	Inf vermis/4th V	Not known	Not known
Karafin *et al.*	53	18, ?	Developmental delay	Posterior fossa	GTR	–
Solis *et al.*	55	16, F	Headache, vomiting	Pineal region	PR	–
Xiong *et al.*	56	38, M	Visual disturbance	Septum pellicidum	PR	–
Podlesek *et al.*	57	70, M	Persistant vertigo	Vermis, 4. V	GTR	–
Present study	58	29, M	Neurological deterioration with somnolence	Vermis, 4. V	NGTR	–

PR – partial removal, GTR – gross total removal, RT – radiotherapy, NGTR – nearly gross total removal
**This case reported again in Marhold serious*
***One of the cases presented in this report had been published previously by Adachi et al.*

Case report

A 29-year-man was admitted with an acute neurological deterioration and somnolence. His neurological examination was normal except a positive Babinski sign on his right side. In his medical history, there was a diagnosis of an incidental and asymptomatic hydrocephalus that was seen in his cranial computed tomography (CT) following a mild head injury three years before. A cranial CT showed a three ventricular hydrocephalus and a hypodensity around vermis in the posterior fossa (Fig. 1A). A cranial magnetic resonance imaging (MRI) revealed a partly cystic lesion located in vermis. It was hypointense on T1 and hyperintense on T2 weighted images and had no contrast enhancement (Fig. 1B-D). The lesion was hyperintense on flair sequences. The neurological status of the patient improved promptly following an emergent external ventricular drainage insertion. On the following day, the patient underwent an operation and a nearly gross total tumour removal was performed.

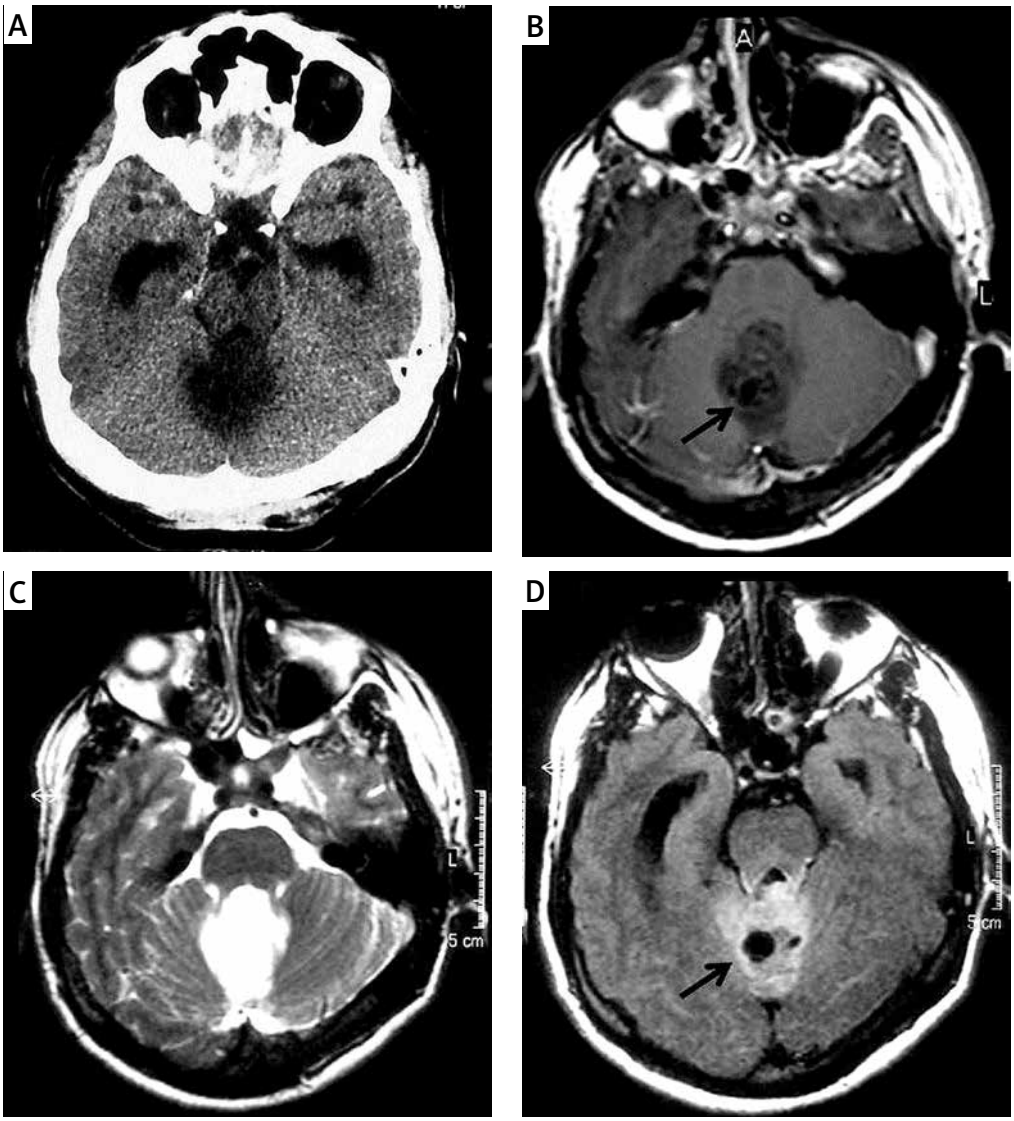

Fig. 1. A) Non-contrast computed tomography scan shows a hypodense lesion at vermis. **B**) On T1 weighted magnetic resonance scans this lesion shows heterogeneous contrast enhancement and a cystic component also is found (arrow) in the lesion. **C**) The lesion seems hyperintense on T2 weighted magnetic resonance imaging (MRI). **D**) On flair weighted MRI images the lesion seems hyperintense but the cystic component is hypointense (arrow).

The resected tumour specimen was transferred to the pathology department after fixing in a phosphate buffered 4% solution of formalin. Serial sections of 5 µm thick paraffin-embedded tumour tissues were stained with hematoxylin and eosin (HE). Additionally, an immunohistochemical (IHC) staining with monoclonal antibodies against glial fibrillary acidic protein (GFAP) (1 : 75; Neomarkers, Fremont, CA, USA), synaptophysin (1 : 100; Neomarkers) and Ki 67 (1 : 50; Neomarkers) was performed. Immunohistochemical staining was performed using an enhancement method based on a repetitive microwave heating technique using sodium citrate buffer. In microscopic examination, the tumour consisted of two components and it was also well demarcated from cerebellar tissue. The tumour was characterized by glial and neuronal components (Fig. 2A). In the area of the glial component, the cytoplasmic processes formed a compact textured fibrillary background. Some areas resembled pilocytic astrocytoma and oligodendroglioma (Fig. 2D). There were a few Rosenthal fibres and hemosiderin deposits. The neurocytic component consisted of uniform neurocytes which are forming rosettes and pseudorosettes (Fig. 2B-C). Neurocytic tumour cells had ovoid or round nuclei with fine chromatin pattern, inconspicuous nucleoli and delicate cytoplasmic processes. Overall, cellularity was low. Mitosis, atypia, necrosis or vascular proliferations were not seen. In immunohistochemical examination, synaptophysin immunoreactivity was only restricted in the peripapillary area of perivascular pseudorosette and rosette

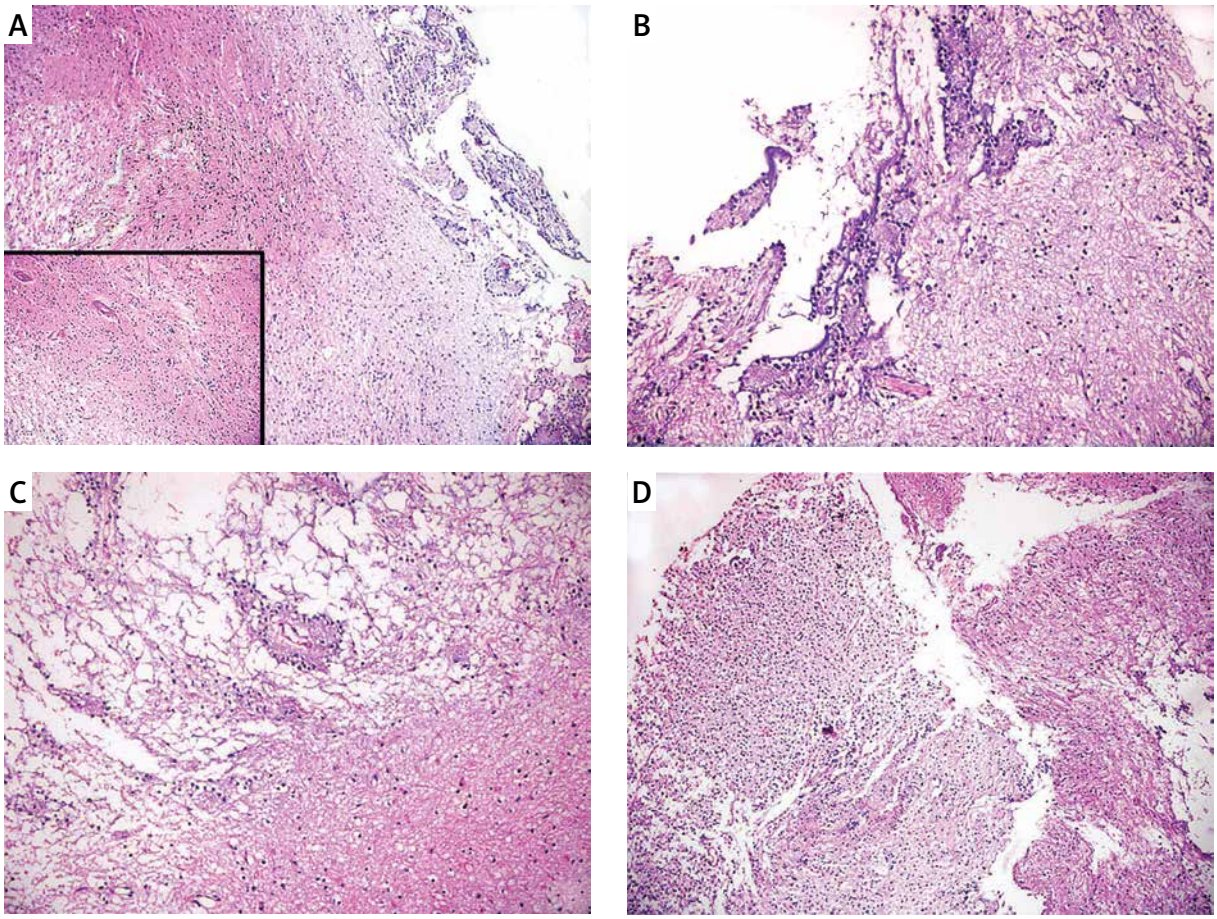

Fig. 2. Two components: neurocytic and astrocytic (H&E x40), pilocytic astrocytoma like component on the left side (H&E x200). **A**) Neurocytic pseudorosettes and rosettes around the astrocytic component. **B**) Neurocytic pseudorosette: delicate cell processes radiating toward a capillary (H&E ×100). **C**) The other glial area resembling oligodendroglioma intermingle with pilocytic astrocytoma like area (H&E ×100). **D**) There is no mitosis and atypical histopathological findings.

(Fig. 3A). Staining with GFAP antibody was positive in the astrocytic component of the tumour (Fig. 3B). Ki 67 labelling index was very low (1% and below). The tumour was reported to be a rosette-forming glioneuronal tumour of the fourth ventricle.

The postoperative period was unremarkable. He was followed for 32 months without evidence of progressive clinical deterioration.

Discussion

Kuchelmeister *et al*. [20] reported a dysembryoplastic neuroepithelial tumour (DNT) in cerebellum which morphologically resembled RGNT in 1995. The term rosette-forming glioneuronal tumour was used to define the low-grade tumour of the fourth ventricle by Komori *et al*. [18] for the first time in 1998. The characteristic features of these tumours were explained as 1) its unique location, 2) neurocytic pseudo-rosette formation and 3) the presence of a pilocytic astrocytoma component. Until the publishing of two cases that were located in chiasma [31] and spinal cord [5], these tumours were believed to be found only in posterior fossa. So, the "unique location" of these tumours seems to need some change. Anan *et al*. [5] suggested that the lesion might derive from the gray matter or the middle motor nuclei in the spinal cord, so RGNT may not be limited in distribution [5]. Scheithauer *et al*. [31] reported that periventricular germinal matrix is the likely origin of RGNTs and so, they may be occurring in "ectopic" sites. Rosette-forming glioneuronal tumours may be located in different areas such as the pineal region [9,10] and lateral ventricles [35] and some satellite tumours may also be seen in the patients [6,18,27,33].

Rosette-forming glioneuronal tumour is encountered more frequently in females. Thirty-one of the 56 reported cases in the English literature, including the present case, up to date were seen in women. Patient age was 12-70 years with a mean of 29 years (Table I).

Headache and cerebellar signs as ataxia and nystagmus are the most common initial clinical symptoms. Diplopia, ptosis [13], dysarthria [13,19], blurred vision [19], seizure [19,35], dizziness [25], vertigo [14,34], vomiting [21,34), clumsy walking [21,23] and neck pain and rigidity [2,19] are the other signs and symptoms of this tumour. Lethargy [13], somnolence, loss of conscious [35] and anisocoria [23] due to increased intracranial pressure may also be seen in these patients as in the presented case. However, there are some cases which are diagnosed incidentally [1,19,27], too.

A three ventricular hydrocephalus may be seen in RGNT patients. It can be so serious that a ventriculo-peritoneal shunt [13] or insertion of an external ventricular drainage (EVD) may be required [10,23]. We also performed an EVD in the emergency room for the presented case, because the patient was admitted with an acute neurological deterioration with somnolence. Fortunately, most of these tumours are slowly growing lesions. The development of ventriculomegaly can be chronic and may be clinically compensated [23].

The radiological findings of RGNTs may show some variations. These lesions are relatively circumscribed and heterogeneous, they may have some cal-

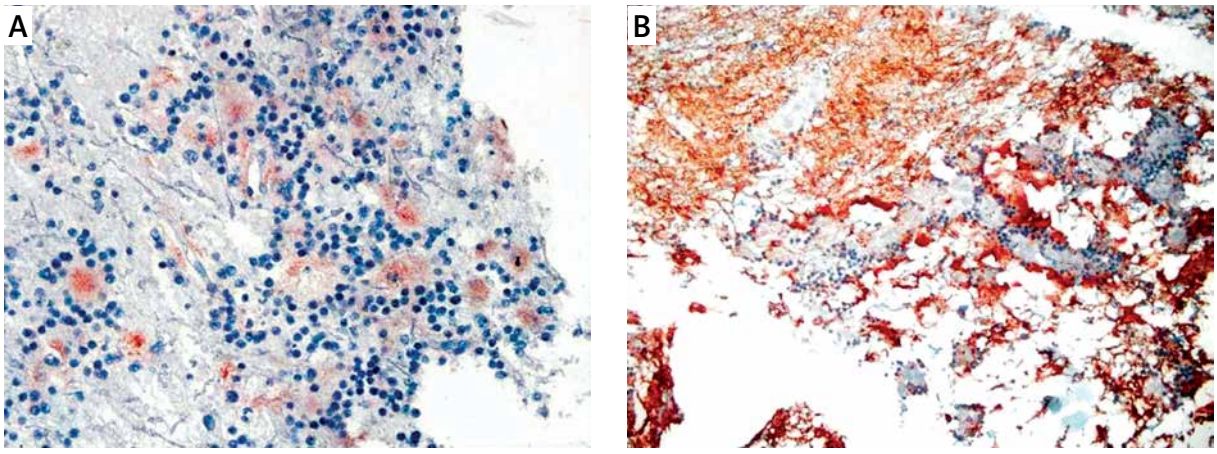

Fig. 3. In immunohistochemical study synaptophysin is present at the centre of neurocytic rosettes (**A**) and glial fibrillary acidic protein (GFAP) immunoreactivity is present in the glial component (**B**).

cifications and cystic components [4,11,13,21,23,27]. Some smaller tumour nodules may accompany these tumours [19,23,27]. These tumours are usually hypointense on T1 and hyperintense or isointens on T2 weighted MRI sequences [10]. They may have no contrast enhancement as in our case or may have a ring shaped contrast enhancement that led to consideration of malignancy [24,27]. Low density on non-enhanced CT as in the presented case is also typical of these lesions [4]. These tumours may show evidence of previous intratumoral haemorrhage on MRI [21,30].

Rosette-forming glioneuronal tumours have two components of both neurocytic and glial areas, but usually the glial component of the tumour predominates [3]. Rosette-forming glioneuronal tumours are low-grade tumours with no histopathological signs of malignancy [1,27]. They have a low labelling index of Ki-67 antigen, minimal or no cellular atypia and there is no evidence of recurrence, increase in tumour size or metastasis until now [19]. Solis *et al*. [32] found mutations of isocitrate dehydrogenase 1 (IDH1) and IDH2 that are relatively specific of diffuse gliomas; but Xiong *et al*. [36] did not detect somatic mutations of IDH1 and IDH2 in their cases. PIK3CA mutations were other mutations reported in RGNT [7]. PIK3CA mutants are seen with high frequencies in glioblastomas and anaplastic oligodendrogliomas.

The recommended treatment modality of these tumours is surgery. As these tumours are accepted low-grade in nature, an aggressive approach can increase surgical morbidity [15]; so, subtotal removal or gross total removal may be chosen. Until now, 4 cases of recurrence have been reported. The recurrence time of the tumours was 10 years in 2 cases [13,19] and 9 and 4 years in the others [7].

The main differential diagnosis of RGNT includes pilocytic astrocytoma (PA), dysembryoplastic neuroepithelial tumour, central neurocytoma, plexus papilloma, oligodendroglioma, ependymoma, primitive neuroectodermal tumour (PNET), glioneuronal tumour with neuropil-like islands (rosette) glioneuronal tumour, papillary glioneuronal tumour and metastasis [3,15,19,29]. Pilocytic astrocytoma is the most difficult tumour type for differential diagnosis with RGNT. Pilocytic astrocytoma has small round cells as well as astrocytic cells but rosette structures like those of RGNT are not found in PA [17,19]. There is also no evidence of neural differentiation in the rounded cells of pilocytic astrocytoma [3]. Dysembryoplastic neuroepithelial tumour has mature neurons in mucinous pools that help for differentiating from RGNT. Rosette-forming glioneuronal tumour does not have "floating neurons" as is the case for the "specific glioneuronal element" of DNT [34]. Central neurocytoma is characterized by uniform round cells and has similar immunohistochemical features of neuronal differentiation as in RGNT, but it does not have biphasic architecture with a distinctly separate glial component and true neurocytic rosette formation [35]. Central neurocytomas have no astrocytic components as RGNTs. Although neurocytes or well-formed rosettes may be found in oligodendrogliomas, oligodendroglial components are not seen in RGNTs [6]. The distribution pattern of synaptophysin and GFAP staining in ependymomas are quite the opposite to that seen in RGNTs [34].

In conclusion, RGNTs are clinically slow-growing tumours and typically occur in the midline. They affect mainly young adults with a slight female predominance. They can be seen outside the posterior fossa as ectopic tumours. They have biphasic cytoarchitecture with two elements; neurocytic rosettes resembling Homer-Wright rosettes and astrocytic component resembling a pilocytic astrocytoma. Glioneuronal tumours are a heterogeneous entity; so, further pathologic and clinical subclassifications may be required for prognostication and treatment. Careful and long-term follow-up monitoring will be wise for these uncommon tumours.

Disclosure

Authors report no conflict of interest.

References

1. Adachi J, Nishikawa R, Hirose T, Matsutani M. Mixed neuronal-glial tumor of the fourth ventricle and successful treatment of postoperative mutism with bromocriptine: case report. Surg Neurol 2005; 63: 375-379.
2. Albanese A, Mangiola A, Pompucci A, Sabatino G, Gessi M, Lauriola L, Anile C. Rosette-forming glioneuronal tumour of the fourth ventricle: report of a case with clinical and surgical implications. J Neurooncol 2005; 71: 195-197.
3. Allende DS, Prayson RA. The expanding family of glioneuronal tumors. Adv Anat Pathol 2009; 16: 33-39.
4. Amemiya S, Shibahara J, Aoki S, Takao H, Ohtomo K. Recently established entities of central nervous system tumors: review of radiological findings. J Comput Assist Tomogr 2008; 32: 279-285.
5. Anan M, Inoue R, Ishii K, Abe T, Fujiki M, Kobayashi H, Goya T, Nakazato Y. A rosette-forming glioneuronal tumor of the spinal

cord: the first case of a rosette-forming glioneuronal tumor originating from the spinal cord. Hum Pathol 2009; 40: 898-901.
6. Arai A, Sasayama T, Tamaki M, Sakagami Y, Enoki E, Ohbayashi C, Kohmura E. Rosette-forming glioneuronal tumor of the fourth ventricle – case report. Neurol Med Chir (Tokyo) 2010; 50: 224-228.
7. Ellezam B, Theeler BJ, Luthra R, Adesina AM, Aldape KD, Gilbert MR. Recurrent PIK3CA mutations in rosette-forming glioneuronal tumor. Acta Neuropathol 2012; 123: 285-287.
8. Gessi M, Waha A, Setty P, Waha A, Pietsch T. Analysis of KIAA1549-BRAF fusion status in a case of rosette-forming glioneuronal tumor of the fourth ventricle (RGNT). Neuropathology 2011; 31: 654-657.
9. Ghosal N, Furtado SV, Hegde AS. Rosette forming glioneuronal tumor pineal gland and tectum: An intraoperative diagnosis on smear preparation. Diagn Cytopathol 2010; 38(8):590-593.
10. Frydenberg E, Laherty R, Rodriguez M, Ow-Yang M, Steel T. A rosette-forming glioneuronal tumour of the pineal gland. J Clin Neurosci 2010; 17:1326-1328.
11. Fushimi Y, Miyasaki A, Taki H, Aoyama K, Hirato J, Kanagaki M, Togashi K. Rosette-forming glioneuronal tumor of the fourth ventricle with bilateral olivary degeneration. Jpn J Radiol 2011; 29: 445-448.
12. Hainfellner JA, Scheithauer BW, Giangaspero F, Rosenblum MK. Rosette-forming glioneuronal tumor of the 4th ventricle (RGNT). In: World Health Organization Classification of Tumours of the Central Nervous System. Louis DN, Ohgaki H, Wiestler OD, Cavenee W (eds.). IARC, Lyon 2007; 115-116.
13. Jacques TS, Eldridge C, Patel A, Saleem NM, Powell M, Kitchen ND, Thom M, Revesz T. Mixed glioneuronal tumour of the fourth ventricle with prominent rosette formation. Neuropathol Appl Neurobiol 2006; 32: 217-220.
14. Johnson M, Pace J, Burroughs JF. Fourth ventricle rosette-forming glioneuronal tumor. Case report. J Neurosurg 2006; 105: 129-131.
15. Joseph V, Wells A, Kuo YH, Halcrow S, Brophy B, Scott G, Manavis J, Swift J, Blumbergs PC. The 'rosette-forming glioneuronal tumor' of the fourth ventricle. Neuropathology 2009; 29: 309-314.
16. Karafin M, Jallo GI, Ayars M, Eberhart CG, Rodriguez FJ. Rosette forming glioneuronal tumor in association with Noonan syndrome: pathobiological implications. Clin Neuropathol 2011; 30: 297-300.
17. Kinno M, Ishizawa K, Shimada S, Masaoka H, Doi M, Seyama S, Komori T, Hirose T. Cytology is a useful tool for the diagnosis of rosette-forming glioneuronal tumour of the fourth ventricle: a report of two cases. Cytopathology 2010; 21: 194-197.
18. Komori T, Scheithauer BW, Sung JH. Rosette-forming mixed neuronal-glial tumour in the fourth ventricle. Neuropathol Exp Neurol 1998; 57: 520 [Abstract].
19. Komori T, Scheithauer BW, Hirose T. A rosette-forming glioneuronal tumor of the fourth ventricle: infratentorial form of dysembryoplastic neuroepithelial tumor? Am J Surg Pathol 2002; 26: 582-591.
20. Kuchelmeister K, Demirel T, Schlörer E, Bergmann M, Gullotta F. Dysembryoplastic neuroepithelial tumour of the cerebellum. Acta Neuropathol 1995; 89: 385-390.
21. Li YM, Li WQ, Pan Y, Lu YC, Long NY, Tao XF, Yu HY. Rosette-forming glioneuronal tumour of the fourth ventricle with previous intratumoural haemorrhage: case report and review of the literature. J Int Med Res 2009; 37: 958-966.
22. Luan S, Zhuang D, Sun L, Huang FP. Rosette-forming glioneuronal tumor (RGNT) of the fourth ventricle: Case report and review of literature. Clin Neurol Neurosurg 2010; 112: 362-364.
23. Marhold F, Preusser M, Dietrich W, Prayer D, Czech T. Clinicoradiological features of rosette-forming glioneuronal tumor (RGNT) of the fourth ventricle: report of four cases and literature review. J Neurooncol 2008; 90: 301-308.
24. Matyja E, Grajkowska W, Nauman P, Ozieblo A, Bonicki W. Rosette-forming glioneuronal tumor of the fourth ventricle with advanced microvascular proliferation – a case report. Neuropathology 2011; 31: 427-432.
25. Pimentel J, Resende M, Vaz A, Reis AM, Campos A, Carvalho H, Honavar M. Rosette-forming glioneuronal tumor: pathology case report. Neurosurgery 2008; 62: E1162-1163.
26. Podlesek D, Geiger K, Hendry DJ, Schackert G, Krex D. Rosette-forming glioneuronal tumor of the fourth ventricle in an elderly patient. J Neurooncol 2011; 103: 727-731.
27. Preusser M, Dietrich W, Czech T, Prayer D, Budka H, Hainfellner JA. Rosette-forming glioneuronal tumor of the fourth ventricle. Acta Neuropathol 2003; 106: 506-508.
28. Rickert CH, Jasper M, Sepehrnia A, Jeibmann A. Rosetted glioneuronal tumour of the spine: clinical, histological and cytogenetic data. Acta Neuropathol 2006; 112: 231-233.
29. Rosenblum MK. The 2007 WHO Classification of Nervous System Tumors: newly recognized members of the mixed glioneuronal group. Brain Pathol 2007; 17: 308-313.
30. Sharma P, Swain M, Padua MD, Ranjan A, Lath R. Rosette-forming glioneuronal tumors: a report of two cases. Neurol India 2011; 59: 276-280.
31. Scheithauer BW, Silva AI, Ketterling RP, Pula JH, Lininger JF, Krinock MJ. Rosette-forming glioneuronal tumor: report of a chiasmal-optic nerve example in neurofibromatosis type 1: special pathology report. Neurosurgery 2009; 64: E771-772.
32. Solis OE, Mehta RI, Lai A, Mehta RI, Farchoukh LO, Green RM, Cheng JC, Natarajan S, Vinters HV, Cloughesy T, Yong WH. Rosette-forming glioneuronal tumor: a pineal region case with IDH1 and IDH2 mutation analyses and literature review of 43 cases. J Neurooncol 2011; 102: 477-484.
33. Tan CC, Gonzales M, Veitch A. Clinical implications of the infratentorial rosette-forming glioneuronal tumor: case report. Neurosurgery 2008; 63: E175-176.
34. Vajtai I, Arnold M, Kappeler A, Jeless O, Lukes A, Mariani L, Paulus W. Rosette-forming glioneuronal tumor of the fourth ventricle: report of two cases with a differential diagnostic overview. Pathol Res Pract 2007; 203: 613-619.
35. Wang Y, Xiong J, Chu SG, Liu Y, Cheng HX, Wang YF, Zhao Y, Mao Y. Rosette-forming glioneuronal tumor: report of an unusual case with intraventricular dissemination. Acta Neuropathol 2009; 118: 813-819.
36. Xiong J, Liu Y, Chu SG, Chen H, Chen HX, Mao Y, Wang Y. Rosette-forming glioneuronal tumor of the septum pellucidum with extension to the supratentorial ventricles: rare case with genetic analysis. Neuropathology 2012; 32: 301-305.

Instructions to Authors

This instruction is based upon *Uniform Requirements for Manuscripts Submitted to Biomedical Reviews* (the complete document appears in N Engl J Med 1997; 336, 309-315).

Aims and scope

Folia Neuropathologica is an official journal of the Mossakowski Medical Research Centre Polish Academy of Sciences and the Polish Association of Neuropathologists. The journal publishes original articles and reviews that deal with all aspects of clinical and experimental neuropathology and related fields of neuroscience research. The scope of journal includes surgical and experimental pathomorphology, ultrastructure, immunohistochemistry, biochemistry and molecular biology of the nervous tissue. Papers on surgical neuropathology and neuroimaging are also welcome. The reports in other fields relevant to the understanding of human neuropathology might be considered.

Publication charge

Please note that there is an obligatory charge (250 Euro) for the manuscript being accepted for publication in *Folia Neuropathologica*. We send invoice for payment after the article is accepted for publication. There are no additional charges based on color figures or other elements.

Ethical consideration

Papers describing animal experiments can be accepted for publication only if the experiment conforms to the legal requirements in Poland as well as with the European Communities Council Directive of November 24, 1986 or the National Institute of Health Guide (National Institute of Health Publications No. 80-23, Revised 1978) for the care and use of Laboratory Animals for experimental procedure. Authors must provide a full description of their anesthetics and surgical procedures. Papers describing experiments on human subjects must include a statement that experiments were performed with the understanding and consent of each subject, with the approval of the appropriate local ethics committee.

Submission of manuscripts

Articles should be written in English. **All new manuscripts should be submitted through the online submission** at http://panel2.termedia.pl/fn
For authors unable to submit their manuscript online, please contact with Prof. E. Matyja, Editor-in-Chief of *Folia Neuropathologica*, ematyja@imdik.pan.pl
The Editorial Board reserves the right to reject a paper without reviewers' opinion if the content or the form of the paper does not meet minimum acceptance criteria or if the subject of the paper is beyond the aims and scope of the journal.

Legal aspects

In sending the manuscript the author(s) confirm(s) that (s)he has (they have) not previously submitted it to another journal (except for abstracts of no more than 400 words) or published it elsewhere. The author(s) also agree(s), if and when the manuscript is accepted for publication, to automatic and free transfer of copyright to the Publisher allowing for the publication and distribution of the material submitted in all available forms and fields of exploitation. The author(s) accept(s) that the manuscript will not be published elsewhere in any language without the written consent of the copyright holder, i.e. the Publisher.
All manuscripts submitted should be accompanied by an authors' statement including signed confirmation of the above and confirming that this publication has been approved by all co-authors (if any), as well as by the responsible authorities at the institution where the work has been carried out. The authors' statement should be signed by ALL co-authors. Additionally, the author(s) confirm(s) that (s)he is (they are) familiar with and will observe the "Instruction to Authors" included in *Folia Neuropathologica* and also that all sources of financial support have been fully disclosed. Materials previously published should be accompanied by written consent for reprinting from the relevant Publishers. In the case of photographs of identifiable persons, their written consent should also be provided. Any potential conflict of interest will be dealt with by the local court specific to the Publisher. Legal relations between the Publisher and the author(s) are in accordance with Polish law and with international conventions binding on Poland.
Authors agree to waive their royalties.

Anonymous review

All manuscripts will be subject to a process of anonymous editorial review.

Preparation of manuscripts

Articles must be written in English, with British spelling used consistently throughout. Authors not entirely familiar with English are advised to correct the style by professional language editors or native English speakers.
• The length of original article should not exceed 20 printed pages including text, illustrations, tables, and references.

- Manuscripts should be typed using 12pts.font, double-spaced, and fully corrected. Allow a margin at least 2.5 cm at the top, bottom and left side of the page. Text should not be justified.
- The title page should contain: the author's full names, title of the paper, all authors' affiliations, full name and address of the communicating author (including e-mail address and fax number), running title (not exceed 40 characters including spaces).
- The abstract should not exceed 350 words. A list of 3–10 key words is recommended below the abstract.
- The manuscript body should be organized in a standard form with separate sections: Introduction, Material and Methods, Results, Discussion, and References. Review articles should be divided into sections and subsections as appropriate without numbering.
- Do not underline in the text. Avoid footnotes.
- All dimensions and measurements must be specified in the metric system.
- The source of any drug and special reagent should be identified.
- Particular attention needs to be paid to the selection of appropriate analysis of data and the results of statistical test should be incorporated in the results section.
- The nomenclature used should conform to the current edition of the Nomina Anatomica or Nomina Anatomica Veterinaria.
- Acknowledgements should be made in a separate sheet following Discussion and before References. These should contain a list of dedications, acknowledgements, and funding sources.
- Legends of figures and tables should be typed on separate pages.
- The editor reserves the right to make corrections.

Tables

- Tables numbered in Roman numerals require a brief but descriptive heading.
- The major divisions of the table should be indicated by horizontal rules.
- Explanatory matter should be included in footnotes, indicated in the body of the table in order of their appearance.
- Tables must not duplicate material in the text or in illustration.

Illustrations

All figures should be supplied electronically at resolution 300dpi in all standard formats (tiff, jpg, Adobe Photoshop, Corel Draw, and EPS). Name your figure files with "Fig" and the figure number, e.g., Fig1.tif

- The maximum figure size is 84 mm or 174 mm for use in a single or double column width, respectively.
- When possible, group several illustrations on one block for reproduction. Like all other figures, block should be prepared within a rectangular frame to fit within a single or double column width of 84 and 174 mm, respectively, and a maximum page height of 226 mm.
- Each figure should include scale magnification bar; do not use magnification factors in the figure legends.
- All figures, whether photographs, graphs or diagrams, should be numbered using Arabic numerals and cited in the text in consecutive numerical order
- **Immunohistochemical study requires color illustrations of very good quality. The papers with white and black immunohistochemistry will not be accepted.**
- **For the paper accepted before 01.04.2016 the publication charge includes only the expense of color illustrations.** The cost of color print for every successive 8 pages is 200 euro irrespective of the number of color pages, i.e., the price remains the same whether there is one or eight pages.

The Publisher makes out the bill to the communicating Author.

References

The list of references (written on a separate page) should include only those publications that are cited in the text. Avoid citation of academic books, manuals and atlases. References may be arranged alphabetically and numbered consecutively. References should be given in square brackets with no space between the comma and the consecutive number, e.g. [3,4,6-12].

References should be written as follows:

Journal papers: initials and names of all authors, full title of paper, journal abbreviation (according to Index Medicus), year of publication, volume (in Arabic numerals), first and last page (example below):

1. Valverde F. The organization of area 18 in the monkey. Anat Embryol 1978; 154: 305-334.
2. Uray NJ, Gona AG. Calbindin immunoreactivity in the auricular lobe and interauricular granular band of the cerebellum in bullfrogs. Brain Behav Evol 1999; 53: 10-19.

Book and monographs: initials and names of all authors, full title, edition, publisher, place, year (examples below):

1. Pollack RS. Tumor surgery of the head and neck. Karger, Basel 1975.
2. Amaral DG, Price JL, Pitkanen A, Carmichael ST. Anatomical organization of the primate amygdaloid complex. In: Aggleton JP (ed.). The amygdala. Wiley-Liss, New York 1992; pp. 1-66.

Reference to articles that are accepted for publication may be cited as „in press" or Epub.

Proofs

Corrections to the proofs should be restricted to printer's errors only; other alterations will be charged to the authors. In order to maintain rapid publication, proofs should be returned within 48 hours, preferably by e-mail, fax or courier mail. If the Publisher receives no response from the authors after 10 days, it will be assumed that there are no errors to correct and the article will be published.

Subscription information

The journal is published in one volume per year consisting of four numbers. The annual subscription price is 160 PLN for Institutions from Poland and 80 PLN for individual subscribers from Poland and 140 Euro for foreign Institutions and 70 Euro for foreign individual subscribers.
Payment should be made to:
Termedia sp. z o.o., ul. Kleeberga 8, 61-615 Poznań
BZ WBK III O/Poznań PL 61 1090 1359 0000 0000 3505 2645
SWIFT: WBKPPLPP

The publisher must be notified of a cancellation of a subscription not later than two months before the end of the calendar year. After that date the subscription is automatically prolonged for another year.
Publishing, Subscription and Advertising Office:
TERMEDIA Publishing House
ul. Kleeberga 2
61-615 Poznań, Poland
phone/fax +48 61 822 77 81
e-mail: termedia@termedia.pl
http://www.folianeuro.termedia.pl

Folia
Neuropathologica

AUTHOR'S STATEMENT

Title of the article

.....

.....

.....

The author(s) hereby confirm(s) that:

☐ The above-mentioned work has not previously been published and that it has not been submitted to the Publishers of any other journal (with the exception of abstracts not exceeding 400 words).

☐ All co-authors named and the relevant authorities of the scientific institutions at which the work has been carried out are familiar with the contents of this work and have agreed to its publication.

☐ In sending the manuscript together with illustrations and tables agree(s) to automatic and free transfer of copyright to the Publisher allowing for the publication and distribution of the material submitted in all available forms and fields of exploitation, without limits of territory or language, provided that the material is accepted for publication. At the same time the author(s) accept(s) that the submitted work will not be published elsewhere and in whatever language without the earlier written permission of the copyright holder, i.e. the Publisher.

☐ (S)he (they) agree to waive his(her)(their) royalties (fees).

☐ (S)he (they) empower(s) the Publisher to make any necessary editorial changes to the submitted manuscript.

☐ All sources of funding of the work have been fully disclosed.

☐ The manuscript has been prepared in accordance with the Publisher's requirements.

☐ (S)he (they) is (are) familiar with the regulations governing the acceptance of works as published in *Folia Neuropathologica* and agree(s) to follow them.

☐ (S)he (they) agree to accept appropriate invoice from the Publisher in case colour illustrations are implemented.

Date *Signatures of **all authors***

The covering letter formula can be found at: www.folianeuro.termedia.pl
-The covering letter should be sent to Associate Editor:

Milena Laure-Kamionowska
-Editorial Office of Folia Neuropathologica
Mossakowski Medical Research Centre, Polish Academy of Sciences
Poland Medical Research Centre
ul. Pawinskiego 5
02-106 Warszawa, Poland

CONTENTS